ISSN 2095-8137 CN 53-1229/Q
Volume 36 Issue 1
18 January 2015

ZR
动物学研究

ZOOLOGICAL RESEARCH

CODEN: DOYADI
www.zoores.ac.cn

Science Press

ZOOLOGICAL RESEARCH

Volume 36, Issue 1 18 January 2015

CONTENTS

Cover image: Brown forest skink, *Sphenomorphus indicus* (Gray, 1853). Photo by Ying-Chao HU

Growing and evolving: remarks for the 35th anniversary of the founding of *Zoological Research*

The beginning of a new year is always a time for reflection, contemplation and optimism. For the past thirty-five years, since its founding in 1980, *Zoological Research* (*ZR*) has experienced many highs and lows, seeing great advances but also overcoming numerous hurdles. *Zoological Research* has made many valuable contributions to the progress of biological sciences in China and won prestige both at home and abroad. Currently, it serves as a key journal focusing on Genome Evolution and Genetic Diversity, Animal Ecology and Ethology, Primates and Animal Models of Human Diseases. The journal also publishes high quality papers related to taxonomy and DNA barcoding, developmental biology, physiology, biochemistry, immunology, and neuroscience. The growth achieved by *ZR* is not only due to our excellent readers and reviewers, but also to the evolution of our authors into renowned scholars. Accordingly, we would like to thank you all for your constant support and generous help.

Zoological Research has always put the needs of its readers and authors first. To facilitate communication between our domestic colleagues and the international community, in 2013 to 2014 we successfully transitioned from a Chinese-language only journal, into a Chinese-English bilingual journal and finally into an internationally aimed English-language only journal. To help expand author view-points, we also included new Editorial and Letter to the Editor columns. Furthermore, the editorial board and editorial members continued to refine our publishing period, editing quality, typesetting, and journal marketing. In addition to *ZR* being selected as a high-quality publication for the dissemination of research findings, both the visibility and influence of *ZR* has continued to increase.

As a respectable scientific publication in China, *ZR* had made impressive progress over the past few years, particularly in regards to its high academic value and leading role in advancing the quality of academic journals in China. In 2014, *ZR* was ranked among the top 300 “Outstanding S&T Journals of China”, the second time *ZR* has been recognized by this prestigious award since 2008. In addition, four articles published in *ZR* between 2009 to 2013 were also included in the “Project of Frontrunner 5000” (F5000), which aims to promote scientific communication and the internationalization of Chinese S&T journals.

The contributions from our colleagues have enabled our continued growth and advance. From a pool of more than 4600 journals, *ZR* was among the top 10% of Chinese publications and was awarded the “The Highest / The International Impact Academic Journals of China” in Science, Technology and Engineering from 2012 to 2014 for its achievements in internationalizing life science research, as determined by its increasing international annual citation frequency and international impact factor.

In September 2014, we were greatly honored to have a group of renowned academic experts from home and abroad join us as members of the editorial board. Thus, with dedicated assistance from our editorial team and first-rate reviewers, we will continue to expand and improve our publication, and in particular we welcome manuscripts on Genetics and Evolution, Primates and Animal Models of Human Diseases, and Biodiversity Conservation and Ecology. We also extend a special invitation to our colleagues to serve as single-issue Guest Editors, and if any author would like to advance a topic that is prospective, controversial and worth exploring, please feel free to contact us.

Once again, we would like to thank you all for your enduring support and faith. Our continued growth and evolution together will ensure that *ZR* remains a respected publication platform that provides ever greater possibilities to you.

Sincerely yours,

Yong-Gang YAO, Editor-in-Chief

Kunming Institute of Zoology, *Chinese Academy of Sciences*, *Kunming* 650223, *China*

Yun ZHANG, Executive Editor-in-Chief

Kunming Institute of Zoology, *Chinese Academy of Sciences*, *Kunming* 650223, *China*

ZOOLOGICAL RESEARCH

Genomic organization and evolution of ruminant lysozyme *c* genes

David M. IRWIN[1,2,*]

[1] *Department of Laboratory Medicine and Pathobiology, University of Toronto, Toronto, Canada*

[2] *Banting and Best Diabetes Centre, University of Toronto, Toronto, Canada*

ABSTRACT

Ruminant stomach lysozyme is a long established model of adaptive gene evolution. Evolution of stomach lysozyme function required changes in the site of expression of the lysozyme *c* gene and changes in the enzymatic properties of the enzyme. In ruminant mammals, these changes were associated with a change in the size of the lysozyme *c* gene family. The recent release of near complete genome sequences from several ruminant species allows a more complete examination of the evolution and diversification of the lysozyme *c* gene family. Here we characterize the size of the lysozyme *c* gene family in extant ruminants and demonstrate that their pecoran ruminant ancestor had a family of at least 10 lysozyme *c* genes, which included at least two pseudogenes. Evolutionary analysis of the ruminant lysozyme *c* gene sequences demonstrate that each of the four exons of the lysozyme *c* gene has a unique evolutionary history, indicating that they participated independently in concerted evolution. These analyses also show that episodic changes in the evolutionary constraints on the protein sequences occurred, with lysozyme *c* genes expressed in the abomasum of the stomach of extant ruminant species showing the greatest levels of selective constraints.

Keywords: Lysozyme *c*; Ruminants; Gene family; Gene duplication; Concerted evolution; Mosaic evolution

INTRODUCTION

Ruminant mammals such as cow, sheep, and deer, rely on foregut fermentation to extract nutrients from their diet of plant material (Clauss et al, 2010; Janis, 1976; Mackie, 2002; Stevens & Hume, 1998). Foregut fermentation, by bacteria and microbes, produces short chain fatty acids that are absorbed through the stomach wall and provide energy for the ruminant animals; however, the microbial population responsible for this fermentation incorporates many of the other nutrients, such as nitrogen based compounds, into their own growing populations (Mackie, 2002; Stevens & Hume, 1998). To extract these essential nutrients from the microbial population, ruminant animals must break open these bacterial and microbial cells, to release their contents, to allow the stomach digestive enzymes in the abomasum to extract nutrients from their contents (Stevens & Hume, 1998). Since bacterial cells are typically resistant to mammalian digestive enzymes, ruminant species have recruited the anti-bacterial enzyme, lysozyme *c*, to break open these cells (Callewaert & Michiels, 2010; Dobson et al, 1984; Irwin et al, 1992; Mackie, 2002; Prager & Jollès, 1996). Recruitment of lysozyme *c* as a digestive enzyme has occurred at least twice within mammals, on the lineages leading to the ruminant artiodactyls and the leaf-eating monkeys (Dobson et al, 1984; Stewart et al, 1987; Stewart & Wilson, 1987), with a similar recruitment of a calcium-binding lysozyme occurring in the hoatzin, a leaf-eating bird (Kornegay et al, 1994; Kornegay, 1996).

Recruitment of lysozyme *c* to become a digestive enzyme required changes both in the site of expression of the gene encoding this enzyme and in the amino acid sequence of the enzyme to allow function in the acidic stomach (Dobson et al, 1984; Irwin et al, 1992; Irwin, 1996; Prager, 1996). The major site of expression of lysozyme in mammals is macrophages, but it also secreted into some body fluids (such as tears), where it participates in host defense against bacterial infection (Callewaert & Michiels, 2010; Prager & Jollès, 1996; Short et al, 1996). The molecular basis for the recruitment of expression, at high levels, of lysozyme *c* in stomach cells is unknown. Typical mammalian lysozyme *c*

Received: 08 October 2014; Accepted: 02 December 2014

Foundation item: This study was supported by grants from the Natural Sciences and Engineering Research Council (RGPIN 183701)

*Corresponding author, E-mail: david.irwin@utoronto.ca

DOI:10.13918/j.issn.2095-8137.2015.1.1

enzymes function in an environment at a neutral pH, and one that is free of digestive enzymes (Callewaert & Michiels, 2010; Prager & Jollès, 1996; Prager, 1996). Lysozyme *c* function in the abomasum of the stomach of ruminant animals, to digest bacterial cell walls, required adapting the lysozyme *c* protein sequence to function at an acidic pH and becoming resistant to the actions of stomach digestive enzymes and acids found in the abomasum (Dobson et al, 1984; Jollès et al, 1989; Prager, 1996). A number of convergent amino acid changes were seen between the lysozyme *c* sequences that have adapted for function in the stomachs of the langur, a leaf-eating monkey, and ruminants, have been identified and presumed to account for much of the functional adaptation (Stewart & Wilson, 1987; Stewart et al, 1987; Swanson et al, 1991; Prager, 1996). Some of these adaptive changes include replacement of lysine residues with arginine, which removes potential cleavage sites for digestive enzymes found in the stomach, and the loss of an aspartate-proline dipeptide, which is an acid-labile peptide bond (Jollès et al, 1989; Prager, 1996; Stewart & Wilson, 1987; Stewart et al, 1987; Swanson et al, 1991). These putative adaptive amino acid replacements are inferred to occur early in ruminant evolution, and thus may parallel the origin and evolution of the ruminant lifestyle (Irwin et al, 1992; Irwin, 1996).

Recruitment of lysozyme *c* to a digestive role in ruminants is associated with an expansion of the size of the lysozyme *c* gene family (Jiang et al, 2014; Irwin & Wilson, 1989; Irwin et al, 1989, 1992). Most mammals have only one or a few lysozyme *c* genes, while ruminant species have 10 or more (Callewaert & Michiels, 2010; Irwin & Wilson, 1989; Irwin et al, 1989, 1996; Prager & Jollès, 1996; Irwin et al, 2011; Jiang et al, 2014). The lysozyme *c* gene family of the cow has been better characterized than those of most other ruminants, where it was found that only some of the genes are expressed in the abomasum, while others retain more ancestral type of roles (Irwin & Wilson, 1989; Irwin et al, 1993; Irwin, 2004). Similar observations have been made for the lysozyme *c* genes of sheep (Jiang et al, 2014). Several lysozyme *c* proteins, and their cDNAs, have been characterized from the abomasums of the cow, sheep and deer (Dobson et al, 1984; Jollès et al, 1989; Irwin & Wilson, 1989, 1990). Intriguingly, phylogenetic analysis of the coding and 3' untranslated portions of the lysozyme *c* cDNA sequences yielded different trees, with the coding sequences implying duplications of the genes on each species lineage and the 3 untranslated region indicating more ancient duplications before the divergence of these species (Irwin & Wilson, 1990). Selection at the protein level (e.g., lineage-specific adaptation of the protein sequences) does not explain the differences in the phylogenies for the two regions, as synonymous difference (those that do not change the coding potential) also yield the same conclusions. It was concluded that the differences in the phylogenies was due to concerted evolution, mediated by gene conversion, acting on the coding sequences, while the 3' untranslated regions only experienced divergent evolution (Irwin & Wilson, 1990; Irwin et al, 1992; Irwin, 1996; Wen & Irwin, 1999; Yu & Irwin, 1996). Characterization of the genomic sequences of lysozyme genes expressed in the abomasum from the cow and sheep suggested that the concerted evolution was limited to only the coding exons, and did not involve the intronic sequences separating these exons (Irwin et al, 1993; Wen & Irwin, 1999). An analysis of larger number of lysozyme mRNA sequences, including genes that are not expressed in the stomach, suggested that some of the genes expressed in non-stomach tissues might have also experienced concerted evolution (Irwin, 1995, 2004; Takeuchi et al, 1993).

The previous analyses were largely limited to lysozyme *c* genes expressed in ruminant species. With the recent completion of draft genomic sequences from several ruminant species (including, cow, yak, zebu, goat, Tibetan antelope, and sheep: Canavez et al, 2012; Dong et al, 2013; Ge et al, 2013; Jiang et al, 2014; Qiu et al, 2012; Zimin et al, 2009) it now possible to more completely characterize the complete complement of lysozyme *c* genes (including genenes that are not expressed) in the genomes of these species and examine the molecular evolution of these genes. Here we describe the lysozyme *c* gene complements of the cow and several other ruminant species. The lysozyme *c* gene cluster has largely been maintained within true ruminant (Infraorder Pecora) species. Analysis of these sequences shows that the ancestor of cow, sheep, and goats had 10 lysozyme *c* genes, several of which were pseudogenes that were retained by diverse species. The exons of the lysozyme *c* genes have differing evolutionary histories, suggesting that concerted evolution acted independently on each exon.

MATERIALS AND METHODS

Database searches

Previous searches of mammalian genomes indicated that the cow genome had about 12 lysozyme *c* genes located in a cluster on cow chromosome 5, many of which were incompletely annotated in the Ensembl assembly (Irwin et al, 2011). To better characterize the lysozyme *c* gene cluster in the cow (*Bos taurus*) genome we used the Blast algorithm (Altschul et al, 1990) to search the UMD 3.1 cow genome assembly (from Ensembl release 75 in June 2014; http://www.ensembl. org/index.html) with known and predicted cow lysozyme *c* cDNA and protein sequences. Lysozyme *c* genes from the sheep (*Ovis aries*; Oar_v3.1), pig (*Sus scrofa*; Sscrofa10.2), bottlenose dolphin (*Tursiops truncates*; Turtru1), dog (*Canis lupus familiaris*; CanFam3.1), panda (*Ailuropoda melanoleuca*; AilMel1), horse (*Equus caballus*; EquCab2), and rhinoceros (*Ceratotherium simum simum*; CerSimSim1 - preEnsembl) genomes from the Ensembl database were characterized by the approaches described above. A similar search strategy was used to identify lysozyme *c* genes in the yak (*Bos grunniens*), zebu (*Bos indicus*), water buffalo (*Babalus babalis*), Tibetan antelope (chiru; *Pantholopus hodgsonii*), goat (*Capra hircus*), aplaca

(*Vicugna pacos*), minke whale (*Balaenoptera acutorostrara scammoni*), killer whale (*Orcinus orca*), Yangtze River dolphin (*Lipotes vexillifer*), and sperm whale (*Physeter catodon*) genomes from the NCBI Genomes (chromosome), Whole-genome shotgun contigs (wgs), and Nucleotide collection (nr/nt) databases (http://blast.ncbi.nlm.nih.gov/Blast.cgi).

Genomic alignments and assignment of orthology

Genomic sequences encompassing lysozyme *c* genes were downloaded from the Ensembl and NCBI databases. Intron-exon boundaries of the 4 exons and the 5' and 3' flanking sequences of the new lysozyme *c* genes were annotated based on genomic alignments of genes using MultiPipMaker (Schwartz et al, 2000, 2003), using previously characterized artiodactyl lysozyme *c* genes (Irwin et al, 1993, 1996; Irwin, 1995; Yu & Irwin, 1996; Wen & Irwin, 1999) as guides. Gene neighborhood organization was assessed as previously described for lysozyme *c* genes (Irwin et al, 2011) with the flanking *Yeats*4 and *Cpsf*6 genes identified using Blast. Ruminant lysozyme *c* genes were named based on orthology (based on phylogeny, see below) and genomic location. Genes present in the common ancestor of sheep and cow were numbered (*Lyz*1-*Lyz*10), while lineage-specific duplicates have a letter (a-c) that follows the gene number. The alpaca lysozyme *c* genes were numbered arbitrarily, thus their numbers do not indicate orthology with the ruminant genes. All other species examined here have a single copy lysozyme *c* gene.

Phylogenetic analysis

Predicted protein coding sequences for lysozyme *c* cDNA sequences, extracted from the genomic alignments, were aligned with Muscle (Edgar, 2004) as implemented in Mega6.06 (Tamura et al, 2013). Alignments were edited manually to insert gaps to maintain open reading frames (due to the presence of frame shifting insertions in some pseudogenes). Phylogenetic trees were constructed by the maximum likelihood, neighbor-joining and parsimony methods using Mega6.06 (Tamara et al, 2013). Alternative phylogenetic hypothesis, derived from the phylogenies of the different exons, were tested using Tree-puzzle (Strimmer & von Haeseler, 1996) as implemented on the Mobyle @Pasteur web site (http://mobyle. pasteur.fr/cgi-bin/portal.py?#welcome; Néron et al, 2009).

RESULTS AND DISCUSSION

Number and organization of lysozyme *c* genes in the cow genome

Analyses of genomic Southern blots had concluded that there were about 10 lysozyme *c* genes in the cow genome (Irwin & Wilson, 1989; Irwin et al, 1989), with many of these genes clustered on chromosome 5 (Gallagher et al, 1993). A recent (2011) search of the Btau4.0 (2nd release, assembled 2007) of the cow genome sequence assembly identified 12 lysozyme *c* genes on chromosome 5 of the cow genome (Irwin et al, 2011). The genes identified in this search account for all of the previously characterized cow lysozyme *c* cDNA and protein sequences (Irwin et al, 2011). To better characterize the cow lysozyme *c* gene cluster, we searched the most current version (UMD3.1 – 3rd release) of the cow genome assembly (assembled 2009; Zimin et al, 2009) with Blast using the previously characterized lysozyme *c* cDNA and protein sequences. Our new searches identified a total of 14 lysosome *c* genes, 11 of which were annotated by Ensembl as genes (Table 1 and Figures 1, 2, and S1, supporting information at http://www.zoores.ac.cn/). The difference in the number of intact genes identified by the searches of the two different genome assemblies (12 in Btau4.0 and 11 in UMD3.1) is due to the earlier Btau4.0 assembly containing two copies of the tracheal lysozyme *c* gene (*CowC* and *CowD* in Irwin et al, 2011) while the most current assembly UMD 3.1 contains only single copy of this gene (here named *Lyz*2b).

In addition to the 11 annotated genes, each of which is composed of 4 exons consistent with the structure of a typical mammalian lysozyme *c* gene (Irwin et al, 1996; Callewaert & Michiels, 2010), Blast hits were found to map to additional locations that were distant from the annotated genes. Examination of these Blast hits suggested that they belong to three partial genes, which had not previously been annotated, with each being composed of only two, not four, exons (Table 1 and Figures 1, 2, and S1). The newly identified partial *Lyz*3a and *Lyz*3c genes contain exons 1 and 2 and exons 3 and 4, respectively, but are separated from each other by the *Lyz*3b gene that contains all 4 coding exons (Table 1 and Figures 1 and 2). No sequences similar to the missing exons were found near the *Lyz*3a and *Lyz*3c genes. The third partial gene, *Lyz*9, contains only exons 1 and 4, with the sequences between these exons showing no similarity to exons 2 or 3 of other lysozyme *c* genes. Most of the lysozyme *c* genes have the same orientation (annotated as the minus strand), but 4 of the 14 are on the opposite strand, indicating that the origin of this gene family is not just a simple series of tandem gene duplications. The cow genome, therefore, was found to contain 14 identifiable lysozyme *c* genes (Table 1 and Figures 1,2, and S1).

Pairwise sequence comparisons revealed that the DNA sequence identities of the coding sequences among the 14 genes ranged from 74.8% to 97.5%, with most pairs showing 80%-90% identity (Table 2). The similarity between *Lyz*3a and *Lyz*3c could not be measured, as there is no overlap between these two genes (*Lyz*3a has exons 3 and 4, while *Lyz*3c has exons 1 and 2, see Table 1). These two partial genes were most similar to the *Lyz*3b gene, showing greater than 96% identify in the coding sequence (Table 2), raising the possibility that they are recent gene duplicates. The *Lyz*3a, *Lyz*3b, and *Lyz*3c genes are also adjacent to each other in the genome, suggesting that the *Lyz*3a and *Lyz*3b gene were generated by partial tandem duplications of different parts of the *Lyz*3b gene (Figure 1). The partial gene *Lyz*9 did not show particularly strong similarity to any other specific cow lysozyme *c* gene (Table 2), suggesting

that it is not a product of a very recent segmental duplication event (Liu et al, 2009; Seo et al, 2013). Among the intact lysozyme genes, the coding sequence of the genes encoding the lysozymes expressed in the abomasum (Irwin & Wilson, 1989; Irwin et al, 1993) *Lyz*5/*Lyz*6/*Lyz*7 share about 97% identity and the *Lyz*2a/*Lyz*2b/*Lyz*2c genes, which includes the tracheal lysozyme gene (Takeuchi et al, 1993), share about 96% identity (Table 2). The high level of identity

Table 1 Locations of cow lysozyme *c* genes

Gene	Chromosome	Strand	Bases	Ensembl gene ID	Other name	Unigene	Sites of expression	Functional
Lyz1	5	Minus	44 421 190-44 426 117	ENSBTAG00000011941	Milk	Bt.67194: 448 ESTs	Rumen, omasum	Intact
Lyz2a	5	Plus	44 421 190-44 426 117	ENSBTAG00000022971		None[b]		Intact
Lyz2b	5	Plus	44 443 587-44 448 198	ENSBTAG00000000198	Trachael	Bt.64327: 121 ESTs	Rumen	Intact
Lyz3a	5	Minus	44 489 738-44 491 389	NA (exons 3 and 4)[a]		None[b]		Pseudogene
Lyz3b	5	Minus	44 502 011-44 507 108	ENSBTAG00000039170	ψNS4	None[b]		Pseudogene
Lyz3c	5	Minus	44 521 088-44 522 921	NA (exons 1 and 2)[a]		None[b]		Pseudogene
Lyz2c	5	Plus	44 533 912-44 538 847	ENSBTAG00000020564		Bt.105675: 31 ESTs	Rumen, intestine	Intact
Lyz4	5	Plus	44 554 351-44 559 113	ENSBTAG00000026323	Intestinal	Bt.49176: 162 ESTs	Intestine	Intact
Lyz5	5	Minus	44 573 344-44 578 495	ENSBTAG00000026088	Stomach 2	Bt.29367: 363 ESTs	Abomasum	Intact
Lyz6	5	Minus	44 599 815-44 607 109	ENSBTAG00000046511	Stomach 1	Bt.89770: 102 ESTs	Abomasum	Intact
Lyz7	5	Minus	44 631 778-44 638 267	ENSBTAG00000046628	Stomach 3	Bt.80498: 74 ESTs	Abomasum	Intact
Lyz8	5	Minus	44 652 535-44 656 613	ENSBTAG00000026322		None[b]		Pseudogene
Lyz9	5	Minus	44 673 817-44 676 391	NA (exons 1 and 4)[a]		None[b]		Pseudogene
Lyz10	5	Minus	44 713 289-44 720 946	ENSBTAG00000026779	Kidney	Bt.64645: 61 ESTs	Lymphoreticular, blood	Intact

[a] – Not annotated as a gene by Ensembl.

[b] – No ESTs with greater than 95% sequence identity identified in the NCBI EST database.

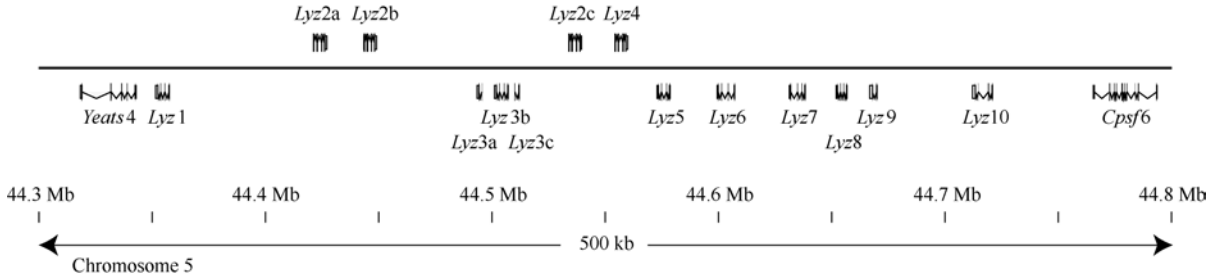

Figure 1 Organization of lysozyme *c* genes in the cow genome

Schematic of the arrangement of lysozyme *c* genes. And their neighbors, in the cow genome. Vertical lines represent exons, with splicing indicated by the lines joining the exons. Gene names are indicated above (plus strand) or below (minus strand) indicating strand with coding potential. Sizes of genes and distances are proportional. The genes are located between 44.3 and 44.8 Mb on chromosome 5.

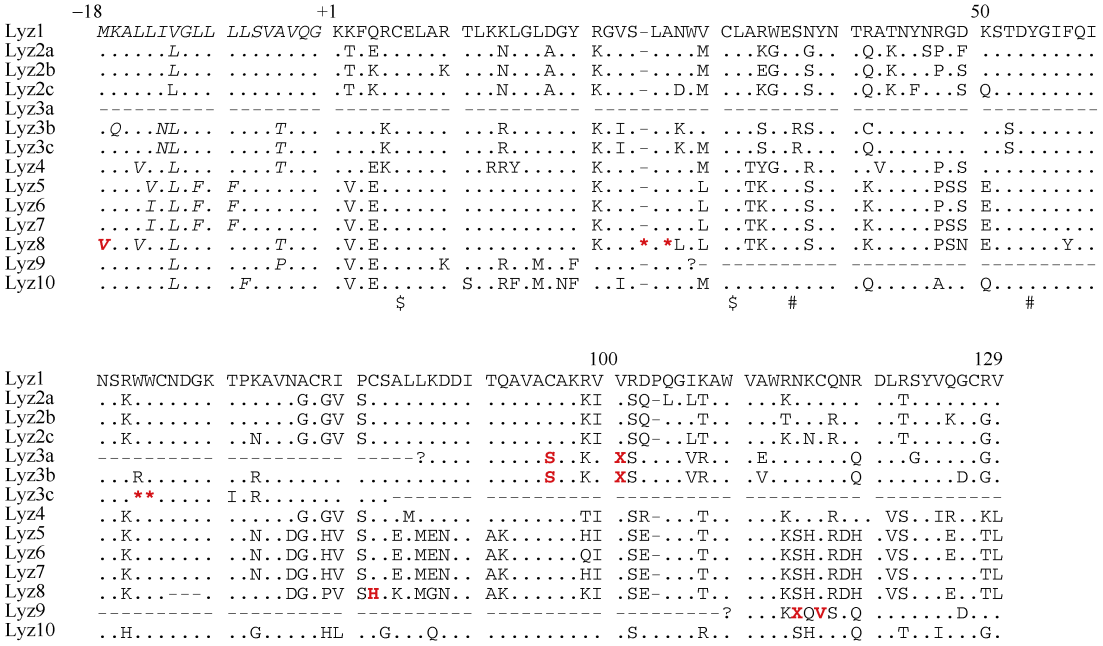

Figure 2 Amino acid sequences predicted by cow lysozyme *c* genes

Sequences of predicted lysozyme *c* proteins from the cow genome are shown in single letter code, with differences from the Cow Lyz1 sequence shown and identities indicated by dots (.). Sequence is numbered avove the sequences from the N-terminus of the Lyz1 sequence, with the signal peptide numbered backwards and in italics. Dashes (-) indicate gaps introduced to maximize alignment. Question marks (?) indicate incomplete codons due to missing sequence. Residues involved in disulfide bridging ($) and active site residues (#) are marked below the sequences. Residues marked in red are likely damaging pseudogenes and disrupt initiation, disrupt disulfide bridging or introduce stop codons. Asterisks (*) indicate inframe stop codons. Xs refer to codons that have less than 3 bases and thus cause frame shifts. The initiation codon of Lyz8 is not methionine (M).

Table 2 Pairwise percent DNA sequence identity between cow lysozyme *c* coding sequences

	Lyz2a	*Lyz2b*	*Lyz3a*	*Lyz3b*	*Lyz3c*	*Lyz2c*	*Lyz4*	*Lyz5*	*Lyz6*	*Lyz7*	*Lyz8*	*Lyz9*	*Lyz10*
Lyz1	89.4	88.7	91.3	91.3	90.7	89.0	86.5	82.2	83.1	82.9	80.9	85.6	89.0
Lyz2a		96.2	87.4	85.3	84.4	96.6	90.1	84.7	85.6	85.4	82.8	84.7	84.5
Lyz2b			88.1	85.3	84.1	96.8	90.5	84.9	85.8	85.4	82.8	83.2	84.5
Lyz3a				96.4	NA[a]	88.1	83.0	74.8	75.6	76.3	76.3	77.3	89.9
Lyz3b					96.3	85.3	85.3	79.0	79.5	79.7	77.6	84.2	86.5
Lyz3c						84.1	86.0	82.1	82.4	82.4	79.5	86.0	86.4
Lyz2c							89.6	84.9	85.8	85.6	82.8	83.7	84.7
Lyz4								84.7	84.7	85.4	83.0	83.7	83.3
Lyz5									96.4	97.5	92.2	83.2	82.9
Lyz6										96.8	92.2	84.2	82.0
Lyz7											92.4	84.7	82.9
Lyz8												82.7	80.0
Lyz9													85.6

[a] – These two genes do not overlap.

shared by these sets of genes suggests that these triplets are products of recent segmental duplication / gene duplication events (Liu et al, 2009; Seo et al, 2013). *Lyz5*/*Lyz6*/*Lyz7* are adjacent to each other and are in the same orientation (Table 1; Figure 1), thus could be generated by a simple series of tandem gene duplication

events. A more complicated duplication history is needed to explain the diversification of the *Lyz*2a/*Lyz*2b/*Lyz*2c genes. While *Lyz*2a and *Lyz*2b are in tandem, several other lysozyme *c* genes (*Lyz*3a, *Lyz*3b, and *Lyz*3c) are located between the *Lyz*2a/2b gene pair and the *Lyz*2c gene (Table 1 and Figure 1).

Since the three partial genes *Lyz*3a, *Lyz*3b, and *Lyz*9 do not contain all four coding exons; they cannot predict intact open reading frames. In addition to the missing exon sequence, all three of these genes also contain in frame stop codons or frameshifts that also would prevent translation (Figure 2). Among the lysozyme *c* genes possessing all four exons, two, *Lyz*3b and *Lyz*8, fail to predict intact open reading frames (Figure 2). *Lyz*3b, which was previously called lysozyme ψNS4 (Irwin, 1995) contains a frameshift, which is shared with *Lyz*3a, which prevents translation of the reading frame, while *Lyz*8 contains both in frame stop codons and a replacement at the initiating codon (Figure 2). Thus of the 14 lysozyme *c* genes found in the cow genome, only 9 potentially encode functional lysozyme *c* proteins. To further investigate the functional potential of these lysozyme *c* genes we searched for evidence of expression for all 14 cow lysozyme *c* genes in the NCBI expressed sequence tag (EST) database. ESTs were found for only 8 of the 9 intact genes, and for none of the 5 pseudogenes (Table 1). While *Lyz*2a has an intact open reading frame (Figure 2), no ESTs highly similar (>98% identity) to it were found in the NCBI database (Table 1), raising the possibility that this gene is not expressed.

Many of the cow lysozyme *c* gene annotations in the Ensembl database do not include 5' and/or 3' untranslated sequences. Since previous work had shown that the 5' and 3' untranslated sequences of known lysozyme *c* genes from diverse mammalian species have considerable sequence similarity (Irwin & Wilson, 1989; Irwin, 1995, 2004), we used this similarity to predict the extent of these regions for each gene (see Figure S1) from alignments generated by MultiPipMaker (Schwartz et al, 2000, 2003). Complete 5' untranslated regions could be predicted for all of the lysozyme *c* genes that had exon 1, however the full 3' untranslated regions could not be predicted for all exon 4 sequences, as the 3' end of the 3' untranslated region could not be found for the cow *Lyz*3a and *Lyz*3b genes (see Figure S1). This observation is consistent with an earlier failure to identify homologous sequences for the entire 3' untranslated region of the cow ψNS4 (*Lyz*3b) gene (Irwin, 1995, 2004).

Lysozyme *c* genes in other ruminant genomes

To better characterize the evolutionary history of the ruminant lysozyme *c* genes, we identified lysozyme *c* genes in the genomes of other ruminant species and their close relatives (Table 3 and Figures 3 and S1). As expected, from previous work (Callewaert & Michiels, 2010; Irwin et al, 1989, 1996, 2011; Prager & Jollès, 1996), only a single lysozyme *c* gene was found in the genomes of carnivores (dog, *Canis lupus familiaris*; and panda, *Ailuropoda melanoleuca*) and perrisodactyls (horse, *Equus caballus*; and rhinoceros, *Ceratotherium simum simum*) (Table 3 and Figures 3 and S1). The single lysozyme *c* gene in the outgroup species is located between the *Yeats*4 and *Cpsf*6 genes (Figure 3), as found in most other mammalian species (Irwin et al, 2011). This ancestral mammalian genomic arrangement has been retained in the cow, with the amplification of the lysozyme *c* genes occurring between the *Yeats*4 and *Cpsf*6 genes (Irwin et al, 2011) (Figures 1 and 3). The tylopod lineage (e.g., camels and alpacas) represents one branch of the earliest divergence within artiodactyls (Morgan et al, 2013; Romiguier et al, 2013), with these species being pseudoruminants with a simpler multi-chambered stomach than the true ruminants (Clauss et al, 2010; Janis, 1976; Mackie, 2002). Searches of the alpaca (*Vicugna pacos*) genome in the Ensembl database identified three genomic sequences encoding partial lysozyme *c* gene sequences, indicating that multiple lysozyme *c* genes exist in this genome (results not shown). Searches of the NCBI Genomes (chromosomes) database identified an updated larger genomic contig that predicted 4 complete lysozyme *c* genes (and included all of the gene sequences found in the Ensembl alpaca genome assembly) at one end of a contig sequence (Table 3 and Figure 3). The *Yeats*4 gene was found to be adjacent to one side of the lysozyme *c* gene cluster, however no genes were found on the other side of the lysozyme *c* gene cluster in this genomic contig (Figure 3). The presence of the *Yeats*4 gene adjacent to the alpaca lysozyme *c* genes suggests that a similar genomic neighborhood exists in alpaca, but since the lysozyme *c* genes were at one end of the genomic contig it is possible that additional unsequenced lysozyme *c* genes may exist in the alpaca genome. The pig (*Sus scrofa*) is a representative of the family Suidea, which is the next diverging lineage within artiodactyls (Morgan et al, 2013; Romiguier et al, 2013). As expected, and previously reported (Irwin et al, 1989; Yu & Irwin, 1996), only a single lysozyme gene is found in this species (Table 3, Figures 3 and S1). As previously reported (Irwin et al, 2011), the genomic neighborhood surrounding the pig lysozyme gene differs from that of other mammals, raising the possibility that this genomic area has experienced recombination (Figure 3). Cetaceans (e.g., whales and dolphins) fall within artiodactyls, thus yielding cetartiodactyla (Morgan et al, 2013; Romiguier et al, 2013). A single lysozyme *c* gene was identified in all five cetacean (bottlenose dolphin, *Tursiops truncates*; minke whale, *Balenoptera acutorostrata scammoni*; killer whale, *Orinus orca*; Yangtze river dolphin, *Lipotes vexilllifer*; and sperm whale, *Physeter catodon*) genomes (Table 3 and Figure S1), which is found in genomic location consistent with the ancestral genomic organization (Figure 3).

Pecoran artiodactyls (cow, sheep, deer, and relatives) are true ruminants with a stomach composed of four chambers (Clauss et al, 2010; Janis, 1976; Mackie, 2002). In addition to the sheep (*Ovis aires*) genome (Jiang et al, 2014), which is available from Ensembl, genome sequences of 5 other pecoran ruminant species (yak, *Bos grunniens* (Qiu et al,

Table 3 Locations of lysozyme *c* genes in diverse artiodactyls and relatives

Gene	Chromosome / scaffold	Strand	Bases	Ensembl gene ID / NCBI accession	Missing exons
Yak (*Bos grunniens*)					
Lyz1	NW_005394307	Minus	5 211-9 033	XM_005901148	
Lyz2	NW_005394307	Plus	75 876-81 020	NA[a]	1[b]
Lyz3	NW_005394198	Plus	7 980-12 653	XM_005900299	
Lyz4	NW_005394198	Minus	27 041-32 422	XM_005900300	
Lyz5	NW_005394198	Minus	53 712-61 005	XM_005900301	
Lyz6	NW_005394198	Minus	83 939-90 419	XM_005900302	
Lyz7	NW_005394198	Minus	104 585-108 706	NA[a]	
Lyz8	NW_005392857	Minus	16 134-18 709	NA[a]	2, 3
Lyz9	NW_005392857	Minus	61 437-66 594	XM_005886999	
Lyz10	NW_005394307	Minus	5 211-9 033	XM_005901148	
Zebu (*Bos indicus*)					
Lyz1	AGFL01046860	Minus	920-2 950	NA[a]	3, 4[b]
Lyz2a	AGFL01046876	Plus	10 835-14 065	NA[a]	
Lyz2b	AGFL01046877	Plus	11 353-15 933	NA[a]	
Lyz3	AGFL01046880	Minus	12 055-17 431	NA[a]	
Lyz2c	AGFL01046883	Plus	3 743-8 620	NA[a]	
Lyz4	AGFL01046890	Plus	880-5 642	NA[a]	
Lyz5	AGFL01046890	Minus	19 872-25 024	NA[a]	
Lyz6	AGFL01046892	Minus	13 424-20 718	NA[a]	
Lyz7	AGFL01046895	Minus	668-7 157	NA[a]	
Lyz8	AGFL01046896	Minus	13 855-17 933	NA[a]	
Lyz9	AGFL01046897	Minus	889-1 024	NA[a]	2, 3, 4[b]
Lyz10	AGFL01046900	Minus	2 248-9 934	NA[a]	
	AGFL01046860	Minus	920-2 950	NA[a]	3, 4[b]
Water buffalo (*Bubalus bubalis*)					
Lyz1	NW_005784949	Minus	16 204-27 136	XM_006058377	
Lyz2	NW_005785126	Plus	13 244-16 121	NA[a]	4[b]
Lyz3	NW_005785126	Minus	148 364-153 473	NA[a]	
Lyz4	NW_005785126	Plus	173 780-178 474	XM_006064264	
Lyz5	NW_005785126	Minus	194 055-199 224	XM_006064265	
Lyz6	NW_005785126	Minus	220 532-227 898	XM_006064266	
Lyz7	NW_005785126	Minus	245 385-151 911	XM_006064267	
Lyz8	NW_005785126	Minus	269 603-271 738	NA[a]	
Lyz9	NW_005785126	Minus	283 880-286 454	NA[a]	2, 3
Lyz10	NW_005785126	Minus	323 066-328 240	XM_006064268	
	NW_005784949	Minus	16 204-27 136	XM_006058377	
Tibetan antelope / Chiru (*Pantholops hodgsonii*)					
Lyz1	NW_005806187	Minus	948 632-954 099	XM_005957102	
Lyz2	NW_005806187	Plus	1 005 582-1 010 034	XM_005957103	
Lyz3	NW_005806187	Minus	1 045 148-1 051 559	XM_005957104	
Lyz4	NW_005806187	Plus	1 074 291-1 079 230	NA[a]	2, 3[b]
Lyz5	NW_005811703	Minus	9 411-10 957	XM_005968144	3, 4[b]
Lyz6	NW_005811703	Minus	31 570-36 493	XM_005968125	
Lyz7	NW_005811703	Minus	64 104-69 686	XR_318952	
Lyz8	NW_005811703	Minus	83 106-87 330	NA[a]	
Lyz9	NW_005811703	Minus	102 887-105 253	NA[a]	2, 3
Lyz10	NW_005811703	Minus	168 707-174 027	XM_005968126	
Goat (*Capra hircus*)					
Lyz1	NW_005100667	Minus	6 548 409-6 554 516	XM_005680191	
Lyz2	NW_005100667	Plus	6 607 855-6 612 306	XM_005680189	
Lyz3	NW_005100667	Minus	6 638 119-6 644 658	NA[a]	

Continued

Gene	Chromosome / scaffold	Strand	Bases	Ensembl gene ID / NCBI accession	Missing exons
Lyz4	NW_005100667	Plus	6 670 972-6 67 2304	NA[a]	1, 2[b]
Lyz5	NW_005100667	Minus	6 689 705-6 694 702	XM_005680192	
Lyz6	NW_005100667	Minus	6 715 083-6 719 993	NM_001287566	
Lyz7	NW_005100667	Minus	6 741 973-6 747 565	NA[a]	
Lyz8	NW_005100667	Minus	6 761 023-6 765 243	XM_005680235	
Lyz9	NW_005100667	Minus	6 783 196-6 785 752	NA[a]	2, 3
Lyz10	NW_005100667	Minus	6 834 500-6 839 640	NM_001285711	
Sheep (*Ovis aries*)					
Lyz1	3	Minus	150 165 176-150 170 352	ENSOARG00000020393	
Lyz2	3	Plus	150 225 205-150 229 630	ENSOARG00000020417	
Lyz3	JH921983.1	Minus	4 380-1 032	ENSOARG00000000543	
Lyz4	3	Plus	150 266 228-150 270 937	ENSOARG00000020429	
Lyz5	3	Minus	150 288 480-150 293 529	ENSOARG00000020393	
Lyz6	3	Minus	150 313 875-150 318 810	ENSOARG00000020439	
Lyz7	3	Minus	150 342 914-150 348 498	NA[a]	
Lyz8	3	Minus	150 362 122-150 366 351	ENSOARG00000020476	
Lyz9	3	Minus	150 385 062-150 387 578	NA[a]	2, 3
Lyz10	3	Minus	150 434 372-150 439 510	ENSOARG00000020515	
Pig (*Sus scrofa*)					
Lyz	5	Minus	36 179 949-36 185 488	ENSSSCG00000000492	5
Alpaca (*Vicugna pacos*)					
Lyz1	NT_167289.2	Minus	1 670 090-1 675 333	NA[a]	
Lyz2	NT_167289.2	Minus	1 707 719-1 713 452	NA[a]	
Lyz3	NT_167289.2	Plus	1 722 393-1 728 285	NA[a]	
Lyz4	NT_167289.2	Plus	1 760 703-1 766 608	NA[a]	
Bottlenose dolphin (*Tursiops truncates*)					
Lyz	scaffold_114746	Plus	182 136-187 936	ENSTTRG00000013948	
Minke whale (*Balaenoptera acutorostrata scammoni*)					
Lyz	NW_006733011	Minus	27 704 269-27 709 850	XM_007195043	
Killer whale (*Orcinus orca*)					
Lyz	NW_004438568	Plus	1 319 177-1 324 490	XM_004281877	
Yangtze River dolphin (*Lipotes vexillifer*)					
Lyz	NW_006790307	Minus	1 455 813-1 461 420	XM_007463554	
Sperm whale (*Physeter catodon*)					
Lyz	NW_006716048	Minus	6 880-11 985	XM_007118874	
Dog (*Canis lupus familiaris*)					
Lyz	10	Plus	11 346 500-11 350 639	ENSCAFG00000000426	
Panda (*Ailuropoda melanoleuca*)					
Lyz	GL192893.1	Plus	308 956-313 372	ENSAMEG00000011820	
Horse (*Equus caballus*)					
Lyz	6	Plus	84 276 158-84 280 173	ENSECAG00000018113	
Rhinoceros (*Ceratotherium simum simum*)					
Lyz	JH767750.1	Plus	25 463 742-25 467 903	ENSP00000261267_1	

[a] – Not annotated as a gene in Ensembl or NCBI.

[b] – Possibly missing due to incomplete gene.

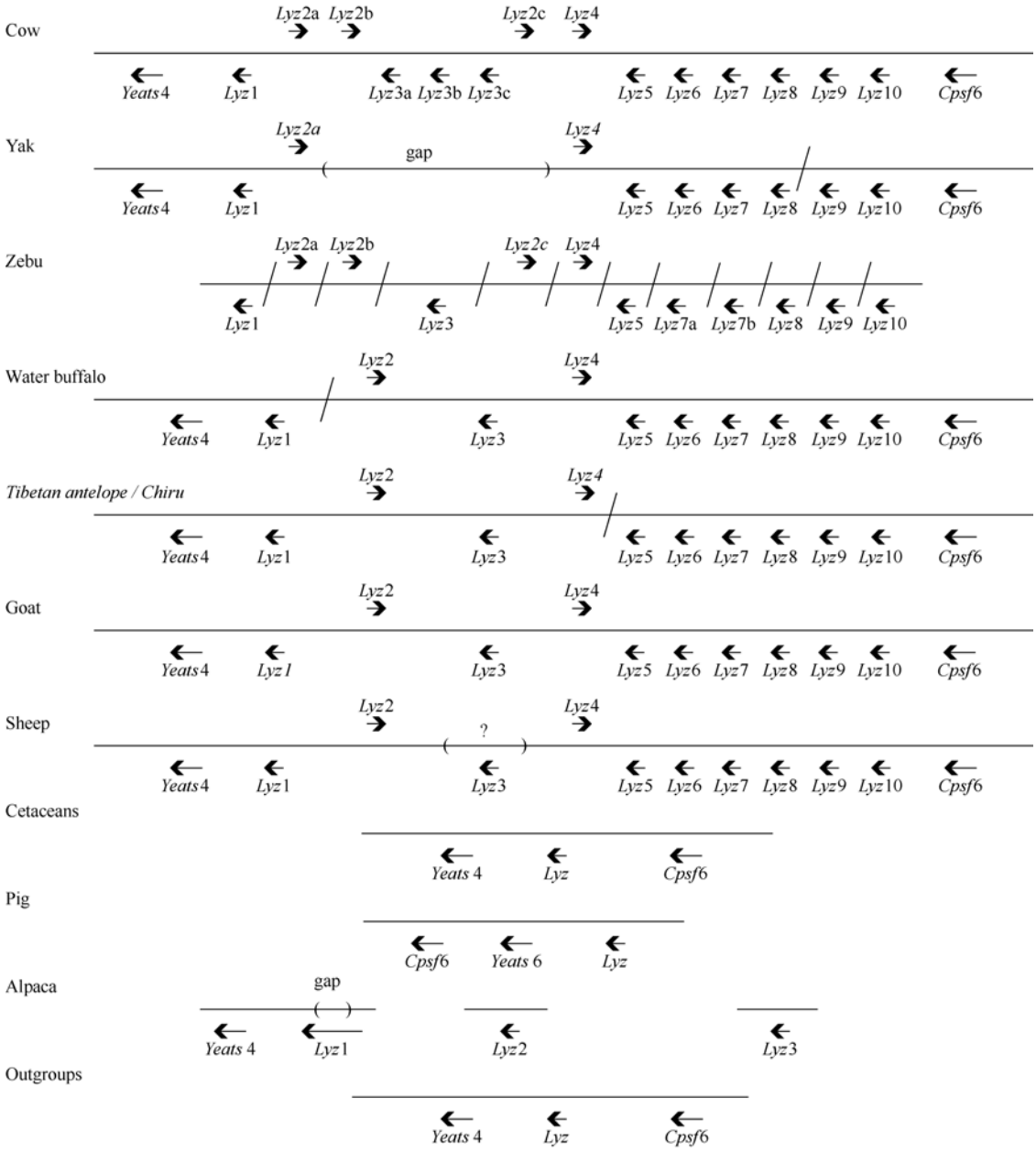

Figure 3 Organization of lysozyme *c* genes in diverse Artiodactyls and relatives

Schematic of the genomic arrangement of lysozyme *c* genes, and their neighbors, derived from genomic sequences in the Ensembl and NCBI databases. Sizes of genes, and distances between genes are not to scale. Genes shown above the lines are encoded by the plus strand, while those below are on the minus strand. Genomic sequences are listed in Table 3.

2012); zebu, *Bos indicus* (Canavez et al, 2012); water buffalo, *Bubalus bubalis*; Tibetan antelope (chiru) (Ge et al, 2013), *Pantholops hodgsonii*; and goat, *Capra hircus* (Dong et al, 2013)) are available in the NCBI database. The genomes of all pecoran ruminant species contained multiple lysozyme *c* genes (Table 3 and Figures 3 and S1), in accord with previous results (Irwin & Wilson, 1989; Irwin et al, 1989, 2011). For most pecoran species, lysozyme *c* genes could be mapped to large genomic contigs, or chromosomes, that show organizations similar to that seen in the cow (Table 3 and Figure 3). In the sheep, one gene (*Lyz*3) was not mapped to chromosome 3, but instead to an unmapped contig (Table 3). Since the goat genes all map to one contig (Table 3) it is possible that the sheep *Lyz*3 gene has been

misplaced (Figure 3), although movement to a new location through recombination cannot be excluded. The yak lysozyme *c* genes map to two contigs, with one containing a large gap that corresponds to the location where one or more missing lysozyme *c* genes might exist (Table 3 and Figure 3). The lysozyme *c* genes in both the Tibetan antelope and water buffalo map to two genomic contigs that might be adjacent in their genomes (Table 3 and Figure 3). Lysozyme *c* genes in the zebu are each on separate contigs, but could be arranged as seen in the cow and other pecoran species (Table 3 and Figure 3).

Mosaic evolutionary histories for exons of cow lysozyme *c* genes

To examine the evolutionary history of the cow lysozyme *c* genes, a phylogeny of the sequences was established. Phylogenetic trees were constructed for each exon of the lysozyme *c* genes (Figure 4) as previous analyses suggested that they might have experienced different histories (Irwin, 2004; Irwin & Wilson, 1990; Irwin et al, 1993, 1996; Wen & Irwin, 1999). As shown in Figure 4, different phylogenies were identified for each exons, with similar trees found if different outgroup species were used or if phylogenies were constructed using distance or parsimony methods or if only synonymous substitutions were used (results not shown). Some consistent phylogenetic patterns were observed across all exons, such as the clustering of the *Lyz*2a, *Lyz*2b, and *Lyz*2c genes and *Lyz*3a or *Lyz*3c being closest to *Lyz*3b (Figure 4). In contrast, the placement of some genes differed greatly between exons, such as the placement of *Lyz*1 or *Lyz*4 (Figure 4). To test whether there were statistically significant differences between the tree topologies estimated by each exon, we used Tree-puzzle (Strimmer & von Haeseler, 1996) to compare the four separate exon tree topologies with data for each exon. Despite the short lengths of some exons, at least two of the three alternative topologies could be excluded by all three of the KH, SH, and ELW statistical tests used by Tree-puzzle, with all three being excluded by at least one of the tests (Table 4). We cannot exclude the possibility that exons 2 and 3 share an identical evolutionary history, as these trees were not excluded by all three of the statistical tests, but exons 1 and 4 have evolutionary histories that are incompatible with each other and with exons 2 and 3 indicating that at least three different histories are represented by these four exons (Table 4). The differences in the topologies are unlikely to be due to convergent evolution acting on the lysozyme *c* protein sequences as the differences in the topologies were also seen when only synonymous differences were examined (results not shown).

Table 4 Phylogenies predicted from different cow lysozyme *c* gene exons are significantly different

Tree/Data	Log L	Difference	*SE*	KH[a]	SH[a]	ELW[a]	
Exon 1 Tree							
Exon 1 Data	–703.05	0.00		1.0000	1.0000	0.9425	BEST
Exon 2 Data	–738.42	35.37	13.1770	0.0080	0.0110	0.0001	EXCLUDED[b]
Exon 3 Data	–722.37	19.32	9.2124	0.0270	0.1170	0.0095	
Exon 4 Data	–733.42	30.37	14.3425	0.0280	0.0320	0.1540	EXCLUDED[b]
Exon 2 Tree							
Exon 1 Data	–844.36	113.94	22.9026	0.0000	0.0000	0.0000	EXCLUDED[b]
Exon 2 Data	–730.42	0.00		1.0000	1.0000	0.9438	BEST
Exon 3 Data	–746.39	15.97	8.3002	0.0400	0.3250	0.0136	
Exon 4 Data	–829.74	99.32	20.0394	0.0000	0.0000	0.0000	EXCLUDED[b]
Exon 3 Tree							
Exon 1 Data	–391.39	59.87	13.7897	0.0000	0.0000	0.0000	EXCLUDED[b]
Exon 2 Data	–343.01	11.49	6.7348	0.0580	0.3190	0.0136	
Exon 3 Data	–331.52	0.00		1.0000	1.0000	0.5948	BEST
Exon 4 Data	–365.58	34.06	13.4375	0.0070	0.0160	0.0002	EXCLUDED[b]
Exon 4 Tree							
Exon 1 Data	–1804.06	95.06	18.8423	0.0000	0.0000	0.0000	EXCLUDEDb
Exon 2 Data	–1780.35	71.35	20.9871	0.0010	0.0020	0.0000	EXCLUDED[b]
Exon 3 Data	–1767.23	58.23	20.2572	0.0020	0.0070	0.0000	EXCLUDED[b]
Exon 4 Data	–1709.00	0.00		1.0000	1.0000	0.9756	BEST

[a] – Probability of observing the tree, given the data, from the statistical one sided KH test based on pairwise SH tests (KH), the Shimodaira-Hasegawa test (SH), and the expected likelihood weight test (ELW) from Tree-puzzle (Strimmer & von Haesler, 1996).

[b] – Probability that the data is compatible with the tree is less than 0.05.

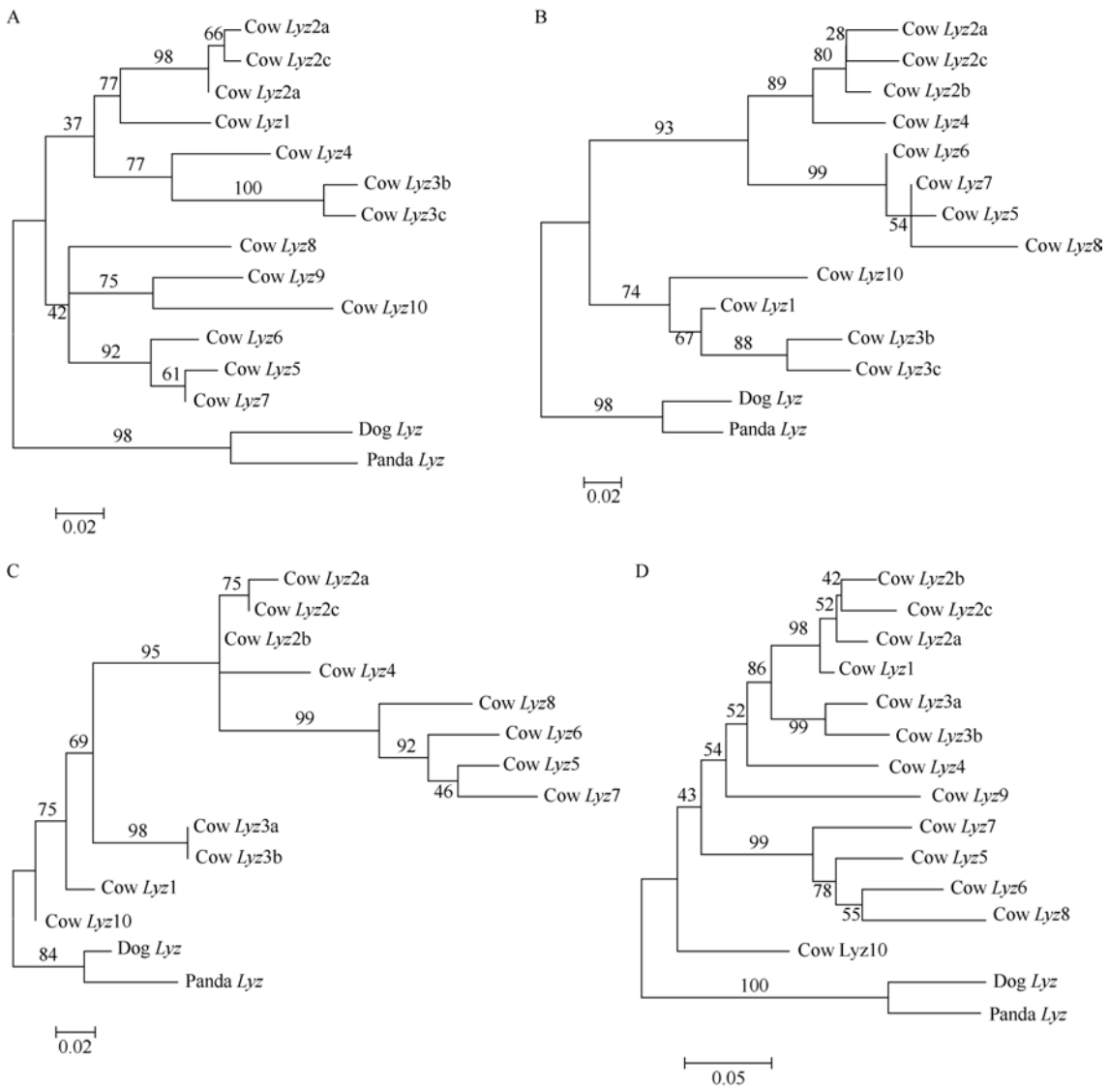

Figure 4 Phylogeny of cow lysozyme *c* genes derive from sequences of (A) exon 1, (B) exon 2, (C) exon 3, and (D) exon 4

Phylogenies for each of the 4 exons of the lysozyme *c* genes were estimated using maximum likelihood, as implemented in Mega6.06 (Tamura et al, 2013), using the Kimura 2-paramater model with a gamma distribution, which was the best fitting model for the sequence data. Similar results were obtained with the neighbor-joining method or parsimony, or the use of different outgroups. Phylogenies were generated from 152, 156, 74, and 306 aligned bases present in all sequences for exons 1, 2, 3, and 4, respectively. The presented phylogenies were bootstrapped 500 times.

These results are in agreement with previous conclusions that lysozyme *c* genes expressed in the abomasum of ruminants have experienced mosaic evolution due to gene conversion occurring between the coding exons (Irwin, 2004; Irwin & Wilson, 1990; Irwin et al, 1993, 1996; Wen & Irwin, 1999), and suggested that the 3' untranslated (exon 4) sequences likely best reflect the evolutionary history of the divergent genes, as this sequence appears to have experienced the fewest number of concerted evolution events.

Origin and evolutionary history of lysozyme *c* genes in ruminant genomes

To better examine the evolution of the duplicated lysozyme *c* genes in ruminant species, a phylogenetic tree was established for the lysozyme *c* sequences from the diverse ruminants (e.g., cow, sheep, and Tibetan antelope) and their close relatives (e.g., pig, cetaceans, and carnivores) (Figure 5). Exon 4 sequences were chosen to construct this phylogeny as they likely best reflect the divergence of the genes, and have experienced lower levels of concerted

evolution (see above). The phylogeny shown in Figure 5 was derived by maximum likelihood, and similar phylogenies were generated when neighbor-joining or parsimony was used (results not shown). The exon 4 phylogeny shown in Figure 5 of the lysozyme *c* genes yield strong evidence for the orthology of 8 of 10 types of lysozyme *c* genes found in ruminants (Figure 5). *Lyz*3, *Lyz*4, *Lyz*5, *Lyz*6, *Lyz*7, *Lyz*8, *Lyz*9, and *Lyz*10 orthology groups each have high (88%-100%) bootstrap support, with the species relationships within each group in general accord with the accepted species relationships (Figure 5). This observation implies that these 8 genes existed in the common ancestor of pecoran ruminants. The phylogenetic analysis did not resolve *Lyz*1 or *Lyz*2 genes as monophyletic groups, but instead suggested some intermixing of these genes (Figure 5). *Lyz*1 and *Lyz*2 sequences from species of tribe Bovine (cow, yak, zebu, and water buffalo) formed a moderately supported monophyletic group that had a primary divergence between the *Lyz*1 and *Lyz*2 sequences. The tribe Bovini *Lyz*1 and *Lyz*2 sequences were then grouped with *Lyz*1 sequences from the other pecoran ruminants (Tibetan antelope, goat and sheep), with the *Lyz*2 sequences from these same species being the outgoup to all of the *Lyz*1 and *Lyz*2 sequences. While it is possible that this distribution could be explained by an ancestor having four genes, and pairs of genes being lost in each species, an alternative explanation is that the pecoran ancestor possessed two genes, and that a concerted evolution event transferred sequences from the tribe Bovini *Lyz*1 exon 4 sequence to the tribe Bovini *Lyz*2 gene, resulting in the grouping of these sequences. Support for the monophyly of the *Lyz*1 and *Lyz*2 genes was found from phylogenies of exon 2 and exon 3 sequences (results not shown). These results suggest that the ancestor of pecoran ruminants possessed 10 lysozyme *c* genes.

While the ancestor of modern pecoran ruminants may have had 10 lysozyme *c* genes, several extant species have a higher number of genes, such as cow with 14 genes and the zebu with 12 genes (Tables 1 and 3). The increased numbers of lysozyme *c* genes in some ruminant species appear to be due to lineage-specific gene duplications. The phylogeny presented in Figure 5 implies lineage-specific duplications in three genes, *Lyz*2, *Lyz*3 and *Lyz*7, all of which occurred in species (cow and zebu) of the genus *Bos*. Both cow and zebu have three *Lyz*2 genes (*Lyz*2a, *Lyz*2b, and *Lyz*2c) (Tables 1 and 3). Only a single *Lyz*2 gene was found in the yak, however a gap in the genome assembly was found at this location (Table 3), thus it is possible that additional *Lyz*2 genes exist in this genome. Better assembly of the *Bos* genome sequences are needed to determine whether the triplicated genes have a single origin, or represent parallel duplication, a conclusion that does have some support from the phylogenetic analysis (Figure 5). Duplicated *Lyz*3 genes were only found in the cow, although the lack of this gene in the yak, potentially due to a gap in the assembly, and the poor assembly of the zebu genome do not rule out the possibility that multiple *Lyz*3 genes exist in these species (Tables 1 and 3). The duplications of the *Lyz*2 and *Lyz*3 genes in *Bos* likely represent products of segmental duplications (Liu et al, 2009; Seo et al, 2013). It is possible that segmental duplications may also exist in other pecoran ruminant species, but were collapsed as single genes during the genome sequence assembly process, and thus the increased numbers seen in the genus *Bos* simple reflect the better cow genome assembly.

The distribution of the numbers of lysozyme *c* genes in the genomes of ruminant species and their close relatives is consistent with an amplification of the lysozyme *c* gene on the lineage leading to true ruminants as previously proposed (Irwin & Wilson, 1989; Irwin et al, 1989, 1992, 2011; Yu & Irwin, 1996). In contrast, our current phylogenetic analysis of the 3' untranslated regions of lysozyme *c* genes suggests that the amplification of these genes was initiated very early in the artiodactyl lineage, before the divergence of the ruminants and tylopod (e.g., alpaca) lineages, and implying that the pig and cetaceans have lost genes, however these early divergences are very poorly supported (Figure 5). Indeed, phylogenetic analysis of exon 1, exon 2, or exon 3 sequences by themselves yielded differing conclusions concerning these earliest duplications, although again, none of these analysis yielded strong conclusions (results not shown). Analysis of larger amounts of genomic sequences (e.g., intronic and flanking sequence) potentially could resolve the order of the earliest divergences of the paralogous lysozyme *c* genes and cetartiodactyl species. While the alpaca has multiple lysozyme *c* genes (Table 3), our phylogenetic analysis suggests that they originated through a parallel series of lineage-specific independent duplications.

Rates of evolution in ruminant lysozyme *c* genes

Duplication of the lysozyme *c* gene on the ruminant lineage has allowed the specialization of gene expression in distinct tissues, such as different chambers of the stomach, and thus evolution of novel gene function (Callewaert & Michiels, 2010; Jiang et al, 2014; Irwin et al, 1992; Irwin, 1995, 2004; Prager & Jollès, 1996). Changes in the function of lysozyme *c* likely leads to changes in the evolutionary constraints acting upon these genes. To examine this issue we calculated the divergence at nonsynonymous and synonymous sites among lysozyme *c* genes, with the results from three divergent representatives of pecoran ruminants (cow, goat, and Tibetan antelope), and between genes in these three species and the single copy lysozyme *c* gene sequences found in pig and horse shown in Table 5 (similar results were seen with the other pecoran ruminant species). The relative rates of nonsynonymous to synonymous substitutions (dn/ds) varied between genes when compared among ruminants, from low values for the *Lyz*5 and *Lyz*6 genes, which imply that they are strongly constrained, to high values for the *Lyz*3 and *Lyz*9 genes, suggesting that there is little constraint on their protein sequences (Table 5). The cow *Lyz*3 and *Lyz*9 genes fail to predict intact open reading frames, suggesting that they are pseudogenes

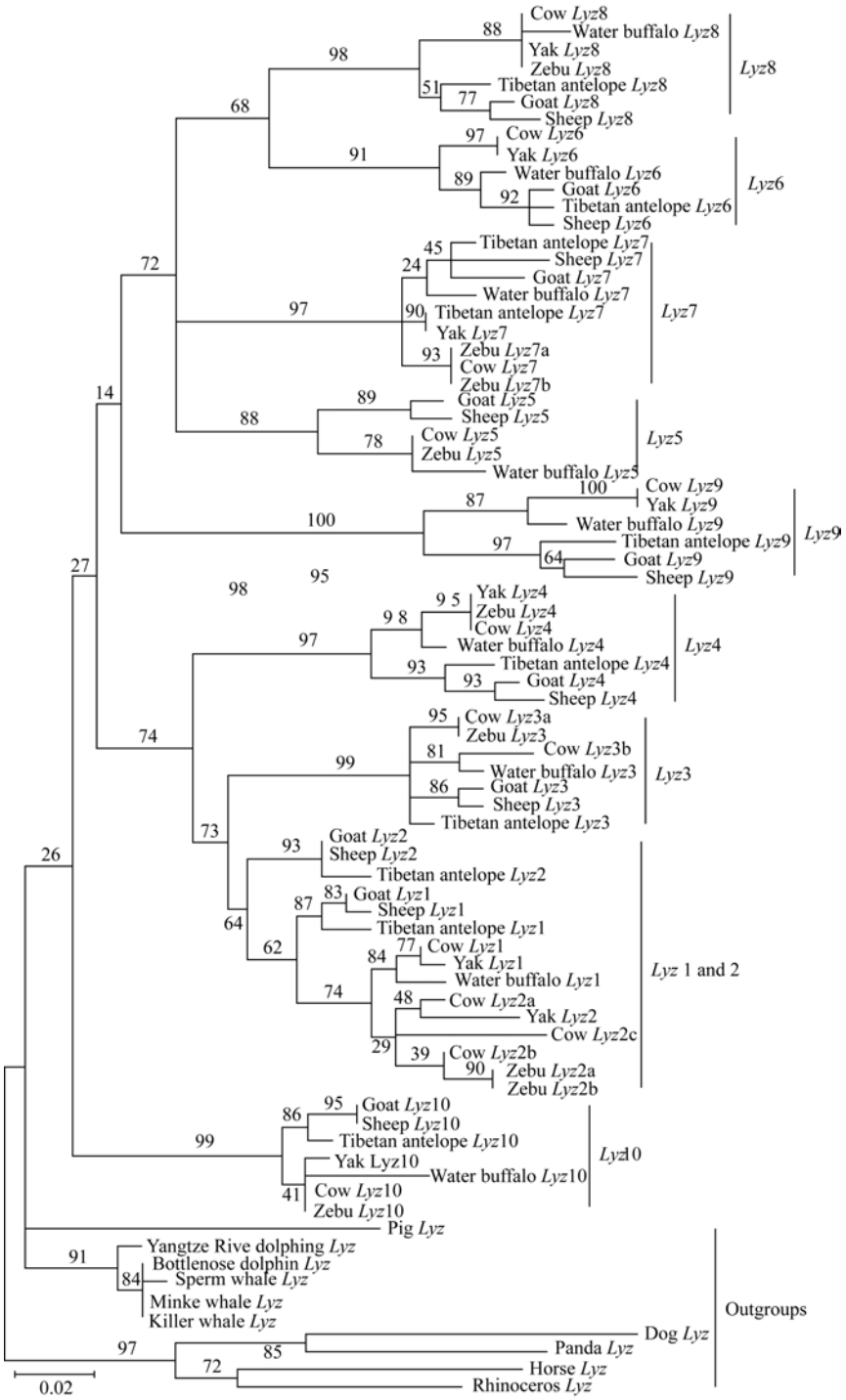

Figure 5 Phylogeny of ruminant lysozyme *c* genes derived from exon 4 sequences of predicted lysozyme *c* genes

The phylogeny of the lysozyme *c* genes was estimated from aligned exon 4 sequences (192 aligned bases in all sequences) using maximum likelihood, as implemented in Mega6.06 (Tamura et al, 2013), using the Kimura 2-paramater model with a gamma distribution, which was the best fitting model for the sequence data. Similar results were obtained with the neighbor-joining method or parsimony. The phylogeny was bootstrapped 500 times. Outgroups used to root the phylogeny are shown at the bottom. The ten types of lysozyme *c* genes are indicated on the right, with the bootstrap values that support 8 of these clades (all except the *Lyz*1 and *Lyz*2 clade) shown in bold.

Table 5 Rates of evolution of ruminant lysozyme *c* genes

	Lyz1			*Lyz2*			*Lyz3*			*Lyz4*[a]			*Lyz5*		
	dn	ds	dn/ds	dn	ds	dn/ds	dn	ds	dn/ds	dn	ds	dn/ds	dn	ds	dn/ds
Cow-Goat	0.026	0.043	0.611	0.052	0.081	0.640	0.073	0.054	1.350	0.031	0.048	0.647	0.022	0.114	0.197
Cow-Tibetan antelope	0.041	0.033	1.234	0.045	0.058	0.767	0.043	0.032	1.340	NA	NA	NA	NA	NA	NA
Goat-Tibetan antelope	0.026	0.043	0.610	0.007	0.066	0.105	0.028	0.021	1.314	NA	NA	NA	NA	NA	NA
Pecora average			0.818			0.504			1.334			0.647			0.197
Pig-Cow	0.184	0.327	0.564	0.246	0.342	0.720	0.268	0.268	0.998	0.230	0.264	0.872	0.224	0.354	0.632
Pig-Goat	0.192	0.317	0.604	0.231	0.318	0.726	0.271	0.259	1.048	NA	NA	NA	NA	NA	NA
Pig-Tibetan antelope	0.193	0.272	0.710	0.233	0.307	0.758	0.254	0.287	0.886	NA	NA	NA	NA	NA	NA
Pig average			0.626			0.735			0.977			0.872			0.632
Horse-Cow	0.099	0.438	0.226	0.180	0.467	0.386	0.129	0.459	0.281	0.193	0.345	0.560	0.197	0.394	0.501
Horse-Goat	0.083	0.451	0.184	0.171	0.441	0.388	0.144	0.379	0.380	NA	NA	NA	NA	NA	NA
Horse-Tibetan antelope	0.101	0.372	0.272	0.171	0.482	0.356	0.127	0.404	0.315	NA	NA	NA	NA	NA	NA
Horse average			0.227			0.377			0.325			0.560			0.501
	Lyz6			*Lyz7*			*Lyz8*			*Lyz9*			*Lyz10*		
	dn	ds	dn/ds	dn	ds	dn/ds	dn	ds	dn/ds	dn	ds	dn/ds	dn	ds	dn/ds
Cow-goat	0.025	0.128	0.195	0.043	0.098	0.441	0.058	0.067	0.867	0.052	0.047	1.097	0.033	0.058	0.573
Cow-Tibetan antelope	0.019	0.073	0.258	0.049	0.078	0.627	0.054	0.083	0.652	0.038	0.031	1.215	0.046	0.072	0.635
Goat-Tibetan antelope	0.025	0.065	0.385	0.049	0.071	0.692	0.023	0.028	0.825	0.029	0.014	1.996	0.012	0.026	0.446
Pecora average			0.279			0.587			0.781			1.436			0.551
Pig-Cow	0.215	0.411	0.523	0.229	0.382	0.599	0.256	0.389	0.658	0.247	0.352	0.701	0.191	0.270	0.708
Pig-Goat	0.238	0.427	0.557	0.278	0.445	0.625	0.265	0.316	0.840	0.272	0.393	0.691	0.187	0.248	0.753
Pig-Tibetan antelope	0.218	0.351	0.621	0.261	0.386	0.677	0.260	0.330	0.788	0.253	0.392	0.645	0.190	0.271	0.700
Pig average			0.567			0.634			0.762			0.679			0.721
Horse-Cow	0.185	0.432	0.429	0.193	0.419	0.461	0.221	0.449	0.491	0.129	0.368	0.349	0.113	0.351	0.323
Horse-Goat	0.204	0.411	0.497	0.227	0.457	0.498	0.241	0.416	0.579	0.169	0.406	0.415	0.101	0.366	0.277
Horse-Tibetan antelope	0.189	0.366	0.516	0.220	0.443	0.498	0.230	0.434	0.531	0.152	0.400	0.380	0.094	0.363	0.259
Horse average			0.481			0.485			0.534			0.381			0.286

[a] – Sheep *Lyz*4 used to replace the incomplete goat *Lyz*4 for comparisons.

(Table 1 and Figure 2) and thus should have no evolutionary constraints on their protein sequences.

The cow genome contains three *Lyz*3-like genes, with only one being a full-length gene sequence (*Lyz*3b), and a single copy of this gene was found in most of the other pecoran ruminant species (Tables 1 and 3). Cow *Lyz*3b gene was previously identified as the cow lysozyme *c* pseudogene NS4 (Irwin, 1995, 2004). While the *Lyz*3 gene sequences from tribe Bovini (cow, zebu and water buffalo) all share a frame shift mutation in exon 3 (amino acid residue 100 in Figure 2), which would prevent translation of a functional product, and additional mutations that potentially disrupt functions found in some sequences at other locations, the sequences from sheep, goat, and Tibetan antelope all predict a full-length open reading frame (Figure S1). This observation might suggest that the *Lyz*3 gene became a pseudogene, due to a frame-shifting mutation, on the lineage leading to tribe Bovini, after divergence from the other pecoran ruminant lineages. However, a high rate of nonsynonymous substitutions is also observed between the goat and Tibetan antelope *Lyz*3 gene sequences (Table 5) and between the sheep and both the goat and Tibetan antelope sequences (results not shown) suggesting that few evolutionary constraints were acting on this sequence and that this gene may have been non-functional in the common ancestor of all pecoran ruminants. It is possible that a mutation that prevented expression, or an amino acid substation that that prevented function, rather than a mutation that prevents translation of an intact product, was the initial mutation that created this pseudogene.

The second gene with a very high dn/ds ratio is the *Lyz*9 gene, which is composed of only 2 exons, exons 1 and 4, in the cow, due to the loss of exons 2 and 3 (Table 1 and

Figure 2). Orthologs of the *Lyz*9 genes in other pecoran ruminant species also have similar gene structures (Tables 1 and 3 and Figure S1), suggesting that this structure exited in the Lyz9 gene in the ancestor of all pecoran ruminants. The loss of exon 2 and 3 sequences from *Lyz*9 prevents the translation of a functional lysozyme, thus it can be concluded that this pseudogene originated before the radiation of the pecoran ruminants. Consistent with this conclusion, a high rate of divergence at nonsynonymous sites is observed in the *Lyz*9 gene sequence among all pecoran ruminant species (Table 5 and results not shown).

The *Lyz*3 and *Lyz*9 genes account for 4 of the five predicted lysozyme *c* pseudogenes in the cow genome (Table 1 and Figure 2). In addition to a pair of inframe stop codons (located between amino acid residues 24 and 25, and residue 26, Figure 2), the initiation codon for the cow *Lyz*8 gene is valine rather than methionine (amino acid -18 in Figure 2 and Figure S1). Orthologs of the *Lyz*8 gene from members of the tribe Bovini (yak, zebu, and water buffalo) share the inframe stop codons, as well other mutations such as a 9 base deletion in exon 2 (3 codons – residues 66-68 in Figure 2), while *Lyz*8 sequences from other pecoran species (sheep, goat and Tibetan antelope) do not possess any obvious harmful amino acid substitution, other than the valine substitution at the initiation codon (Figure S1). In contrast to the *Lyz*3 and *Lyz*9 pseudogenes, a much lower dn/ds ratio was observed in the pairwise comparisons among cow, goat, and Tibetan antelope (Table 5), which would be consistent with functional constraints acting on some, but not necessarily all, of the Lyz8 protein sequences. These observations appear to suggest, that despite the replacement of the initiator methionine with valine, the Lyz8 protein sequences in the sheep, goat and Tibetan antelope is functional, while a mutation occurred on the lineage leading to tribe Bovini to producing the *Lyz*8 pseudogene. How a functional protein can be translated from the *Lyz*8 gene, or evolutionary constraints that mirror protein function, is unclear. A downstream ATG, at codon 85 of the mature protein sequence (Figure 2), would be predicted to yield a protein of only 45 amino acid residues, far shorter than the typical 145 amino acid long protein lysozyme *c* precursor, with most of the sequence not being translated and thus not under evolutionary constraint for protein function.

Episodic evolution of ruminant lysozyme *c* genes

The cow lysozyme *c* genes displaying the lowest dn/ds ratios among ruminant species, and thus implying the strongest evolutionary constraints, are the *Lyz*5 and *Lyz*6 genes (Table 5), which are expressed in the abomasum (Table 1). Lysozyme *c* genes expressed predominantly in non-stomach tissues (Irwin, 2004), such as *Lyz*1, in milk, *Lyz*2, in the trachea, and *Lyz*10, in macrophages, have intermediate dn/ds ratios, but ratios that lower than those seen for the *Lyz*3, *Lyz*8, and *Lyz*9 pseudogenes (Table 5). However, when the dn/ds ratios are calculated between the ruminant genes (cow, goat, and Tibetan antelope) and an outgroup sequence (pig or horse), the stomach expressed *Lyz*5 and *Lyz*6 genes are seen to have dn/ds ratios that are either similar (when pig is the outgroup) or higher (horse being the outgroup) than those seen for the non-stomach (*Lyz*1, *Lyz*2, and *Lyz*10) genes (Table 5). To obtain this pattern of results, these observations suggest that the dn/ds ratio on the common ancestral lineage leading to the ruminants, after divergence from pig or horse, but before radiation of the pecoran ruminants, was higher for the lysozyme *c* genes expressed in the abomasum (*Lyz*5 and *Lyz*6) than for those expressed in non-stomach tissues (*Lyz*1, *Lyz*2, and *Lyz*10). This suggests that the rates of evolution of lysozyme *c* genes expressed in the abomasum display an episodic pattern, with more rapid evolution on the early ruminant lineage, and a slower rate within the pecoran ruminants. These results are consistent with previous findings of accelerated evolution of lysozyme *c* protein sequences obtained from the abomasum of ruminant species (Jollès et al, 1989; Irwin & Wilson, 1990; Irwin et al, 1992, 1993).

CONCLUSIONS

Genome sequences have advanced our understanding of the evolution of the lysozyme *c* gene family in ruminant species. Genomic sequences from seven divergent pecoran ruminant species allowed us to demonstrate that the genome of the pecoran ruminant common ancestor possessed at least 10 lysozyme *c* genes, and that these genes have largely been retained by extant ruminant species. More recent gene duplication, likely via segmental duplications (Liu et al, 2009; Seo et al, 2013), have resulted in increases in the number of lysozyme *c* genes on some lineages, with 14 genes found in the cow, but we can not exclude the possibility that some duplications may have been missed during assembly of some genomes. Lysozyme *c* genes have not evolved in a simple divergent manner, but rather by concerted evolution acting independently on each exon, yielding differing phylogenetic relationships for the ten types of lysozyme *c* genes. Some lysozyme *c* genes have become pseudogenes, either due to mutations in their coding sequence (e.g., *Lyz*3 and *Lyz*8) or by deletion of exon sequences (e.g., *Lyz*9). Some pseudogenes may have been generated by incomplete duplication of genes, such as *Lyz*3a and *Lyz*3c in the cow. Despite being presumably non-functional, at least two pseudogenes that exited in the ancestral pecoran ruminant (*Lyz*3 and *Lyz*9) have been retained in diverse ruminant species. A third lysozyme *c* gene has its initiation codon mutated to valine (from methionine), yet shows evidence that its coding sequence is evolutionary constrained on some ruminant lineages. This suggests that some lysozyme *c* pseudogenes may retain biological functions, however, how protein function in this sequence is maintained is unclear. Changes in the rates of nonsynonymous substitutions suggest that changes have occurred in the functional constraints acting on lysozyme *c* protein sequences, and these changes have occurred in an episodic fashion.

ACKNOWLEDGEMENTS

I thank the editor and two reviewers for helpful comments that have improved the manuscript.

REFERENCES

Altschul SF, Gish W, Miller W, Myers EW, Lipman DJ. 1990. Basic local alignment search tool. *Journal of Molecular Biology,* **215**(3): 403-410.

Callewaert L, Michiels CW. 2010. Lysozymes in the animal kingdom. *Journal of Biosciences,* **35**(1): 127-160.

Canavez FC, Luche DD, Stothard P, Leite KR, Sousa-Canavez JM, Plastow G, Meidanis J, Souza MA, Feijao P, Moore SS, Camara-Lopes LH. 2012. Genome sequence and assembly of *Bos indicus*. *Journal of Heredity,* **103**(3): 342-348.

Clauss M, Hume ID, Hummel J. 2010. Evolutionary adaptations of ruminants and their potential relevance for modern production systems. *Animal,* **4**(7): 979-992.

Dobson DE, Prager EM, Wilson AC. 1984. Stomach lysozymes of ruminants. I. Distribution and catalytic properties. *Journal of Biological Chemistry,* **259**(18): 11607-11616.

Dong Y, Xie M, Jiang Y, Xiao NQ, Du XY, Zhang WG, Tosser-Klopp G, Wang JH, Yang S, Liang J, Chen WB, Chen J, Zeng P, Hou Y, Bian C, Pan SK, Li YX, Liu X, Wang WL, Servin B, Sayre B, Zhu B, Sweeney D, Moore R, Nie W, Shen Y, Zhao R, Zhang G, Li J, Faraut T, Womack J, Zhang Y, Kijas J, Cockett N, Xu X, Zhao S, Wang J, Wang W. 2013. Sequencing and automated whole-genome optical mapping of the genome of a domestic goat (*Capra hircus*). *Nature Biotechnology,* **31**(2): 135-141.

Edgar RC. 2004. MUSCLE: multiple sequence alignment with high accuracy and high throughput. *Nucleic Acids Research,* **32**(5): 1792-1797.

Gallagher DS Jr, Threadgill DW, Ryan AM, Womack JE, Irwin DM. 1993. Physical mapping of the lysozyme gene family in cattle. *Mammalian Genome,* **4**(7): 368-373.

Ge RL, Cai Q, Shen YY, San A, Ma L, Zhang Y, Yi X, Chen Y, Yang L, Huang Y, He R, Hui Y, Hao M, Li Y, Wang B, Ou X, Xu J, Zhang Y, Wu K, Geng C, Zhou W, Zhou T, Irwin DM, Yang Y, Ying L, Bao H, Kim J, Larkin DM, Ma J, Lewin HA, Xing J, Platt RN 2nd, Ray DA, Auvil L, Capitanu B, Zhang X, Zhang G, Murphy RW, Wang J, Zhang YP, Wang J. 2013. Draft genome sequence of the Tibetan antelope. *Nature Communications,* **4**: 1858.

Irwin DM. 1995. Evolution of the bovine lysozyme gene family: changes in gene expression and reversion of function. *Journal of Molecular Evolution,* **41**(3): 299-312.

Irwin DM. 1996. Molecular evolution of ruminant lysozymes. *In*: Jollès P. Lysozymes: Model Enzymes in Biochemistry and Molecular Biology. Basel: Birkhäuser Verlag, 347-361.

Irwin DM. 2004. Evolution of cow nonstomach lysozyme genes. *Genome,* **47**(6): 1082-1090.

Irwin DM, Wilson AC. 1989. Multiple cDNA sequences and the evolution of bovine stomach lysozyme. *Journal of Biological Chemistry,* **264**(19): 11387-11393.

Irwin DM, Wilson AC. 1990. Concerted evolution of ruminant stomach lysozymes. Characterization of lysozyme cDNA clones from sheep and deer. *Journal of Biological Chemistry,* **265**(9): 4944-4952.

Irwin DM, Sidow A, White RT, Wilson AC. 1989. Multiple genes for ruminant lysozymes. *In*: Smith-Gill SJ, Sercarz EE. The Immune Response to Structurally Defined Proteins. NY: Adenine Press, 73-85.

Irwin DM, Prager EM, Wilson AC. 1992. Evolutionary genetics of ruminant lysozymes. *Animal Genetics,* **23**(3): 193-202.

Irwin DM, White RT, Wilson AC. 1993. Characterization of the cow stomach lysozyme genes: repetitive DNA and concerted evolution. *Journal of Molecular Evolution,* **37**(4): 355-366.

Irwin DM, Yu M, Wen Y. 1996. Isolation and characterization of vertebrate lysozyme genes. *In*: Jollès P. Lysozymes: Model Enzymes in Biochemistry and Molecular Biology. Basel: Birkhäuser Verlag, 225-241.

Irwin DM, Biegel JM, Stewart CB. 2011. Evolution of the mammalian lysozyme gene family. *BMC Evolutionary Biology,* **11**: 166.

Janis C. 1976. The evolutionary strategy of Equidae and the origins of rumen and cecal digestion. *Evolution,* **30**(4): 757-774.

Jiang Y, Xie M, Chen W, Talbot R, Maddox JF, Faraut T, Wu C, Muzny DM, Li Y, Zhang W, Stanton JA, Brauning R, Barris WC, Hourlier T, Aken BL, Searle SM, Adelson DL, Bian C, Cam GR, Chen Y, Cheng S, DeSilva U, Dixen K, Dong Y, Fan G, Franklin IR, Fu S, Fuentes-Utrilla P, Guan R, Highland MA, Holder ME, Huang G, Ingham AB, Jhangiani SN, Kalra D, Kovar CL, Lee SL, Liu W, Liu X, Lu C, Lü T, Mathew T, McWilliam S, Menzies M, Pan S, Robelin D, Servin B, Townley D, Wang W, Wei B, White SN, Yang X, Ye C, Yue Y, Zeng P, Zhou Q, Hansen JB, Kristiansen K, Gibbs RA, Flicek P, Warkup CC, Jones HE, Oddy VH, Nicholas FW, McEwan JC, Kijas JW, Wang J, Worley KC, Archibald AL, Cockett N, Xu X, Wang W, Dalrymple BP. 2014. The sheep genome illuminates biology of the rumen and lipid metabolism. *Science,* **344**(6188): 1168-1173.

Jollès J, Jollès P, Bowman BH, Prager EM, Stewart CB, Wilson AC. 1989. Episodic evolution in the stomach lysozymes of ruminants. *Journal of Molecular Evolution,* **28**(6): 528-535.

Kornegay JR, Schilling JW, Wilson AC. 1994. Molecular adaptation of a leaf-eating bird: stomach lysozyme of the hoatzin. *Molecular Biology and Evolution,* **11**(6): 921-928.

Kornegay JR. 1996. Molecular genetics and evolution of stomach and nonstomach lysozymes in the hoatzin. *Journal of Molecular Evolution,* **42**(6): 676-684.

Liu GE, Ventura M, Cellamare A, Chen L, Cheng Z, Zhu B, Li C, Song J, Eichler EE. 2009. Analysis of recent segmental duplications in the bovine genome. *BMC Genomics,* **10**: 571.

Mackie RI. 2002. Mutualistic fermentative digestion in the gastrointestinal tract: diversity and evolution. *Integrative and Comparative Biology,* **42**(2): 319-326.

Morgan CC, Foster PG, Webb AE, Pisani D, McInerney JO, O'Connell MJ. 2013. Heterogeneous models place the root of the placental mammal phylogeny. *Molecular Biology and Evolution,* **30**(9): 2145-2156.

Néron B, Ménager H, Maufrais C, Joly N, Maupetit J, Letort S, Carrere S, Tuffery P, Letondal C. 2009. Mobyle: a new full web bioinformatics framework. *Bioinformatics,* **25**(22): 3005-3011.

Prager EM. 1996. Adaptive evolution of lysozyme: changes in amino acid sequence, regulation of expression and gene number. *In*: Jollès P. Lysozymes: Model Enzymes in Biochemistry and Molecular Biology. Basel: Birkhäuser Verlag, 323-345.

Prager EM, Jollès P. 1996. Animal lysozymes *c* and *g*: an overview. *In*:

Jollès P. Lysozymes: Model Enzymes in Biochemistry and Molecular Biology. Basel: Birkhäuser Verlag, 9-31.

Qiu Q, Zhang GJ, Ma T, Qian WB, Wang JY, Ye ZQ, Cao CC, Hu QJ, Kim J, Larkin DM, Auvil L, Capitanu B, Ma J, Lewin HA, Qian XJ, Lang YS, Zhou R, Wang LZ, Wang K, Xia JQ, Liao SG, Pan SK, Lu X, Hou HL, Wang Y, Zang XT, Yin Y, Ma H, Zhang J, Wang ZF, Zhang YM, Zhang DW, Yonezawa T, Hasegawa M, Zhong Y, Liu WB, Zhang Y, Huang ZY, Zhang SX, Long RJ, Yang HM, Wang J, Lenstra JA, Cooper DN, Wu Y, Wang J, Shi P, Wang J, Liu JQ. 2012. The yak genome and adaptation to life at high altitude. *Nature Genetics,* **44**(8): 946-949.

Romiguier J, Ranwez V, Delsuc F, Galtier N, Douzery EJ. 2013. Less is more in mammalian phylogenomics: AT-rich genes minimize tree conflicts and unravel the root of placental mammals. *Molecular Biology and Evolution,* **30**(9): 2134-2144.

Schwartz S, Zhang Z, Frazer KA, Smit A, Riemer C, Bouck J, Gibbs R, Hardison R, Miller W. 2000. PipMaker--a web server for aligning two genomic DNA sequences. *Genome Research,* **10**(4): 577-586.

Schwartz S, Elnitski L, Li M, Weirauch M, Riemer C, Smit A; NISC Comparative Sequencing Program, Green ED, Hardison RC, Miller W. 2003. MultiPipMaker and supporting tools: Alignments and analysis of multiple genomic DNA sequences. *Nucleic Acids Research,* **31**(13): 3518-3524.

Seo S, Larkin DM, Loor JJ. 2013. Cattle genomics and its implications for future nutritional strategies for dairy cattle. *Animal,* **7**(S1): 172-183.

Short ML, Nickel J, Schmitz A, Renkawitz R. 1996. Lysozyme gene expression and regulation. *In*: Jollès P. Lysozymes: Model Enzymes in Biochemistry and Molecular Biology. Basel: Birkhäuser Verlag, 243-257.

Stevens CE, Hume ID. 1998. Contributions of microbes in vertebrate gastrointestinal tract to production and conservation of nutrients. *Physiological Reviews,* **78**(2): 393-427.

Stewart CB, Wilson AC. 1987. Sequence convergence and functional adaptation of stomach lysozymes from foregut fermenters. *Cold Spring Harbor Symposium on Quantitative Biology,* **52**: 891-899.

Stewart CB, Schilling JW, Wilson AC. 1987. Adaptive evolution in the stomach lysozymes of foregut fermenters. *Nature,* **330**(6146): 401-404.

Strimmer K, von Haeseler A. 1996. Quartet puzzling: A quartet maximum likelihood method for reconstructing tree topologies. *Molecular Biology and Evolution,* **13**(7): 964-969.

Swanson KW, Irwin DM, Wilson AC. 1991. Stomach lysozyme gene of the langur monkey: tests for convergence and positive selection. *Journal of Molecular Evolution,* **33**(5): 418-425.

Takeuchi K, Irwin DM, Gallup M, Shinbrot E, Kai H, Stewart CB, Basbaum C. 1993. Multiple cDNA sequences of bovine tracheal lysozyme. *Journal of Biological Chemistry*, **268**(36): 27440-27446.

Tamura K, Stecher G, Peterson D, Filipski A, Kumar S. 2013. MEGA6: Molecular evolutionary genetics analysis version 6.0. *Molecular Biology and Evolution,* **30**(12): 2725-2729.

Wen Y, Irwin DM. 1999. Mosaic evolution of ruminant stomach lysozyme genes. *Molecular Phylogenetics and Evolution,* **13**(3): 474-482.

Yu M, Irwin DM. 1996. Evolution of stomach lysozyme: the pig lysozyme gene. *Molecular Phylogenetics and Evolution,* **5**(2): 298-308.

Zimin AV, Delcher AL, Florea L, Kelley DR, Schatz MC, Puiu D, Hanrahan F, Pertea G, Van Tassell CP, Sonstegard TS, Marçais G, Roberts M, Subramanian P, Yorke JA, Salzberg SL. 2009. A whole-genome assembly of the domestic cow, *Bos taurus*. *Genome Biology,* **10**(4): R42.

The coexistence of seven sympatric fulvettas in Ailao Mountains, Ejia Town, Yunnan Province

Ji XIA[1,2,#], Fei WU[1,#], Wan-Zhao HU[1,2], Jian-Ling FANG[3], Xiao-Jun YANG[1,*]

[1]*State Key Laboratory of Genetic Resources and Evolution*, *Kunming Institute of Zoology*, *Chinese Academy of Sciences*, *Kunming, Yunnan* 650223, *China*

[2]*University of Chinese Academy of Sciences*, *Beijing* 100049, *China*

[3]*Shuangbai Ailaoshan Nature Reserve Management Bureau*, *Shuangbai*, *Yunnan* 675107, *China*

ABSTRACT

The coexistence of ecologically similar species sharing sympatric areas is a central issue of community ecology. Niche differentiation is required at least in one dimension to avoid competitive exclusion. From 2012-2014, by adopting the methods of mist-nets and point counts to evaluate spatial niche partitioning and morphological differentiations, we explored the coexistence mechanisms of seven sympatric fulvettas in Ailao Mountains, Ejia town, Yunnan Province, China. The microhabitats of these seven fulvettas were significantly different in elevation, roost site height and vegetation coverage, indicating a spatial niche segregation in different levels. Approximately, 90.30% of the samples were correctly classified by linear discriminant analysis (LDA) with correct rates at 91.20%-100%, except the White-browed fulvetta (*Alcippe vinipectus*) (65.4%) and the Streak-throated fulvetta (*A. cinereiceps*) (74.6%). The seven fulvettas were classified into four guilds based on their specific morphological characters, suggesting that the species in each guild use their unique feeding ways to realize resource partitioning in the overlapped areas. These finding indicate that through multi-dimensional spatial niche segregation and divergence in resource utilizing, the inter-specific competition among these seven fulvettas is minimized, whereas, coexistence is promoted.

Keywords: Fulvettas;Coexistence;Niche segregation; Ailao Mountains

INTRODUCTION

The competition and coexistence of ecologically similar species sharing sympatric areas is one of the hot topics in community ecology (Macarthur, 1958). According to the competitive exclusion principle, to reduce inter-specific competition, niche segregation is required at least in one dimension among sympatric congeners (Bagchi et al, 2003; Denoël et al, 2004; Munday et al, 2001; Schoener, 1974; Tschapka, 2004). The differentiation in resource use can be taken as a standard to judge niche partitioning (Fox, 2004; Svenning, 1999). Lots of studies have shown that niche partitioning was principally along three dimensions: time, space and diet (Chesson, 2000; Davies et al, 2007; Martínez-Freiría et al, 2010; Schoener, 1974). Temporal partitioning includes daily (Di Bitetti et al, 2009; Lara et al, 2011; Lucherini et al, 2009) or seasonal differences (Martínez-Freiría et al, 2010; Schuett et al, 2005) in animals' activity patterns. Spatial partitioning includes differences in habitat selection (Chiang et al, 2012; Quillfeldt et al, 2013) or in microhabitat utilization (Langkilde & Shine, 2004; Vidus-Rosin et al, 2012). Trophic partitioning includes differences in prey size (Kaifu et al, 2013) or prey type (Ward-Campbell et al, 2005). Niche segregation may occur along either some combination of these dimensions or just upon one of them (Loveridge & Macdonald, 2003). Furthermore, niche segregation could be related to species' morphology (Gustafsson, 1988) because different morphological characteristics may result in different behaviors (Miles et al, 1987) and different behaviors allow animals to partition the limited resources in different ways, hence reduce the inter-specific competitive interactions (Guillemain et al, 2002). Therefore, it is necessary to evaluate the influences of various factors in different ways as well as at different scales when exploring the mechanisms of animals'

Received: 02 July 2014; Accepted: 25 September 2014

Foundation items: This project was supported by the National Natural Science Foundation of China (Y201011041), the National Science and Technology Basic Project of the Ministry of Science and Technology of China (2008FY110300) and the Natural Science Foundation of Yunnan Province (Y103841101)

[*]Corresponding author, E-mail: yangxj@mail.kiz.ac.cn

[#]Authors contributed equally to this work

DOI:10.13918/j.issn.2095-8137.2015.1.18

coexistence (Li et al, 2013).

Closely related species usually have similar ecological characteristics and occupy similar ecological niches. When they contact, the inter-specific competition may arouse (Wiens & Graham, 2005). Studies on the sympatric congeners of birds in China were focused on species such as pheasants (Cui et al, 2008; Li et al, 2006), herons (Wen et al, 1998; Ye et al, 2006; Zhu et al, 1998), tits (Gao & Yang, 1991; Liu et al, 1989; Yang et al, 2012), woodpeckers (Gao et al, 1997), larks (Zhao & Zhang, 2004) and prinias (Zhou & Fang, 2000), but never on fulvettas. Alcippe is a group of Timaliidae includes 18 species worldwide (Zheng, 2002) with 15 of them distributing in China (Zheng, 2011) and 12 of them in Yunnan Province, in specific (Yang & Yang, 2004). The range of body length in fulvettas is 11-15 cm. Different species of fulvettas have similar morphology, plumage color and stripes and sexual differences are difficult to distinguish morphologically. They inhabit the undergrowth in broadleaf forests, mixed coniferous broad-leaved forests, bamboo groves, scrubs and brambles and feed on animal-based food, such as insects, caterpillars and mollusks, but sometimes on plant food (Yang & Yang, 2004). The Golden-breasted Fulvetta (*Alcippe chrysotis*), Rufous-winged Fulvetta (*A. castaneceps*), White-browed Fulvetta (*A. vinipectus*), Spectacled Fulvetta (*A. ruficapilla*), Streak-throated Fulvetta (*A. cinereiceps*), Rusty-capped Fulvetta (*A. dubia*) and Grey-cheeked Fulvetta (*A. morrisonia*) are the seven species of fulvettas coexisting in Ailao Mountains, Ejia town, Yunnan Province, China, which are excellent subjects in the study on coexistence mechanisms of sympatric congeners. In this study, we aim to: (1) understand the coexistence mechanisms of these fulvettas through exploring their spatial niche partitioning and morphological differentiation; (2) test the niche theory on animal communities in the subtropical mountain forest; and (3) discuss the necessity to evaluate the influences of various factors in different ways as well as at different scales when exploring the coexistence mechanisms of sympatric congeners.

MATERIALS AND METHODS

Study area

The study site consisted of two adjacent areas, the Ailaoshan National Nature Reserve and Konglong River Nature Reserve, was located in the steep (30°- 40°, or even 60°) eastern slope (800-2 800 m a.s.l.) of north central of Ailao Mountains, Ejia Town, Yunnan Province (Chen & Ye, 1988; Liu et al, 1988; Wu & Yang, 2008). Because of the west monsoon climate, annual temperature differences are small, whereas, daily temperature differences are large. The large elevation gradients also lead to the vertical climatic spectrum. The radiation, rainfall, temperature and forest types are all featured with obvious vertical variations (Wang et al, 1988). Four major forest types from low to high elevation are observed: (1) savanna shrub and grass; (2) dry evergreen broadleaved forest; (3) semi-moist evergreen broadleaved forest and Burma pine (*Pinus yunnanensis*) forest; and (4) moist evergreen broadleaved forest. However, most of the original vegetation in lower elevations have been destroyed or replaced by cultivated land and villages due to long-term human disturbance (Liu et al, 1988).

Birds sampling

Fieldwork was conducted during breeding seasons and winters of 2012-2014. Mist-nets work best in field survey because fulvettas inhabit the undergrowth (Bibby et al, 1998). Point counts are effective in species survey and in montane forest bird community survey (Wu et al, 2010). Mist-nets combined with point counts will offset the weakness of each other, and provide a more accurate survey result (Pagen et al, 2002; Rappole et al, 1998). Birds inhibit in lower elevations start to reproduce earlier due to the higher temperature there. So, in breeding seasons, the fieldwork was carried out from valley to montane crest, whereas, in winters, the order was inversed.

We divided the study area into 10 units along elevation gradients with each unit containing a 200 m elevation differences. Ten mist-nets of the same specification (12 m×2.5 m, 36 mm mesh) were set up symmetrically in each unit. Due to the rugged terrain and limited access, it was difficult to set up each mist-net with 20 m elevation differences exactly. When different habitat types occurred in one unit, mist-nets were set up in each different habitat proportionally. The location, elevation and working time were recorded by GPS (NAVA 100) and the habitat type as well as environment information were also recorded meanwhile. We chose a rectangular patch (with the diagonal of 20 m×20 m) around the mist-net to estimate vegetation coverage. Observers walked along the diagonal of the rectangular patch to record the vegetation (tree, shrub and herb) of every 1 m. At each point of 1 m, if vegetations were found, then it was recorded as 1, while, if not, it was 0. Then the vegetation coverage of each type (tree, shrub and herb) was estimated according to the percentages of the vegetations recorded at all points. Mist-nets were kept open for 3 days and were remained closed during raining. We checked each mist-net hourly during the day and marked each captured individual with metal ring. Time, species and numbers of birds were recorded. Body weight (BW) was measured by an electronic balance (DIAMOND, precision=0.1 g) and other morphological characteristics such as body length (BL), wing length (WL), tail length (TL), tarsus-metatarsus length (TML), claw length (CLL), finger length (FL) and culmen length (CUL) were recorded by a vernier caliper (precision=0.05 mm) according to Zheng (1995). All the juveniles or certain species with too small sampling size were excluded from measuring.

Unlimited radius point counts were conducted in our study and the points were established on either pre-existing trails or low traffic volume roads along the elevation gradient in each unit. The points were systematically 200 m apart in a three-dimensional space. Surveys were conducted during the peak period of birds' activities from sunrise to 4 h after sunrise. We used GPS receiver (NAVA 100) to record the location of each point. There were 160 points in total in our study area and each count lasted for 10 min. During this period, we used

binoculars (Eagle 8×40) to observe birds and the indentified ones were recorded (Table 1).

Table 1 Information recorded by point counts

Items	Details
Distance	Horizontal distance from the observer to the detected bird or the average horizontal distance to a group of birds
Roost site	Position of a bird was initially sighted (A: trunk of a tree; B: branches of a tree; C: substratum of crown canopy; D: superstratum of crown canopy; E: inner part of a shrub; F: outer part of a shrub; G: ground)
Roost site height	Vertical distance from ground to the position of a bird was initially sighted or to the central position of a group of birds
Time	Time when the bird was detected
Animal subject	Bird species and numbers of each species

Data analysis

Statistical analysis was conducted using R software (R Core Team, 2013). Shapiro and Levene statistics were used to test for normality and homogeneity. Function "pair-wise-*t*-test" was used to conduct multiple comparisons for unbalanced design when variance analysis was afforded (Crawley, 2012). Kruskal-Wallis rank sum test was used when data was not in normality or homogeneity (Crawley, 2012) and function "gao_cs" in the "nparcomp" package (Gao et al, 2008) was applied to conduct unbalanced multiple comparisons. The tested variables were morphological characteristics and habitat variables. All the data was displayed in mean±*SD*. Statistical tests were two-tailed-tests and the confidence level was 95%. We used model selection based on generalized linear models (GLM) with Poisson error to find major factors affecting birds' habitat selection. Morphological characteristics were applied in linear discriminant analysis (LDA) to estimate the similarity among different species and to predict resource partition. Morphological data was standardized by dividing the cubic root of body weight to avoid the influence of body size (Amadon, 1943). Culmen length was excluded from standardization because it was primarily related to the size of food (Hespenheide, 1973). Logarithmic transformation was conducted before the relative length data (L'=L/BW1/ 3, L: the relative length of morphological characteristics) was applied to LDA ($Z'=\log_{10}Z$, Z: the relative length data) (Atchley et al, 1976). Data collected by mist-nets and point counts were analyzed independently to avoid influences of different methods (Barlow et al, 2007).

RESULTS

Habitat variables

Elevational distribution All of the seven fulvettas in Ailao Mountains, Ejia Town, Yunnan Province, were documented in this study and their elevation distributions were demonstrated in Figure 1. The Grey-cheeked Fulvetta occupied the lowest elevation, while the Golden-breasted Fulvetta preferred relatively higher elevation. Numbers documented by mist-nets and point counts was 413 and 417, respectively (Table 2). Significant differences in elevation were detected both by mist-nets (χ^2=253.6158, P<0.01) and point counts (χ^2= 269.1986, P<0.01). Further analysis of data from mist-nets showed that there were no significant differences among White-browed Fulvettas, Streak-throated Fulvettas and Golden-breasted Fulvettas and similar results were also occurred between Rusty-capped Fulvettas and Spectacled Fulvettas. Significant differences were detected among the other pairs. Rufous-winged Fulvettas were excluded from analyses because of the small sample size (only two records). However, non-significant differences were only found between Streak-throated Fulvettas and Rufous-winged Fulvettas in all of the 21 combinations of point counts (Table 3).

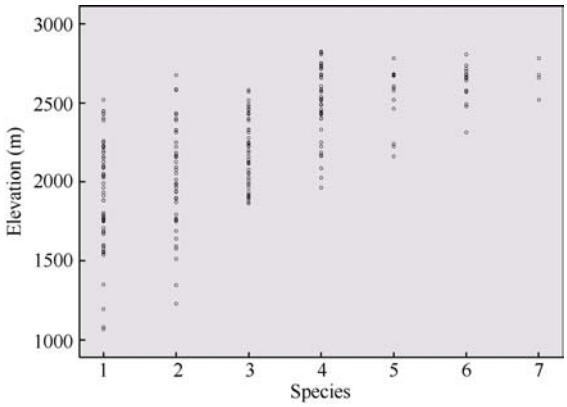

Figure 1 Scatter diagram of fulvetta species' distribution along elevation gradients

1: Grey-cheeked Fulvetta (*A.morrisonia*); 2: Rusty-capped Fulvetta (*A.dubia*); 3: Spectacled Fulvetta (*A.ruficapilla*); 4: Streak-throated Fulvetta (*A.cinereiceps*); 5: Golden-breasted Fulvetta (*A.chrysotis*); 6: White-browed Fulvetta (*A.vinipectus*); 7: Rufous-winged Fulvetta (*A.castaneceps*).

Roost site choice and roost site height Significant differences (χ^2=248.811, P<0.01) were found in the roost site height of the 417 fulvettas documented by point counts. Only three combinations consisted of White-browed Fulvettas, Spectacled Fulvettas and Streak-throated Fulvettas did not show significant differences in all of 21 combinations of the seven fulvettas in nonparametric multiple tests (Table 4). Rufous-winged Fulvettas occupied the highest roost site while Rusty-capped Fulvettas held the lowest one (Table 4). Although five species mainly chose the inner part of a shrub to roost, subtle differences were still detected (Figure 2). Golden-breasted Fulvettas preferred the substratum of crown canopy and Rufous-winged Fulvettas preferred branches of trees. White-browed Fulvettas and Streak-throated Fulvettas, which did not show significant differences in distribution elevations or roost site height, made similar choices over roost sites located in the inner part of shrubs, and the percentage was more than 80%.

Table 2 Numbers of each fulvetta species recorded by mist-nets or point counts

Species	Numbers of each species recorded by mist-nets (*n*)	Numbers of each species recorded by point counts (*n*)
White-browed Fulvetta (*A.vinipectus*)	31	22
Rufous-winged Fulvetta (*A.castaneceps*)	2	23
Golden-breasted Fulvetta (*A.chrysotis*)	32	46
Streak-throated Fulvetta (*A.cinereiceps*)	74	92
Spectacled Fulvetta (*A.ruficapilla*)	85	50
Rusty-capped Fulvetta (*A.dubia*)	41	78
Grey-cheeked Fulvetta (*A.morrisonia*)	148	106
Total	413	417

Table 3 Comparisons of the distribution elevations of the fulvetta species recorded by mist-nets or point counts (m)

Species	Elevations of the species recorded by mist-nets	Elevations of the species recorded by point counts
Rufous-winged Fulvetta (*A.castaneceps*)		2 552.130±66.213^{b}
White-browed Fulvetta (*A.vinipectus*)	2 633.742±108.005^{a}	2 516.455±65.236^{c}
Golden-breasted Fulvetta (*A.chrysotis*)	2 600.438±163.993^{a}	2 576.478±31.804^{a}
Streak-throated Fulvetta (*A.cinereiceps*)	2 554.919±223.930^{a}	2 559.185±140.016^{b}
Spectacled Fulvetta (*A.ruficapilla*)	2 190.459±211.938^{b}	2 159.380±234.746^{d}
Rusty-capped Fulvetta (*A.dubia*)	2 090.634±332.147^{b}	2 023.295±361.512^{e}
Grey-cheeked Fulvetta (*A.morrisonia*)	1 838.588±334.220^{c}	1 728.330±260.232^{f}

Same superscripts indicate non-significant differences.

Table 4 Sampling size and roost site height of the seven fulvetta species

Species	Numbers (*n*)	Roost site height (*m*)
Rufous-winged Fulvetta (*A.castaneceps*)	23	11.087±2.109^{a}
White-browed Fulvetta (*A.vinipectus*)	22	3.386±6.353^{d}
Golden-breasted Fulvetta (*A.chrysotis*)	46	5.978±3.480^{b}
Streak-throated Fulvetta (*A.cinereiceps*)	92	1.328±1.345^{d}
Spectacled Fulvetta (*A.ruficapilla*)	50	1.300±0.909^{d}
Rusty-capped Fulvetta (*A.dubia*)	78	0.559±0.408^{e}
Grey-cheeked Fulvetta (*A.morrisonia*)	106	3.774±2.737^{c}

Same superscripts indicate non-significant differences.

Vegetation coverage and mountain slope inclination

Significant differences were found in tree coverage (χ^2=34.9663, P<0.01), shrub coverage (χ^2=49.2832, P<0.01), herb coverage (χ^2=50.828, P<0.01) as well as in the shrub and herb coverage between White-browed Fulvettas and Streak-throated Fulvettas (Table 5). Because no niche segregation was found between these two Fulvetta species in earlier analysis, these differences in vegetation coverage indicate the specific choices of these two species over microhabitat utilization and their relaxed inter-specific competition. No significant differences were found in the mountain slope inclination (χ^2= 10.1526, P=0.1184). Rufous-winged Fulvetta was excluded from analyses due to the small sampling size.

Key factors affect habitat selection

According to earlier analyses of habitat variables, we chose the elevation, tree coverage, shrub coverage and herb coverage as habitat selection factors and used function "aictab" in the "AICcmodavg" package (Mazerolle, 2013) to determine the key factors affecting habitat selection. The results showed that the first 4 models' cumulative weight of QAICc (Cum.Wt) reached 100%. The first two models' delta QAICc were<2 and their cumulative weight reached 81%. The first one had the smallest QAICc and its weight reached 57% (Table 6). Because the weight of the first model was more than twice of the second one and it was succinct, the first model was considered as the optimal model. Because the

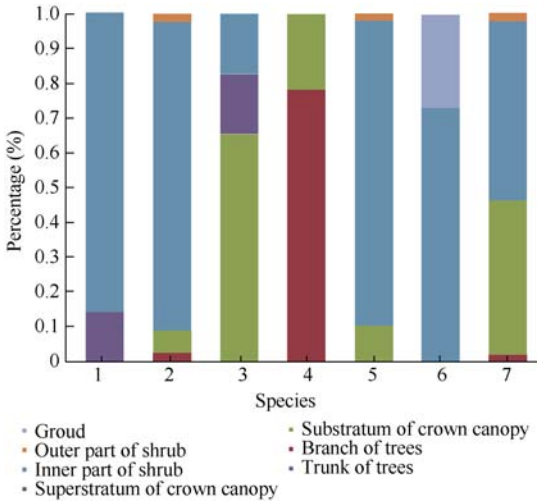

Figure 2 Comparison of roost site choices of species

1: White-browed Fulvetta (*A.vinipectus*); 2: Streak-throated Fulvetta (*A.cinereiceps*); 3: Golden-breasted Fulvetta (*A.chrysotis*); 4: Rufous-winged Fulvetta (*A.castaneceps*); 5: Spectacled Fulvetta (*A.ruficapilla*); 6: Rusty-capped Fulvetta (*A.dubia*); 7: Grey-cheeked Fulvetta (*A.morrisonia*).

first model was composed of elevation, herb coverage and shrub coverage, these factors were taken as the key factors affecting fulvettas' habitat selection.

We conducted model average of these four factors (elevation, tree coverage, shrub coverage and herb coverage) to learn effect trends. The results (Table 7) also showed that tree coverage did not significantly affect fulvettas' habitat selection because 0 occurred within its 95% confidence interval. The estimators of elevation and shrub were >0, indicating their positive effects on fulvettas' habitat selection. Herb coverage had negative effects on fulvettas' habitat selection because its estimator<0. Therefore, we concluded that fulvettas prefer the habitats with relatively high elevation and thick shrubs.

Morphological characteristics

Significant differences were detected in body weight (χ^2=292.4995, P<0.01), body length (χ^2=273.2875, P<0.01), wing length (χ^2=270.8071, P<0.01), tail length (χ^2=252.251, p<0.01), tarsus-metatarsus length (χ^2=183.7224, P<0.01), claw length (χ^2=81.1642, P<0.01), finger length (χ^2=169.0881, P<0.01) and culmen length (χ^2=264.6239, P<0.01). The Rufous-winged Fulvetta had the smallest tail length and tarsus-metatarsus length, while, the Golden-breasted Fulvetta was the smallest in the other morphological characteristics. Data of the Rusty-capped Fulvetta and the Grey-cheeked Fulvetta were relatively large (Table 8).

Table 5 Comparisons of vegetation coverage of the habitats of seven fulvetta species

Species	Percentage of tree coverage (%)	Percentage of shrub coverage (%)	Percentage of herb coverage (%)
White-browed Fulvetta (*A.vinipectus*)	60.461±30.204^{abc}	40.268±37.980^{b}	78.148±39.234^{b}
Golden-breasted Fulvetta (*A.chrysotis*)	64.853±14.120^{bc}	61.050±17.664^{b}	84.141±17.565^{a}
Streak-throated Fulvetta (*A.cinereiceps*)	67.850±24.946^{ab}	72.761±32.170^{a}	52.393±41.027^{c}
Spectacled Fulvetta (*A.ruficapilla*)	53.357±26.087^{c}	80.808±26.292^{a}	38.211±43.193^{c}
Rusty-capped Fulvetta (*A.dubia*)	63.019±25.633^{abc}	72.461±30.159^{a}	40.637±43.533^{c}
Grey-cheeked Fulvetta (*A.morrisonia*)	71.719±24.159^{a}	77.666±24.346^{a}	34.364±42.520^{c}

Same superscripts indicate non-significant differences.

Table 6 Results of model selection according to quasi-likelihood of the second-order Akaike's information criterion

Candidate models	QAICc	Delta_QAICc	QAICcWt	Cum.Wt	Quasi.LL
1/3/4	295.87	0.00	0.57	0.57	–142.83
1/2/3/4	297.62	1.75	0.24	0.81	–142.67
1/3	299.14	3.27	0.11	0.92	–145.5
1/4	299.77	3.9	0.08	1	–145.82
1	312.52	16.65	0	1	–153.22
3/4	322.2	26.33	0	1	–157.03
3	325.07	29.2	0	1	–159.49
4	339.48	43.61	0	1	–166.7

1: Elevation; 2: Percentage of tree coverage; 3: Percentage of shrub coverage; 4: Percentage of herb coverage.

Table 7 Model-averaged parameter estimations of habitat factors

Factors	Estimator	*SE*	Lower 95% CI	Upper 95% CI
Elevation	0.0012	2e-04	7e-04	0.0016
Percentage of tree coverage	–0.0021	0.0037	–0.0094	0.0051
Percentage of shrub coverage	0.0094	0.0041	0.0013	0.0175
Percentage of herb coverage	–0.0064	0.0028	–0.0118	–0.001

Table 8 Comparison of morphological characteristics of species

Species	*n*	Body weight (g)	Claw length (mm)	Culmen length (mm)	Wing length (mm)	Body length (mm)	Tail length (mm)	Tarsus-metatarsus length (mm)	Finger length (mm)
White-browed Fulvetta (*A.vinipectus*)	26	10.150±0.858^{c}	5.571±1.299^{c}	5.598±0.287^{c}	57.837±3.049^{b}	111.038±5.495^{b}	55.577±3.177^{b}	24.946±0.827^{a}	11.848±0.730^{b}
Streak-throated Fulvetta (*A.cinereiceps*)	63	9.756±0.680^{c}	6.551±1.386^{ab}	5.629±0.321^{c}	54.817±2.489^{c}	107.873±6.831^{c}	52.397±3.314^{c}	24.495±0.931^{a}	11.618±1.029^{b}
Rusty-capped Fulvetta (*A.dubia*	31	15.803±1.086^{a}	6.861±0.884^{a}	6.842±0.354^{a}	59.452±1.748^{b}	132.032±4.199^{a}	61.677±3.250^{a}	25.079±0.961^{a}	13.848±1.403^{a}
Grey-cheeked) Fulvetta (*A.morrisonia*)	120	14.496±1.187^{b}	5.828±0.733^{c}	6.751±0.362^{a}	64.208±1.878^{a}	133.000±3.043^{a}	62.192±3.537^{a}	23.634±0.830^{b}	11.927±0.876^{b}
Golden-breasted Fulvetta (*A.chrysotis*)	31	7.126±0.390^{e}	4.716±0.613^{d}	4.771±0.236^{d}	52.742±1.751^{d}	99.645±4.079^{d}	48.903±3.944^{d}	22.792±0.944^{c}	10.132±0.661^{d}
Rufous-winged Fulvetta (*A.castaneceps*)	10	9.610±0.985^{c}	6.575±0.834^{ab}	5.875±0.196^{b}	56.100±2.132^{bc}	104.100±6.999^{cd}	42.600±2.836^{e}	20.210±0.778^{d}	12.300±0.707^{b}
Spectacled Fulvetta (*A.ruficapilla*)	58	8.479±0.876^{d}	5.911±1.235^{bc}	5.650±0.237^{c}	53.517±2.011^{d}	105.483±3.267^{c}	50.741±3.081^{d}	22.516±1.076^{c}	10.635±0.630^{c}

Same superscripts indicate non-significant differences.

Linear discriminant analysis

We conducted LDA to the eight morphological characteristics in Table 8, and got six linear discriminant functions. The cumulative proportion of LD1 and LD2 reached 0.9284 (Table 9), indicating that they could account for 92.84% variability in the linear discriminant model. The proportions of the last four linear discriminant functions were small, indicating the weak influences they exert on the results. The absolute values of coefficients of body length (BL) and tarsus-metatarsus length (TML) in LD1 were high, indicating that LD1 primarily reflected the discriminant effects of body length and tarsus-metatarsus length. The absolute value of coefficient of wing length (WL) in LD2 was the largest coefficient, indicating that LD2 primarily reflected the discriminant effect of wing length (Table 10).

Approximately, 90.3% of the samples were correctly classified into different species via LDA. Samples were divided into four groupings and two of them were consisted of a single species, Golden-breasted Fulvettas and Rufous-winged Fulvettas, respectively. One group was consisted of Grey-cheeked Fulvettas and Rusty-capped Fulvettas, and the fourth group was consisted of White-browed Fulvettas, Streak-throated Fulvettas and spectacled Fulvettas (Table 11). The accuracy rates of LDA for each species were relatively high (91.20%-100%) except for White-browed Fulvettas (65.40%) and Streak-throated Fulvettas (74.60%). Misclassifications were found among White-browed Fulvettas, Streak-throated Fulvettas and spectacled Fulvettas, as well as between Grey-cheeked Fulvettas and Rusty-capped Fulvettas. Misclassification rate was relatively high between White-browed Fulvettas and Streak-throated Fulvettas (Table 11).

Table 9 Proportion of trace of linear discriminant analysis

Functions	LD1	LD2	LD3	LD4	LD5	LD6
Proportion of trace	0.8523	0.0761	0.0516	0.0139	0.0051	0.001

Table 10 Coefficients of linear discriminant analysis

Morphological characteristics	LD1	LD2	LD3	LD4	LD5	LD6
BW	–0.8811885	0.3735774	–0.4774164	0.624646	0.1744586	0.2523426
CUL	–1.340453	0.1253922	1.2647371	–1.54594	1.4543998	–1.077508
CLL	0.7308699	4.5448938	3.6643598	–4.682241	6.6273355	5.5899434
WL	–14.8874514	–48.0531867	–12.1749091	30.530741	42.8527554	–2.7700184
BL	–22.2927648	–2.5958555	–15.5078565	4.240833	–26.0764156	15.6511549
TL	–3.5438221	9.4093755	–14.3753771	–29.584098	–7.0460453	–16.0740137
TML	20.7689209	37.1068074	–33.2364027	16.419393	25.9016113	7.8645413
FL	3.1495686	8.2214066	17.5987326	12.287153	–6.1706657	–17.0493372

Table 11 Classification rates of linear discriminant analysis of morphological characteristics

Species	White-browed Fulvetta (*A.vinipectus*)	Streak-throated Fulvetta (*A.cinereiceps*)	spectacled Fulvetta (*A.ruficapilla*)	Rusty-capped Fulvetta (*A.dubia*)	Grey-cheeked Fulvetta (*A.morrisonia*)	Golden-breasted Fulvetta (*A.chrysotis*)	Rufous-winged Fulvetta (*A.castaneceps*)
White-browed Fulvetta (*A.vinipectus*)	65.40%	30.80%	3.80%				
Streak-throated Fulvetta (*A.cinereiceps*)	15.90%	74.60%	9.50%				
Spectacled Fulvetta (*A.ruficapilla*)		8.80%	91.20%				
Rusty-capped Fulvetta (*A.dubia*)				93.50%	6.50%		
Grey-cheeked Fulvetta (*A.morrisonia*)					100%		
Golden-breasted Fulvetta (*A.chrysotis*)						100%	
Rufous-winged Fulvetta (*A.castaneceps*)							100%

DISCUSSION

Spatial niche segregation in different scales

According to the competitive exclusion principle, niche segregation was required among sympatric congeners to avoid competitive exclusion (Hardin, 1960; Levin, 1970; Schoener, 1974). Niche theory could well explain species coexistence in temperate forest (Nakashizuka, 2001). According to this study, the niche theory could also be used in subtropical montane forest to explain the coexistence of the seven fulvettas in Ailao Mountains, Ejia Twon, Yunnan Province. Through spatial niche segregation in different scales, fulvettas reduced inter-specific competition and promoted species coexistence.

Habitat partitioning was relatively more important than other dimensions (Schoener, 1974). Habitat heterogeneity was vital for habitat segregation (Vidus-Rosin et al, 2012). In this study, results of model selection based on GLM with Poisson error indicated that the elevation, shrub coverage and herb coverage were the key factors affecting fulvettas' habitats selection (Table 6). Elevation analysis showed that niche segregation was detected through both mist-nets and point counts. No significant differences were found either among the three fulvettas occupying relatively high elevations or between Spectacled Fulvettas and Rusty-capped Fulvettas through mist-nets, whereas, through point counts, only one pair was found with non-significant differences. Chiang et al (2012) reported that elevation gradients might be the main factor in explaining the coexistence of species in spatial dimension. In the study area of this study, elevations were ranged from 800 m to 2 800 m and both the climate and forest types were showed with obvious vertical variations, therefore, the habitat heterogeneity along elevation gradients offered

opportunities of these fulvettas to choose different habitats.

Niche overlaps were also existence for some fulvettas even though segregation in elevation had been detected. Schoener (1983) found that when species were similar in one dimension, resource differentiation would occur in other dimensions to reduce inter-specific competition. Vertical height was an important component of spatial niche. Studies on tits had shown that segregation in vertical height could facilitate species' coexistence (Song, 1983; Yang et al, 2012). Through analysis of roost site height, we found niche overlaps among White-browed Fulvettas, Spectacled Fulvettas and Streak-throated Fulvettas. However, Spectacled Fulvettas had significant differences with the other two in elevation. Golden-breasted Fulvettas was widely overlapped with White-browed Fulvettas and Streak-throated Fulvettas in elevation documented by mist-nets. They had significant differences in roost site height with the other two species. Similar results were also found between Rufous-winged Fulvettas and Streak-throated Fulvettas documented by point counts. Vertical height reflects the activity space chosen by birds. Because of their unique physiological and activity pattern, birds have high demand for energy supply. Foraging behavior accordingly occupies a large proportion in birds' activities. Therefore, differentiation in roost site height mainly reflects segregation in foraging height. Studies on tits (Liu et al, 1989), prinias (Zhou & Fang, 2000), hummingbirds (Lara et al, 2011) and other bird communities (Gao & Yang, 1991) found that foraging height segregation reduced inter-specific competition and facilitated coexistence. Hence, we assumed that foraging height segregation permitted fulvettas that widely overlapped in elevation to relax the intensity of inter-specific competitive interactions.

Through analysis of elevation and vertical height, we did not found significant differences between White-browed Fulvettas and Streak-throated Fulvettas documented by mist-nets. However, significant differences were then detected in the key factors of shrub coverage and herb coverage (Table 5). Vegetation coverage was an important component of microhabitat chosen by animals. Segregation in microhabitat could facilitate species' coexistence (Dammhahn et al, 2013; Traba et al, 2013). Study on Blue Eared Pheasant (*Crossoptilon auritum*) found that concealment condition provided by vegetation coverage had a significant influence on birds' habitat selection (Liu et al, 2005). Study of breeding ecology showed that fulvettas' nests were primarily located in undergrowth consisted of shrubs and herbs (Lee et al, 2010; Gong, 1994; Huang et al, 1988; Zhou, 1989). Therefore, segregation in this scale allowed fulvettas to use different concealment conditions in their home range and avoided complete niche overlap accordingly.

Morphological differentiations

Morphological characteristics provide an insight into the ecology of animals (Landmann & Winding, 1993; Miles et al, 1987). It reflects the adaptions to the environmental conditions consisted of abiotic and biotic factors during animals' life history (Martin, 2001). We detected significant differences in eight morphological characteristics of the seven fulvettas (Table 8) and four qualitative groupings were resulted from LDA (Table 11). Numerous of studies on the relationships between birds' niche use and morphology found that differences in morphological characteristics led to differentiation in their competitive abilities (Kalinoski, 1975; Gao et al, 1997), their foraging behaviors (Salewski et al, 2003), their resource preferences (Hill & Lein, 1988) and the varieties, sites and vertical height of trees they chose (Alatalo, 1981; Richards et al, 2000; Salewski et al, 2003). In this study, LDA primarily reflected discriminant effects of body length, tarsus-metatarsus length and wing length. These three characteristics have great influences on bird's activities. Studies on herons (Wen et al, 1998; Ye et al, 2006; Zhu et al, 1998), hummingbirds (Lara et al, 2011) and woodpeckers (Gao et al, 1997) showed that body size played a key role in deciding birds' competitive ability. Wing length decides birds' flying ability. Tarsus-metatarsus length has a strong correlation with birds' behavior and influences habitat selection (Liu et al, 2013). Therefore, we predicted that fulvettas of different groupings present different features in resource use which helped them to realize niche partition. Misclassifications within groups indicated the similarity in resource use among group members. However, we also detected segregations among fulvettas within each group. For example, in the first group, White-browed Fulvettas was different from Streak-throated Fulvettas in microhabitat use, and they had significant differences with Spectacled Fulvettas in elevation. Significant differences were also detected in elevation and roost site height between Grey-cheeked Fulvettas and Rusty-capped Fulvettas of the second group (Table 11).

In conclusion, different morphological characteristics of each group benefited fulvettas to partition resource in the overlapped regions and spatial niche segregation relaxed the intensity of inter-specific interactions among members within each group. However, the misclassifications indicated that intense competition could still occur among members within each groups in the overlapped regions and these competitions might become new selective pressures facilitating further differentiations.

The findings of this study showed that niche theory could explain the coexistence mechanisms of the seven fulvettas in the subtropical montane, Ejia Town, Yunnan Province. Through elevation, roost site height and vegetation coverage partitioning, these seven sympatric fulvettas realized spatial niche segregation in different scales. Combined with differentiations in resource use due to different morphological characteristics, they were able to minimize the intensity of inter-specific interactions and promote the coexistence. Moreover, the mutability and unpredictability of environment, the interference effects, the migration of species and the heterogeneity provided by large environmental gradient might also play important roles and

should be considered along with the competition effects when exploring the coexistence mechanisms of sympatric congeners.

ACKNOWLEDGEMENTS

We thank Shuangbai Ailaoshan Nature Reserve Management Bureau for the help in conducting this research. We thank Cheng ZHU, Pei-Qing XU and Meng-Yin AN for their participation in the fieldwork.

REFERENCES

Alatalo RV. 1981. Interspecific competition in tits Parus spp. and the goldcrest Regulus regulus: foraging shifts in multispecific flocks. *Oikos,* **37**(3): 335-344.

Amadon D. 1943. Bird weights as an aid in taxonomy. *The Wilson Bulletin,* **55**(3): 164-177.

Atchley WR, Gaskins CT, Anderson D. 1976. Statistical properties of ratios. I. Empirical results. *Systematic Biology,* **25**(2): 137-148.

Bagchi S, Goyal SP, Sankar K. 2003. Niche relationships of an ungulate assemblage in a dry tropical forest. *Journal of Mammalogy,* **84**(3): 981-988.

Barlow J, Mestre LAM, Gardner TA, Peres CA. 2007. The value of primary, secondary and plantation forests for Amazonian birds. *Biological Conservation,* **136**(2): 212-231.

Bibby CJ, Jones M, Marsden S. 1998. Bird Surveys: Expedition Field Techniques. London: Expedition Advisory Centre, Royal Geographical Society.

Chen YS, Ye LF. 1988. Geology and geomorphy of the Ailaoshan Mountain Natural Reserve and its vicinity. *In*: Xu YC, Jiang HJ. Comprehensive survey of Ailaoshan Nature Reserve. Kunming: Yunnan Ethnic Press, 11-23. (in Chinese)

Chesson P. 2000. Mechanisms of maintenance of species diversity. *Annual Review of Ecology and Systematics,* **31**(1): 343-366.

Chiang PJ, Pei KJC, Vaughan MR, Li CF. 2012. Niche relationships of carnivores in a subtropical primary forest in southern Taiwan. *Zoological Studies,* **51**(4): 500-511.

Crawley MJ. 2012. The R Book. 2nd ed. West Sussex: John Wiley and Sons.

Cui P, Kang MJ, Deng WH. 2008. Foraging habitat selection by sympatric Temminck's tragopan and blood pheasant during breeding season in southwestern China. *Biodiversity Science,* **16**(2): 143-149. (in Chinese)

Dammhahn M, Soarimalala V, Goodman SM. 2013. Trophic niche differentiation and microhabitat utilization in a species-rich montane forest small mammal community of eastern madagascar. *Biotropica,* **45**(1): 111-118.

Davies TJ, Meiri S, Barraclough TG, Gittleman JL. 2007. Species coexistence and character divergence across carnivores. *Ecology Letters,* **10**(2): 146-152.

Denoël M, Schabetsberger R, Joly P. 2004. Trophic specialisations in alternative heterochronic morphs. *Naturwissenschaften,* **91**(2): 81-84.

Di Bitetti MS, Di Blanco YE, Pereira JA, Paviolo A, Pérez IJ. 2009. Time partitioning favors the coexistence of sympatric crab-eating foxes (*Cerdocyon thous*) and pampas foxes (*Lycalopex gymnocercus*). *Journal of Mammalogy,* **90**(2): 479-490.

Fox JW. 2004. Modelling the joint effects of predator and prey diversity on total prey biomass. *Journal of Animal Ecology,* **73**(1): 88-96.

Gao W, Yang ZJ. 1991. The relationship of mixed flock of birds in the artificial larch forest in winter. *Chinese Journal of Zoology,* **26**(4): 9-12. (in Chinese)

Gao W, Li WC, Lü JT. 1997. The niche and competition of three woodpeckers. *Journal of Northeast Normal University: Natural Science Edition,* (1): 78-81. (in Chinese)

Gao X, Alvo M, Chen J, Li G. 2008. Nonparametric multiple comparison procedures for unbalanced one-way factorial designs. *Journal of Statistical Planning and Inference,* **138**(8): 2574-2591.

Gong HS. 1994. The observation of breeding ecology of Golden-breasted Fulvetta (*Alcippe chrysotis*). *Sichuan Journal of Zoology,* **13**(2): 89. (in Chinese)

Guillemain M, Fritz H, Guillon N, Simon G. 2002. Ecomorphology and coexistence in dabbling ducks: the role of lamellar density and body length in winter. *Oikos,* **98**(3): 547-551.

Gustafsson L. 1988. Foraging behaviour of individual Coal Ttis, Parus-Ater, in relation to their age, sex and morphology. *Animal Behaviour,* **36**(3): 696-704.

Hardin G. 1960. The competitive exclusion principle. *Science,* **131**(3409): 1292-1297.

Hespenheide HA. 1973. Ecological inferences from morphological data. *Annual Review of Ecology and Systematics,* **4**(1): 213-229.

Hill BG, Lein MR. 1988. Ecological relations of sympatric black-capped and mountain chickadees in southwestern Alberta. *The Condor,* **90**(4): 875-884.

Huang Y, Wu WG, Huang SM. 1988. The breeding babit of Grey-hooded Fulvetta (A.cinereiceps). *Chinese Wildlife,* **42**(2): 13-15. (in Chinese)

Kaifu K, Miller MJ, Aoyama J, Washitani I, Tsukamoto K. 2013. Evidence of niche segregation between freshwater eels and conger eels in Kojima Bay, Japan. *Fisheries Science,* **79**(4): 593-603.

Kalinoski R. 1975. Intra-and interspecific aggression in House Finches and House Sparrows. *The Condor,* **77**(4): 375-384.

Landmann A, Winding N. 1993. Niche segregation in high-altitude Himalayan chats (Aves, Turdidae): does morphology match ecology? *Oecologia,* **95**(4): 506-519.

Langkilde T, Shine R. 2004. Competing for crevices: interspecific conflict influences retreat-site selection in montane lizards. *Oecologia,* **140**(4): 684-691.

Lara C, Martínez-García V, Ortiz-Pulido R, Bravo-Cadena J, Loranca S, Córdoba-Aguilar A. 2011. Temporal-spatial segregation among hummingbirds foraging on honeydew in a temperate forest in Mexico. *Current Zoology,* **57**(1): 56-62.

Lara C, Martínez-García V, Ortiz-Pulido R, Bravo-Cadena J, Loranca S, Córdoba-Aguilar A. 2011. Temporal-spatial segregation among hummingbirds foraging on honeydew in a temperate forest in Mexico. *Current Zoology*, **57**(1): 56-62.

Lee PY, Wang LJ, Hsu HC, Chou LS, Chen CC. 2010. Habitat selection among nesting, foraging, and singing sites of the Gray-cheeked Fulvetta Alcippe morrisonia in northeastern Taiwan. *Ornithological Science,* **9**(2): 135-140.

Levin SA. 1970. Community equilibria and stability, and an extension of the competitive exclusion principle. *The American Naturalist,* **104**(939): 413-423.

Li L, Zhang L, Yin JX, Liu ZC, Liu H, Wan DM. 2013. Coexistence mechanism of two species passerines in man-made nest boxes. *Acta Ecologica Sinica,* **13**(1): 150-158. (in Chinese)

Li W, Zhou W, Zhang XY, Cao M, Zhang RG. 2006. Spring foraging sites of three pheasants at Nanhua part in Ailaoshan National Nature Reserve. *Zoological Research,* **27**(5): 495-504. (in Chinese)

Liu DY, Wang JX, Lv PY, Chen YY. 1988. Comprehensive report on scientific exploration of the Ailaoshan Nature Reserve. *In*: Xu YC,Jiang HJ. Comprehensive Survey of Ailaoshan Nature Reserve. Kunming: Yunnan Ethnic Press, 1-10. (in Chinese)

Liu LH, Chen XC, Chu H, Sun JC, Zhang XA, Zhao L. 2013. Ecomorphological explanations of passerines coexistence in alpine meadow. *Zoological Research,* **34**(3): 160-165. (in Chinese)

Liu NF, Li Y, Liu JZ. 1989. Studies of interspecific relationship between great tit and willow tit. *Zoological Research,* **10**(4): 277-284. (in Chinese)

Liu ZS, Chao LR, Li ZG, Li T, Wang XM. 2005. Winter habitat selection of blue eared pheasant (*Crossoptilon auritum*) in Helan Mountain, China. *Chinese Journal of Zoology,* **40**(2): 38-43. (in Chinese)

Loveridge AJ, Macdonald DW. 2003. Niche separation in sympatric jackals (*Canis mesomelas* and *Canis adustus*). *Journal of Zoology,* **259**(2): 143-153.

Lucherini M, Reppucci JI, Walker RS, Villalba ML, Wurstten A, Gallardo G, Iriarte A, Villalobos R, Perovic P. 2009. Activity pattern segregation of carnivores in the high Andes. *Journal of Mammalogy,* **90**(6): 1404-1409.

Macarthur RH. 1958. Population ecology of some warblers of northeastern coniferous forests. *Ecology,* **39**(4): 599-619.

Martin TE. 2001. Abiotic vs. biotic influences on habitat selection of coexisting species: climate change impacts? *Ecology*, **82**(1): 175-188.

Martínez-Freiría F, Lizana M, Do Amaral JP, Brito JC. 2010. Spatial and temporal segregation allows coexistence in a hybrid zone among two Mediterranean vipers (*Vipera aspis* and *V. latastei*). *Amphibia-Reptilia*, **31**(2): 195-212.

Mazerolle MJ. 2013. AICcmodavg: Model selection and multimodel inference based on (Q)AIC(c), http://CRAN.R-project.org/package= AICcmodavg.

Miles DB, Ricklefs RE, Travis J. 1987. Concordance of ecomorphological relationships in three assemblages of passerine birds. *The American Naturalist,* **129**(3): 347-364.

Munday PL, Jones GP, Caley MJ. 2001. Interspecific competition and coexistence in a guild of coral-dwelling fishes. *Ecology,* **82**(8): 2177-2189.

Nakashizuka T. 2001. Species coexistence in temperate, mixed deciduous forests. *Trends in Ecology and Evolution,* **16**(4): 205-210.

Pagen RW, Thompson III FR, Burhans DE. 2002. A comparison of point-count and mist-net detections of songbirds by habitat and time-of-season. *Journal of Field Ornithology,* **73**(1): 53-59.

Quillfeldt P, Masello JF, Navarro J, Phillips RA. 2013. Year-round distribution suggests spatial segregation of two small petrel species in the South Atlantic. *Journal of Biogeography,* **40**(3): 430-441.

R Core Team. 2013. R: A language and environment for statistical computing. Vienna, Austria: R Foundation for Statistical Computing

Rappole JH, Winker K, Powell GVN. 1998. Migratory bird habitat use in southern Mexico: Mist Nets versus Point Counts. *Journal of Field Ornithology,* **69**(4): 635-643.

Richards SA, Nisbet RM, Wilson WG, Possingham HP. 2000. Grazers and diggers: exploitation competition and coexistence among foragers with different feeding strategies on a single resource. *The American Naturalist,* **155**(2): 266-279.

Salewski V, Bairlein F, Leisler B. 2003. Niche partitioning of two Palearctic passerine migrants with Afrotropical residents in their West African winter quarters. *Behavioral Ecology,* **14**(4): 493-502.

Schoener TW. 1974. Resource partitioning in ecological communities. *Science,* **185**(4145): 27-39.

Schoener TW. 1983. Field experiments on interspecific competition. *The American Naturalist,* **122**(2): 240-285.

Schuett GW, Hardy DL, Greene HW, Earley RL, Grober MS, Van Kirk EA, Murdoch WJ. 2005. Sympatric rattlesnakes with contrasting mating systems show differences in seasonal patterns of plasma sex steroids. *Animal Behaviour,* **70**(2): 257-266.

Song YJ. 1983. Study of breeding habit of the Coal Tit (Parus ater). *Acta Ecologica Sinica,* **3**(4): 399-407. (in Chinese)

Svenning JC. 1999. Microhabitat specialization in a species-rich palm community in Amazonian Ecuador. *Journal of Ecology,* **87**(1): 55-65.

Traba J, Acebes P, Malo JE, García JT, Carriles E, Radi M, Znari M. 2013. Habitat selection and partitioning of the Black-bellied Sandgrouse (*Pterocles orientalis*), the Stone Curlew (*Burhinus oedicnemus*) and the Cream-coloured Courser (*Cursorius cursor*) in arid areas of North Africa. *Journal of Arid Environments,* **94**: 10-17.

Tschapka M. 2004. Energy density patterns of nectar resources permit coexistence within a guild of Neotropical flower-visiting bats. *Journal of Zoology,* **263**(1): 7-21.

Vidus-Rosin A, Lizier L, Meriggi A, Serrano-Perez S. 2012. Habitat selection and segregation by two sympatric lagomorphs: the case of European hares (*Lepus europaeus*) and Eastern cottontails (*Sylvilagus floridanus*) in northern Italy. *Acta Theriologica,* **57**(4): 295-304.

Wang XF, Tang SF, Gao PL. 1988. The mountain climate of mid-north section of the Ailao Mountains. *In*: Xu YC, Jiang HJ. Comprehensive Survey of Ailaoshan Nature Reserve. Kunming: Yunnan Ethnic Press, 24–34. (in Chinese)

Ward-Campbell BMS, Beamish FWH, Kongchaiya C. 2005. Morphological characteristics in relation to diet in five coexisting Thai fish species. *Journal of Fish Biology,* **67**(5): 1266-1279.

Wen ZZ, Wang QL, Sun RY. 1998. Study of interspecific relationship of the herons. *Chinese Journal of Ecology,* **17**(1): 27-34. (in Chinese)

Wiens JJ, Graham CH. 2005. Niche conservatism: Integrating evolution, ecology, and conservation biology. *Annual Review of Ecology, Evolution, and Systematics,* **36**: 519-539.

Wu F, Yang XJ. 2008. Application of point count method in forest birds survey. *Chinese Journal of Ecology*, **27**(12): 2240-2244. (in Chinese)

Wu F, Yang XJ, Yang JX. 2010. Additive diversity partitioning as a guide to regional montane reserve design in Asia: an example from Yunnan Province, China. *Diversity and Distributions,* **16**(6): 1022-1033.

Yang L, Yang XJ. 2004. The Avifauna of Yunnan, China. Vol. 2 Passeriformes. Kunming: Yunnan Science and Technology Press. (in Chinese)

Yang XN, Zhu L, Hao G, Wen AX, Sun YH. 2012. Niche separation and coexistence of two species of tits at Wawushan. *Chinese Journal of Zoology,* **47**(4): 11-18. (in Chinese)

Ye F, Huang CM, Li HH. 2006. Study on spartial niche of seven species of colonial breeding egrets and herons of Fangcheng, Guangxi Autonomous Region. *Sichuan Journal of Zoology,* **25**(3): 577-583. (in Chinese)

Zhao L, Zhang XA. 2004. Nest-site selection and competition coexistence of Horned Larks and Small Skylarks. *Zoological Research,* **25**(3): 198-204.

(in Chinese)

Zheng GM. 1995. Ornithology. Beijing: Beijing Normal University Press. (in Chinese)

Zheng GM. 2002. A Checklist on the Classification and Distribution of the Birds of the World. Beijing: Science Press. (in Chinese)

Zheng GM. 2011. A Checklist on the Classification and Distribution of the Birds of China. 2nd ed. Beijing: Science Press. (in Chinese)

Zhou F. 1989. Study of breeding ecology of Grey-cheeked Fulvetta (*Alcippe morrisonia*). *Chinese Wildlife,* **52**(6): 54-57. (in Chinese)

Zhou F, Fang HL. 2000. On the interspecific niche relationship between two species of wren warbler. *Zoological Research,* **21**(1): 52-57. (in Chinese)

Zhu X, Zhang LX, Liang J, Xuan ZC. 1998. Spatial niche and interspecific relationships of Ardeidae Birds in Taigongshan Hill, Zhejiang. *Zoological Research,* **19**(1): 45-51. (in Chinese)

Age-related habitat selection by brown forest skinks (*Sphenomorphus indicus*)

Qi-Ping ZHU, Meng-Yao ZHU, Ying-Chao HU, Xue-Ya ZHANG, Guo-Hua DING*, Zhi-Hua LIN

College of Ecology, *Lishui University*, *Lishui* 323000, *China*

ABSTRACT

In reptiles, habitat selection is the process whereby suitable habitat is selected that optimizes physiological functions and behavioral performance. Here, we used the brown forest skink (*Sphenomorphus indicus*) as a model animal and examined whether the frequency of active individuals, environmental temperature, illumination of activity area, and habitat type vary with different age classes. We surveyed the number of active individuals and measured environmental variables at Baiyunshan Mountain in Lishui, Zhejiang, China. We found no difference in the activity frequency of adult and juvenile *S. indicus*; the activity pattern of active individuals was bimodal. The mean environmental temperature selected by adults was higher than that selected by juveniles. The environmental temperature of active areas measured at 0900-1000 h and 1100-1200h was higher than at 1400-1500h; illumination of the active area at 1000-1200h was also higher than at 1400h-1600 h. The number of active individuals, the environmental temperature and illumination of activity areas showed pairwise positive correlation. There was a difference in habitat type between juveniles and adults whereby juveniles prefer rock habitats. We predict that active *S. indicus* select optimal habitats with different environmental temperatures and types to reach the physiological needs particular to their age classes.

Keywords: *Sphenomorphus indicus*; Age-related selection difference; Habitat selection; Temperature; Illumination; Habitat type; Activity frequency

INTRODUCTION

Habitat selection is the process of animals choosing optimal habitat (Buckland et al, 2014; Johnson, 1980). Studies on habitat selection can help us understand animal behavior, population dynamics, propagation, survival and wildlife conservation (Buckland et al, 2014; Manly et al, 2002; Strickland & McDonald, 2006). Because habitat selection variation occurs with spatial dimensional change, we can acquire information about habitat selection by examining animal distributions at specific spatial scales (De La Cruz et al, 2014; Hódar et al, 2000; Oppel et al, 2004). Studies on habitat selection have mainly focused on the three levels of population, home range and microhabitat (Thomas & Taylor, 1990). However, studies at different levels are important in determining the factors vital to habitat utilization and effective conversation measures (Beasley et al, 2007; Buckland et al, 2014; Razgour et al, 2011).

Habitat selection in most ectotherms is determined by specific thermal preferences, social interactions, predator avoidance and other factors (Angilletta et al, 2002; Dochtermann et al, 2012; Downes & Shine, 1998; Hall et al, 1992). Ectotherms are able to optimize their physiological and functional performance through habitat selection, and studies at the microhabitat level are important in understanding the mechanisms of selection. As a representative species and ectothermic group, reptiles not only need to avoid predators during activity, but more importantly, their behavior and physiological capabilities are significantly affected by temperature. It is vital that reptiles find suitable heterogeneous thermal environments to improve fitness (Angilletta et al, 2002; Castilla et al, 1999; Huey, 1982; Webb, 1996). During microhabitat selction, the activities of a reptile are under the influence of other repetiles or other species within the environment (Manicom & Schwarzkopf, 2011; Stamps & Tanaka, 1981; Wasko & Sasa, 2012). Sometimes, competition over environmental resources occurs (e.g., food, thermal resources) (Amarasekare & Coutinho, 2014;

Received: 09 September 2014; Accepted: 27 October 2014

Foundation items: This work was supported by the Open Research Fund program of Laboratory of Lishui University (2014-26-10); the Scientific Research Foundation of Ph.D. in Lishui University (QD1301); the Science and Technology Planning Project of Lishui (20110426) and the Project of Summer Work for Undergraduates in Lishui University (2014-245-23)

*Corresponding author. E-mail: guwoding@qq.com

DOI:10.13918/j.issn.2095-8137.2015.1.29

Marler et al, 1995; Hart & Marshall, 2012) and differences in intraspecies or interspecies habitat selection will follow.

The brown forest skink (*Sphenomorphus indicus*) is a member of the family Scincidae and mainly distributed across sourthen China in dark and wet grass, rock piles or cracks in cliffs (Huang, 1999). They are active away from their caves from early April to late October, and are more likely to be observed in shady areas during the morning and afternoon, and occasionally at noon. Here, we used line transects to investigate the quantity and type of habitat used by *S. indicus* in hilly road areas of Baiyunshan Mountain, Lishui, China. Environmental temperatures and illumination intensity were measured to explore characteristics and underlying mechanisms of habitat selection by *S. indicus* of different ages. Our results will aid the conservation of wild populations of this species.

MATERIALS AND METHODS

Experimental design

From May to early July 2014 we used line transect methods to investigate *S. indicus* and their habitat at Baiyunshan Mountain, Lishui, Zhejiang, China (N27°49′17.50″, E120°32′14.89″). The full length of the line transect was 4 km, and the altitude at the start and end points was 140 m and 360 m, respectively. During the survey observers proceeded at an even pace along hilly road. Active individuals sighted within 2 m of the road along the cliff (width=2 m) and environmental parameters of habitat were recorded. Seventeen surveys were randomly carried out during 0900h-1230h (10 surveys) and 1230h-1600h (7 surveys) over 6 days. The weather and temperature during surveys are shown in Table 1. Active individuals were determined as adults (SVL> 65 mm) or juveniles (SVL<65 mm) (Ji & Du, 2000) by visually estimating body size. The snout-vent length (SVL) of randomly captured individuals was measured by digital square caliper (0.01 mm, Mitutoyo, Japan) and the accuracy of visual estimation was verified. Before being released to the original capture area, the 1st toe on the left hind legs was clipped in individuals to avoid repeated sampling. Because sex can not be determined by visual estimation, gender-related differences were not considered here. The habitat of observed *S. indicus* was determined whereby grass or leaf litter layer was categorized as grass habitat and bare rock or ditch was categorized as rock habitat. An infrared radiation thermometer (UT301A, Uni-T, China) was used to measure the temperature of the spot where a skink was located, defined by a circle with a 10 cm diameter around the animal; the environmental temperature of this habitat was the average value of 10 measurements. A sensitive probe was planted at the center of this circle to measure illumination intensity (lux).

Table 1 Weather conditions during field surveys

Date	Time	Weather	Temperature (ºC)
16/05	1230h-1600h	Sunny	22.8 (20.7-26.5)
21/05	0900h-1230h	Sunny	24.1 (17.1-31.8)
24/05	0900h-1230h	Cloudy	24.8 (20.4-31)
25/05	0900h-1230h	Sunny	26.4 (23.2-32)
27/05	0900h-1600h	Overcast to cloudy	24.1 (22.3-29.4)
01/06	0900h-1600h	Sunny	26.6 (22.7-32.3)
07/06	0900h-1600h	Overcast to cloudy	26.9 (22.0-34.3)
25/06	0900h-1600h	Overcast to sunny	25.4 (20.8-32)
06/07	0900h-1230h	Showers to cloudy	29.6 (26.0-34.0)
07/07	0900h-1600h	Showers to cloudy	26.4 (26.0-36.0)
09/07	0900h-1600h	Cloudy to sunny	29.6 (26.0-36.0)

Statistical analysis

Data were analyzed using STATISTICA (v6.0). The normality and homogeneity of variance of all data were checked by Kolmogorov-Simirnov tests and Bartlet tests, respectively; no parameters required transformation before statistical analyses. The percentage of active *S. indicus* during a survey was equal to the numbers of observed active *S. indicus* during a survey divided by the total numbers of observed *S. indicus* during a survey, multiplied by 100. Contingency tables and *G*-tests were used to analyze age-related activity patterns and habitat type, and activity frequencies during each time period. Two-factor ANOVA was used to determine the effects of age and survey time on environmental temperature and illumination intensity of the active area. One-factor ANOVA was used to determine the effects of age-related individual differences and habitat type on environmental temperature and illumination intensity of the active area. Partial correlation was used to check correlations between numbers of active individuals during a survey period, environmental temperature and illumination intensity of the active area. Group differences were compared using Tukey's *post hoc* test. All data were expressed as mean±*SE* and statistical significance was taken at α=0.05.

RESULTS

We collected 404 *S. indicus* (211 juveniles and 193 adults), and acquired parameters for habitat type, environmental temperature and illumination intensity in active areas. Body size was measured in 96 individuals (31 juveniles and 65 adults). The SVL of adults (74.7± 0.6 mm, 65.8-91.3 mm) was longer than that of juveniles (60.5±0.7 mm, 46.0-64.7 mm) ($F_{1, 94}$=205.82, P<0.001) and no overlap was found between the SVL ranges of adults and juveniles. The activity patterns of adults and juveniles during each survey period were comparable (G=9.04, df=6, P=0.171) (Figure 1A). However, when data from adults and juveniles were grouped together, differences in the proportions of active individuals during each survey period were found (G=178.22, df=6, P<0.001). For example, two activity peaks occurred at 1000-1200 h and 1300-1500 h, and individuals were more active during 1000-1200 h (Figure 1B).

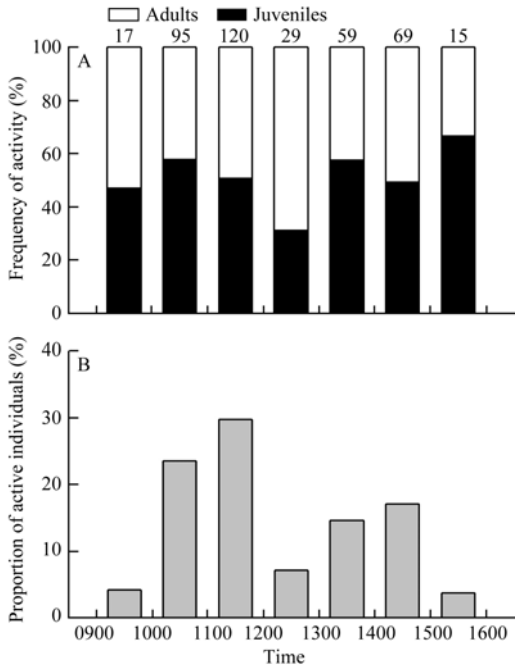

Figure 1 Activity frequency of juvenile and adult *Sphenomorphus indicus* (A) and proportion of active individuals at survey times (B)
Numbers above bars indicate sample size for each time.

Both age and survey time influenced the environmental temperature of areas of activity in *S. indicus*, but the age × urvey time interaction did not. The environmental temperature of areas of adult activity (24.8±0.2 °C) was higher than for juveniles (24.1±0.2 °C) (Tukey's test, P<0.001). The environmental temperatures during 0900-1000 h and 1100-1200 h were both higher that during 1400-1500 h (Tukey's test, both P<0.03); no differences were found across other survey periods (Tukey's test, all P>0.05).

Survey time influenced illumination intensity of the areas frequented by active *S. indicus*, but age and the age× survey time interaction did not. The illumination intensity during 1000-1200 h was higher than during 1400-1600 h (Tukey's test, all P<0.04); no differences were found among other survey periods (Tukey's test, all P>0.05) (Figure 2, Table 2). During each survey period, the number of active individuals, environmental temperature and illumination intensity of the active area were positively correlated (all P<0.04).

Table 2 Statistical results of environmental temperature and illumination in areas where *Sphenomorphus indicus* are active

	Environmental tempera-ture			Illumination intensity		
	F	*df*	*P*	F	*df*	*P*
Age	3.88	1, 390	<0.001	1.10	1, 390	0.295
Measurement time	8.00	6, 390	<0.01	4.58	6, 390	<0.001
Interaction	0.92	6, 390	0.480	0.97	6, 390	0.448

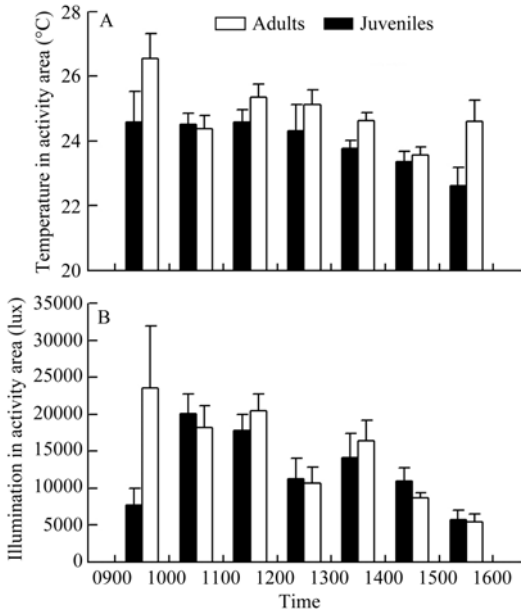

Figure 2 Environmental temperature (A) and illumination intensity (B) of areas where *Sphenomorphus indicus* are active over different survey times

Habitat type in the activity areas did not affect either environmental temperature ($F_{1,402}$=0.05, P=0.829) or illumination intensity ($F_{1,402}$=2.49, P=0.115). Habitat selection between adults and juveniles was different (G=4.70, df=1, P<0.04) (Figure 3).

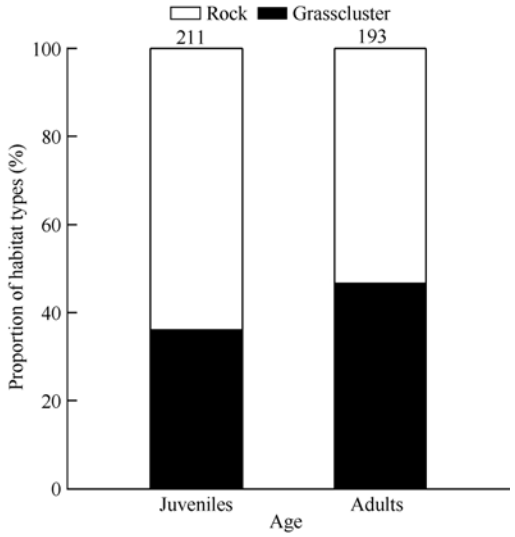

Figure 3 Proportion of habitat types selected by active juvenile and adult *Sphenomorphus indicus*

DISCUSSION

The activity patterns of reptiles is affected by many biotic and

abiotic factors (Cloudsley-Thompson, 1961; Oishi et al, 2004), including age-related energy requirements among different individuals (Liu et al, 2008; Mautz & Nagy, 1987; Oishi et al, 2004; Paulissen, 1987;). For example, the daily activity of common lizard (*Lacerta vivipara*) in juveniles is started later and shorter than in adults (Liu et al, 2008). Here, activity patterns were similar between adult and juvenile *S. indicus* (Figure 1A), indicating that because the habitat of *S. indicus* is relatively shady, wet and closed with high food abundance, skinks are less likely to compete with each other over food. It appears that niche separation over activity time distribution is not induced among individuals of different ages in this species and this is consistent with other studies on diurnal activity rhythms in other diurnal lizards (Liang et al, 2006; Liu et al, 2008; Wen & Zou, 2002;). Activity rhythms with double peaks were found in *S. indicus* during summer. The highest percentage of active individuals occurred during 1000-1200 h, and this decreased during 1200-1300 h and increased again during 1300-1500 h (Figure 1B). Differences between our results and those reported by Wang (1964) on *S. indicus* in Hangzhou are probably the result of local weather and geographic conditions.

As typical ectotherms, the biological function and behavioral performance of reptiles are significantly influenced by the thermal environment (Angilletta et al, 2002; Angilletta, 2009; Shu et al, 2010; Vermunt et al, 2014). Extreme temperatures can be harmful to individuals and good fitness requires a suitable temperature range (Clusella-Trullas & Chown, 2014; Shen et al, 2013). We found that the mean environmental temperature of the active areas frequented by adult *S. indicus* was 0.7 °C higher than the areas used by juveniles (Figure 2); a similar phenomenon has been observed in other thermal biology studies on the Iberian wall lizard (*Podarcis hispanica atrata*), the Mongolia racerunner (*Eremias argus*) and the multi-ocellated racerunner (*Eremias multiocellata*) (Castilla & Bauwens, 1991; Tang et al, 2013; Xu & Ji, 2006). These age-related differences in body temperature and environmental temperature of habitat may be correlated with body size because a small body size is usually characterized by higher thermo-conductivity but weaker heat storage capacity (Castilla & Bauwens, 1991; Tang et al, 2013; Xu & Ji, 2006). Moreover, the differences in feeding activity and predator avoidance during development may induce variation in thermal environments (Christian & Bedford, 1995; Hertz et al., 1993). The similar illumination intensities among habitats of individuals at different ages (Figure 2) indicate that illumination intensity does not affect habitat selection. However, temporal rhythms were found in both adult and juvenile *S. indicus*, i.e., the environmental temperature and illumination intensity of the active areas were both higher in mornings (0900-1200 h) than afternoons (1400-1600 h) (Figure 2), indicating that the rhythms of *S. indicus* choosing environmental factors are consistent with diurnal activity patterns. Positive correlations among the number of active individuals, environmental temperature and illumination intensity also indicate that the activity rhythms of *S. indicus* are interwoven with environmental thermal and illuminative factors.

Reptiles choose optimal habitats to obtain more thermal resources and a better chance of obtaining food (Wang, 1964; Strickland & McDonald, 2006; Buckland et al, 2014). Our study found that juvenile *S. indicus* preferred rock habitats (64%) during diurnal activity (Figure 3), consistent with Wang (1964). However, neither the environmental temperature nor illumination intensity differed between rock habitat and grass habitat, suggesting that the reason juveniles choose rock habitat is not based on acquiring more heat and illumination. The optimal physiological function and behavioral performance of lizards changes during development (Tang et al, 2013; Xu & Ji, 2006), therefore, lizards at different ages should choose different habitats to meet their physiological requirements and avoid predators (Irschick et al, 2000). For example, two species of anole lizards (*Anolis lineatopus* and *Anolis gundlachi*) in India choose habitats located in low and narrow areas to avoid predators (Irschick et al, 2000). Because the dark brown body color of *S. indicus* (Huang, 1999) is close to the color of rocks, we assume that juveniles prefer moving on rocks so as to avoid predators. We therefore predict that active *S. indicus* select optimal habitats with different environmental temperatures and types to reach the physiological needs particular to their age classes.

ACKNOWLEDGEMENTS

We are grateful to Shi-Liang QIN, Yu YU, Xiao-Wei WANG, Jian-Yang XIE, Li-Shuang ZHANG, Qiong-Lu ZHANG, Xue-Ya ZHANG, Xiao-Ning ZHOU for their help during this research.

REFERENCES

Amarasekare P, Coutinho RM. 2014. Effects of temperature on intraspecific competition in ectotherms. *American Naturalist,* **184**(3): E50-E65.

Angilletta MJ Jr. 2009. Thermal Adaptation: A Theoretical and Empirical Synthesis. Oxford: Oxford University Press.

Angilletta MJ Jr, Niewiarowski PH, Navas CA. 2002. The evolution of thermal physiology in ectotherms. *Journal of Thermal Biology,* **27**(4): 249-268.

Beasley JC, Devault TL, Retamosa MI, Rhodes OE. 2007. A hierarchical analysis of habitat selection by raccoons in northern Indiana. *Journal of Wildlife Management,* **71**(4): 1125-1133.

Buckland S, Cole N C, Godsall B, Rodríguez-Pérez JR, Gallagher LE, Henshaw SM, Harris S. 2014. Habitat selection of the Mauritian lowland forest day gecko at multiple spatial scales: a baseline for translocation. *Global Ecology and Conservation,* **1**: 71-79, doi: 10.1016/j.gecco.2014.06.001.

Castilla AM, Bauwens D. 1991. Thermal Biology, microhabitat selection, and conservation of the insular lizard *Podarcis hispanica atrata*. *Oecologia,* **85**(3): 366-374.

Castilla AM, Van Damme R, Bauwens D. 1999. Field body temperatures, mechanisms of thermoregulation and evolution of thermal characteristics in Lacertid lizards. *Natura Croatica,* **8**(3): 253-274.

Christian KA, Bedford GS. 1995. Seasonal changes in thermoregulation by the frillneck lizard, *Chlamydosaurus kingii*, in tropical Australia. *Ecology,* **76**(1): 124-132.

Cloudsley-Thompson JL. 1961. Rhythmic Activity in Animal Physiology and Behaviour. New York: Academic Press.

Clusella-Trullas S, Chown SL. 2014. Lizard thermal trait variation at multiple scales: a review. *Journal of Comparative Physiology B,* **184**(1): 5-21.

De La Cruz SEW, Eadie JM, Miles AK, Yee J, Spragens KA, Palm EC, Takekawa JY. 2014. Resource selection and space use by sea ducks during the non-breeding season: implications for habitat conservation planning in urbanized estuaries. *Biological Conservation,* **169**: 68-78.

Dochtermann NA, Jenkins SH, Swartz MJ, Hargett AC. 2012. The roles of competition and environmental heterogeneity in the maintenance of behavioral variation and covariation. *Ecology,* **93**(6): 1330-1339.

Downes S, Shine R. 1998. Heat, safety or solitude? Using habitat selection experiments to identify a lizard's priorities. *Animal Behaviour,* **55**(5): 1387-1396.

Hall CAS, Stanford JA, Hauer FR. 1992. The distribution and abundance of organisms as a consequence of energy balances along multiple environmental gradients. *Oikos,* **65**(3): 377-390.

Hart SP, Marshall DJ. 2012. Advantages and disadvantages of interference-competitive ability and resource-use efficiency when invading established communities. *Oikos,* **121**(3): 396-402.

Hertz PE, Huey RB, Stevenson R. 1993. Evaluating temperature regulation by field-active ectotherms: the fallacy of the inappropriate question. *The American Naturalist,* **142**(5): 796-818.

Hódar JA, Pleguezuelos JM, Poveda JC. 2000. Habitat selection of the common chameleon (*Chamaeleo chamaeleon*) (L.) in an area under development in southern Spain: implications for conservation. *Biological Conservation,* **94**(1): 63-68.

Huang QY. 1999. *Sphenomorphus indicus* (Gray, 1853). *In*: Zhao EM, Zhao KT, Zhou KY. Fauna Sinica, Reptile Vol. 2, Squamata, Lacertilia. Beijing: Science Press, 340-349. (in Chinese)

Huey RB. 1982. Temperature, physiology, and the ecology of reptiles. *In*: Gans C C, Pough FH. Biology of the Reptilia, Vol. 12. New York: Academic Press, 25-91.

Irschick DJ, Macrini TE, Koruba S, Forman J. 2000. Ontogenetic differences in morphology, habitat use, behavior, and sprinting capacity in two West Indian *Anolis* lizards. *Journal of Herpetology,* **34**(3): 444-451.

Ji X, Du WG. 2000. Sexual dimorphism in body size and head size and female reproduction in a viviparous skink, *Sphenomorphus indicus*. *Zoological Research,* **21**(5): 349-354. (in Chinese)

Johnson DH. 1980. The comparison of usage and availability measurements for evaluating resource preference. *Ecology,* **61**(1): 65-71.

Liang WB, Zhang YX, Su P, Long Q, Huang JQ. 2006. Observation on time budget of *Shinisaurus crocodilurus* in captivity. *Sichuan Journal of Zoology,* **25**(2): 264-266. (in Chinese)

Liu P, Liu ZT, Li DW, Zhao WG. 2008. Diurnal activity rhythm and time budget of *Lacerta vivipara* in simulated habitat. *Chinese Journal of Ecology,* **27**(12): 2146-2152. (in Chinese)

Manicom C, Schwarzkopf L. 2011. Diet and prey selection of sympatric tropical skinks. *Austral Ecology,* **36**(5): 485-496.

Manly BFJ, McDonald LL, Thomas DL, McDonald TL, Erickson WP. 2002. Resource Selection by Animals: Statistical Design and Analysis for Field Studies. 2nd ed. Netherlands: Kluwer Academic Publishers.

Marler CA, Walsberg G, White ML, Moore M. 1995. Increased energy expenditure due to increased territorial defense in male lizards after phenotypic manipulation. *Behavioral Ecology and Sociobiology,* **37**(4): 225-231.

Mautz WJ, Nagy KA. 1987. Ontogenetic changes in diet, field metabolic rate, and water flux in the herbivorous lizard *Dipsosaurus dorsalis*. *Physiological Zoology,* **60**(6): 640-658.

Oishi T, Nagai K, Harada Y, Naruse M, Ohtani M, Kawano E, Tamotsu S. 2004. Circadian rhythms in amphibians and reptiles: ecological implications. *Biological Rhythm Research,* **35**(1-2): 105-120.

Oppel S, Schaefer HM, Schmidt V, Schröder B. 2004. Habitat selection by the pale-headed brush-finch (*Atlapetes pallidiceps*) in southern Ecuador: implications for conservation. *Biological Conservation,* **118**(1): 33-40.

Paulissen MA. 1987. Optimal foraging and intraspecific diet differences in the lizard *Cnemidophorus sexlineatus*. *Oecologia*, **71**(3): 439-446.

Razgour O, Hanmer J, Jones G. 2011. Using multi-scale modelling to predict habitat suitability for species of conservation concern: the grey long-eared bat as a case study. *Biological Conservation,* **144**(12): 2922-2930.

Shen JW, Meng FW, Zhang YP, Du WG. 2013. Field body temperature and thermal preference of the big-headed turtle *Platysternon megacephalum*. *Current Zoology,* **59**(5): 626-632.

Shu L, Zhang QL, Qu YF, Ji X. 2010. Thermal tolerance, selected body temperature and thermal dependence of food assimilation and locomotor performance in the Qinghai toad headed lizard, *Phrynocephalus vlangalii*. *Acta Ecologica Sinica,* **30**(8): 2036-2042. (in Chinese)

Stamps JA, Tanaka S. 1981. The relationship between food and social behavior in juvenile lizards. *Copeia,* **1981**(2): 422-434.

Strickland MD, McDonald LL. 2006. Introduction to the special section on resource selection. *Journal of Wildlife Management,* **70**(2): 321-323.

Tang XL, Yue F, He JZ, Wang NB, Ma M, Mo JR, Chen Q. 2013. Ontogenetic and sexual differences of thermal biology and locomotor performance in a lacertid lizard, *Eremias multiocellata*. *Zoology,* **116**(6): 331-335.

Thomas DL, Taylor EJ. 1990. Study designs and tests for comparing resource use and availability. *Journal of Wildlife Management,* **54**(2): 322-330.

Vermunt A, Hare KM, Besson AA. 2014. Unusual change in activity pattern at cool temperature in a reptile (*Sphenodon punctatus*). *Journal of Thermal Biology,* **42**: 40-45.

Wang PC. 1964. Ecology of four lizards in Hangzhou (1): distribution, activity rhythm and food habits. *Chinese Journal of Zoology,* **6**(2): 70-76. (in Chinese)

Wasko DK, Sasa M. 2012. Food resources influence spatial ecology, habitat selection, and foraging behavior in an ambush-hunting snake (Viperidae: *Bothrops asper*): an experimental study. *Zoology,* **115**(3): 179-187.

Webb J. 1996. Ecology of A Threatened Snake Species, *Hoplocephalus bungaroides* (Elapidae). Ph. D. thesis, University of Sydney, Sydney.

Wen CY, Zou PZ. 2002. Preliminary studies on population ecology and diet of *Eumeces chinensis* in the north of Guangdong province. *Journal of Guangzhou University(Natural Science Edition),* **1**(3): 19-22. (in Chinese)

Xu XF, Ji X. 2006. Ontogenetic shifts in thermal tolerance, selected body temperature and thermal dependence of food assimilation and locomotor performance in a lacertid lizard, *Eremias brenchleyi*. *Comparative Biochemistry and Physiology Part A: Molecular & Integrative Physiology,* **143**(1): 118-124.

Microsatellite analysis of genetic diversity and population structure of freshwater mussel (*Lamprotula leai*)

Jin-Jin MIN[1], Rong-Hui YE[2,*], Gen-Fang ZHANG[2], Rong-Quan ZHENG[1,*]

[1] *Institute of Ecology*, *Zhejiang Normal University*, *Jinhua Zhejiang* 321004, *China*

[2] *Jinhua Polytechnic*, *Jinhua Zhejiang* 321004, *China*

ABSTRACT

Lamprotula leai is one of the most commercially important freshwater pearl mussels in China, but there is limited data on its genetic diversity and population structure. In the present study, 119 individuals from four major geographical populations were investigated using 15 microsatellite loci identified via cross-species amplification. A total of 114 alleles were detected, with an average of 7.6 alleles per locus (range: 2 to 21). Among the four stocks, those from Hung-tse Lake and Poyang Lake had the lowest (0.412) and highest (0.455) observed heterozygosity respectively. The polymorphism information content (*PIC*) ranged from 0.374 to 0.927 (mean: 0.907). AMOVA showed that 12.56% and 44.68% genetic variances were among populations and within individuals, respectively. Pairwise *Fst* ranged from 0.073 to 0.146, indicating medium genetic differentiation among the populations. In aggregate, our results suggest that inbreeding is a crucial factor accounting for deviations from Hardy–Weinberg equilibrium at 12 loci. Moreover, the genetic distance among four stocks ranged from 0.192 to 0.890. Poyang Lake and Hung-tse Lake were clustered together, joined with Dongting Lake and Anqing Lake. Given that specimens from Hung-tse Lake showed the highest average allele richness, expected heterozygosity and *PIC*, this location may be the source of the highest quality germplasm resources and the stock from this area may be the best for future breeding efforts.

Keywords: *Lamprotula leai*; Freshwater mussel; Genetic diversity; Population structure; Microsatellite loci

INTRODUCTION

Genetic diversity is important for sustainable exploitation of cultured resources (Afanas'ev et al, 2006; Laikre et al, 2005), especially as the exploitation of aquatic stocks and environmental degradation of habitat becomes more commonplace. Higher levels of genetic diversity among these stocks often grants them greater ability to respond to environmental changes, artificial selection and pathogen infection, all of which tend to occur in during intensified aquaculture (Liu & Yao, 2013; Wu et al, 2013). For example, *Lamprotula leai* is an endemic species distributed in large and medium rivers and lakes across China (Hu, 2005) that are widely used in pearl aquaculture and indigenous handicrafts due to their large shell, strong ability to secrete pearls, and thick nacre (Wang et al, 2007). Likewise, this mussel is widely consumed as food throughout China (Liu et al, 1979). Despite the importance of this species, little is known about the current state of its genetic diversity, except that among cultured species there is germplasm degradation and general declines genetic diversity, potentially due to intensive farming and the method of cultivation (Ling, 2005). Due to the intensive cultivation of this species, it is now listed as a first-class protected aquatic wildlife species in Anhui province and second-class protected species in Hubei province (Xu et al, 2012).

To date, most of the research into *L. leai* has focused on age and growth (Ling et al, 2005), conservation biology (Ling, 2005), embryonic development (Zhang et al, 2009), abnormal development and effective accumulated temperature of parasitic glochidium (Zhang et al, 2010a), and growth and development of juvenile mussels (Zhang et al, 2010b). However, little work has been done on this species' genetic diversity and population structure. One strategy to improve our understanding of population structure and genetic diversity of many aquaculture species is molecular analysis (Liu & Corde, 2004). Microsatellite markers have been shown to be suitable tools to assess genetic diversity because of their intrinsic genetic characteristics, including high

Received: 28 May 2014; Accepted: 03 December 2014

Foundation items: Public Welfare Projects of Technology Office in Zhejiang Province (2011C32SA700049); Major Science and Technology Specific Projects of Zhejiang Province (2012C12907-9); Science and Technology Plan Projects of Jinhua City (2011A22020)

*Corresponding authors, E-mails: yeronghui@163.com; zhengrq@zjnu.cn

DOI:10.13918/j.issn.2095-8137.2015.1.34

polymorphism, stability and specificity, and co-dominant inheritance (Sun et al, 2008). More promisingly for studying *L. leai,* microsatellites have been previously used to analyze genetic diversity in several mollusks, including *Hyriopsis cumingii* (Ji, 2007), *Cristaria plicata* (Ji et al, 2007), *Pinctada martensii* (Yan et al, 2009), and *Anodonta woodiana* (Wang et al, 2011a). To date, 18 pairs of microsatellite primers have been isolated using magnetic bead hybridization and 5'-anchored PCR methods (Xu et al, 2011, 2012). In this study, we used these microsatellites to analyze the genetic relationships among four different stocks of *L. leai* and provide a novel theoretical basis for genetic resource protection and genetic management.

MATERIALS AND METHODS

Sample collection and DNA isolation

Freshwater mussel specimens originating from four geographical locations across China—Poyang Lake (PY), Dongting Lake (DT), Hung-tse Lake (HZ), and Anqing Lake (AQ)—were obtained from the Weiwang Pearl Cultivation Base in Zhejiang Province (Figure 1), with 31, 31, 28, and 29 samples respectively from PY, DT, HZ and AQ (Hale et al, 2012). Genomic DNA was extracted from muscular tissue following a standard phenol: chloroform protocol as published previously (Sambrook & Russell, 2001).

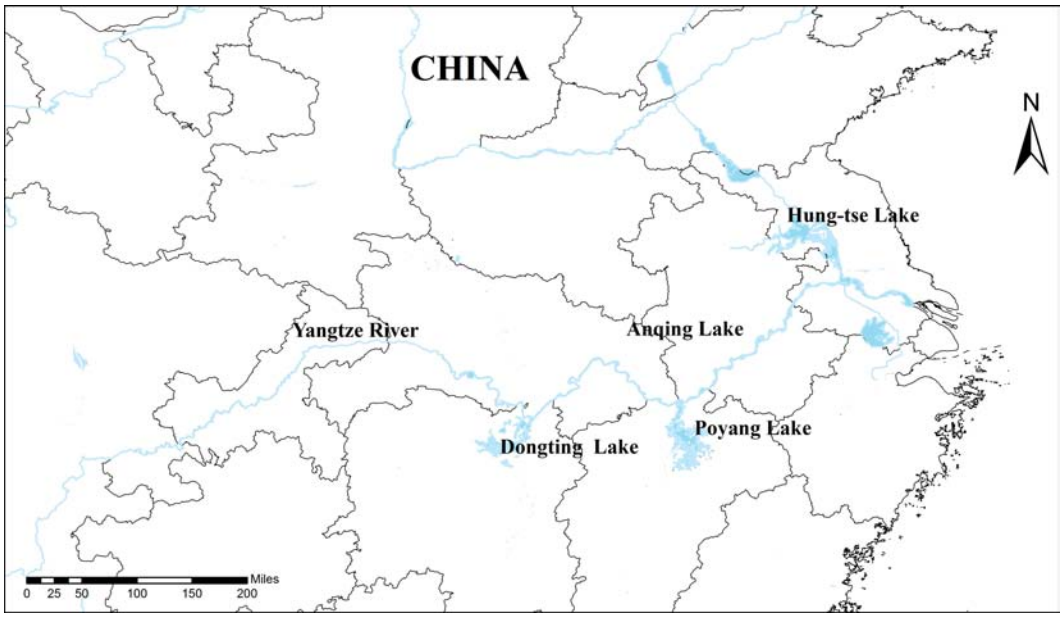

Figure 1 Sampling locations of four *Lamprotula leai* stocks in China

Microsatellite amplification in *L. leai*

We used microsatellite primers published for *H. cumingii* (Bai et al, 2009; Li et al, 2007; Luo, 2006; Wang et al, 2006; Xu et al, 2010; Zhu et al, 2010) and other species closely related to *L. leai* (Ji, 2007; Launey & Hedgecock, 2001). A total of 107 candidate primer pairs (see supplemental Table 1, supporting information of http://www.zoores.ac.cn/) were synthesized (Shanghai Sangon Company) and each microsatellite was amplified in a 25 μL PCR containing 50 ng of DNA, 1 μL each of 10 μmol/L primer, 2.5 μL of 10× buffer, 2 μL of dNTP (10 mmol/L), 1 U of Taq polymerase (5 U/μL), and 17.3 μL of ddH_2O. PCR was conducted under the following conditions: 4 min denaturation at 94 °C 32 cycles of 30 s at 94 °C, 30 s at specific annealing temperatures, and 30 s at 72 °C; and a final extension at 72 °C for 10 min. PCR products were electrophoresed on 2% agarose gel, using 0.5% TBE buffer. Fragment sizes were determined by gel imaging analysis based on DNA Marker (ΦX174-Hinc II digest). Finally genotypes were exported to Excel tables for data analysis (An et al, 2012).

Data analysis

The allele number (N_A) and observed (H_O) and expected (H_E) heterozygosity were analyzed using Popgene 1.32 (Yeh et al, 1999). Allele richness (A_R) was calculated using FSTAT 2.9.3 (Hered, 1995). Since allele number is influenced by sample size, we used allele richness for comparison (Yan & Zhang, 2004). Deviations from Hardy-Weinberg equilibrium (HWE) and linkage disequilibrium were estimated using Genepop 4.2 (Rousset, 2008). Meanwhile the Bonferroni correction was conducted using SPSS 18.0. The presence of null alleles was detected using Micro-checker 2.2.3 (Van Oosterhout et al, 2004). Polymorphism information content (*PIC*) was then confirmed using Microsatellite Toolkit (Zhang et al, 2010c).

The *F*-statistics (*Fis*, *Fst*, and *Fit*) and gene flow (N_m) were calculated by Genetix 4.05. AMOVA was conducted using Arlequin 3.1 to estimate genetic variation within and between populations as well as for individuals (Excoffier et al, 2005). Popgene 1.32 was used to calculate Nei's unbiased genetic distance between populations (Nei, 1978). A UPGMA system evolutionary tree was constructed using MEGA 5.05.

RESULTS

A total of 15 polymorphic microsatellite loci were detected from 107 candidate primer pairs in the four tested stocks of *L. leai* via cross-species amplification. The values of N_A, A_R, H_O, H_E, *PIC* and *P* for testing HWE ($P_{H\text{-}W}$) at each locus in each stock are presented in Table 1. Totally, 114 alleles were detected. The allele number at each locus ranged from 2 to 21 (mean: 7.6). Overall, specimens from HZ showed the highest average allele richness (7.743). *PIC* values for the four stocks ranged from 0.374 to 0.927 (mean: 0.907). Collectively, stocks from DT (0.412) and AQ (0.455) had the lowest and highest *Ho*, respectively, while AQ had the lowest H_E (0.791) whereas HZ had a relatively high H_E value (0.868). When the four stocks were treated as one population, no significant linkage disequilibrium among the loci was detected (P>0.05), though 12 loci showed significant (P<0.05) or highly significant (P<0.01) deviations from HWE (Table 1).

F-statistics for 15 microsatellite loci among all four *L. leai* stocks placed the mean values of *Fis*, *Fst* and *Fit* at 0.462, 0.523 and 0.114, respectively. Pairwise comparisons revealed that the *Fst* ranged from 0.073 to 0.146 (0.05<*Fst*<0.15), indicating a medium differentiation among the four populations that was moderately closer to no differentiation (Wright, 1965). The number of migrats per generation (*Nm*) ranged from 1.46 to 3.18 (Table 2).

AMOVA analysis showed that most (44.68%) of the genetic variation originated within individuals with only 12.56% variation between the four tested populations (Table 3). The genetic distance matrix data indicated that PY and HZ populations had the smallest genetic distance (0.192) and the highest genetic similarity (0.563). Likewise, populations from DT and PY showed the greatest genetic distance (0.890) and lowest genetic similarity (0.287) (Table 4). The UPGMA dendrogram further showed that PY and HZ grouped together and then gathered with DT and AQ, which clustered together (Figure 2).

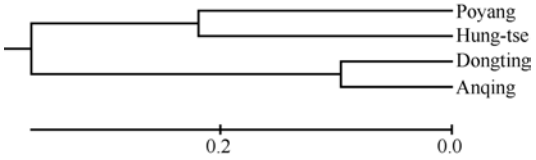

Figure 2 UPGMA dendrogram based on Nei's genetic distances among *Lamprotula leai* stocks

DISCUSSION

Genetic diversity within populations

Higher levels of genetic diversity among intensively cultivated stocks of aquatic species typically grants enhanced evolutionary potential for dealing with enviromental change, artificial selection, and pathogen infection (Liu & Yao, 2013; Wu et al, 2013), thereby improving yields and minimizing economic losses associated with these factors. In the present study, we wanted to provide basic data on the genetic diversity and stock structure of *L. leai* using microsatellite markers to provide a foundaion for a more comprehensive genetic resource protection and genetic management. Previous studies found that sample size do not always correlate with expected heterozygosity, which can be a comparison parameter (Maudet et al, 2002; Sun, 1996). Compared with other mollusks, *L. leai* showed a higher than expected heterozygosity. Previously, Li et al (2009) used eight microsatellite markers to investigate the genetic status of *H. cumingii*, with an expected heterozygosity of *H. cumingii* in PY at 0.706, which was less than the value for *L. leai* (0.835) that we arrived at in this study. Shen et al. (2013) had previously isolated 14 polymorphic loci for *Mytilus coruscus* with an expected heterozygosity averaged at 0.82, while Xu et al (2011) estimated the mean expected heterozygosity 0.683 and 0.759 using magnetic bead hybridization and 5'-anchored PCR methods to isolate microsatellite markers of *L. leai.* The disparity in these disparate findings suggests that cross-amplification may be more effective as compared with other methods. This supposition is supported by our present results, we showed that the overall level of heterozygosity was high and the *PIC* of 15 loci in this study showed high polymorphism (*PIC*>0.5). Together, these findings indicated that the stocks of *L. leai* have abundant genetic diversity (Botstein et al, 1980), but also that microsatellite loci can be used to analyze the genetic diversity and structure of mollusks like *L. leai*. More specifically, our findings showed that specimens from Hung-tse Lake had the highest A_R, average H_E and *PIC*, suggesting specimens from this location have a potentially larger amount of genetic resources, making them ideal candidate for future breeding efforts in China.

Genetic differentiation among populations

Genetic differentiation is commonly measured by *Fst*, *Nm* and genetic distance. Pairwise comparisons revealed medium genetic differentiation among the populations. AMOVA analysis also showed a 12.56% variation existed among these stocks (Wang et al, 2011b). Genetic differentiation can be caused by several different factors, including migration, genetic drift and gene mutation. Since the *Nm* values found in this study were all greater than 1, it is likely that genetic drift is not the main factor among *L. leai* (Slatkin, 1985). However, it seems more likely that this phenomenon may have been caused by short-time farming, as intensive farming could affect the variation among stocks.

The UPGMA cluster indicated that DT and AQ clustered together. One potential reason for this patter is that individuals of *L. leai* in Anqing Lake may have initially came from Dongting Lake. This possibility caused by either manual intervention or species migration. Study showed that genetic communication may related to geographic location (Ma et al, 2007). Here Poyang Lake in the middle and lower reaches of the Yangtze River clustered with Hung-tse Lake, which is in the downstream of Huaihe River (Xu et al, 2013). These two lakes in close geographic proximity had similar genetic relationships. However, this conclusion remains to be more verification.

Table 1 Allele number (N_A), allele richness (A_R), observed heterozygosity (H_O) and expected heterozygosity (H_E), polymorphism information content (*PIC*), and *P* value for testing Hardy–Weinberg equilibrium ($P_{H\text{-}W}$) in four *Lamprotula leai* stocks

GenBank accession no. /Locus	PY(*n*=28)						DT(*n*=31)						HZ(*n*=29)						AQ(*n*=31)						All stocks					
	N_A	A_R	*Ho*	H_E	*PIC*	$P_{H\text{-}W}$	N_A	A_R	*Ho*	H_E	*PIC*	$P_{H\text{-}W}$	N_A	A_R	*Ho*	H_E	*PIC*	$P_{H\text{-}W}$	N_A	A_R	*Ho*	H_E	*PIC*	$P_{H\text{-}W}$	N_A	A_R	*Ho*	H_E	*PIC*	$P_{H\text{-}W}$
GQ302635	12	9.87	0.679	0.922	0.898	0.367	11	10.98	0.355	0.889	0.863	0.000	12	10.96	0.483	0.917	0.893	0.006	10	9.56	0.452	0.849	0.815	0.004	12	10.75	0.487	0.966	0.961	0.000
GQ302636	5	4.90	0.357	0.779	0.726	0.000	7	6.99	0.226	0.812	0.769	0.000	5	4.00	0.241	0.763	0.710	0.002	7	6.00	0.484	0.811	0.771	1.000	5	4.00	0.328	0.820	0.793	0.079
GQ302646	9	7.96	0.643	0.888	0.859	0.000	9	7.97	0.806	0.903	0.879	0.000	9	8.86	0.793	0.854	0.820	1.000	11	10.00	0.161	0.914	0.891	0.000	9	8.02	0.597	0.960	0.954	0.000
GQ302647	4	3.00	0.393	0.788	0.737	0.000	2	1.86	0.226	0.508	0.375	0.000	10	9.89	0.241	0.895	0.867	0.000	3	2.79	0.419	0.648	0.560	1.000	4	3.75	0.319	0.851	0.831	0.093
GQ302656	5	4.00	0.607	0.721	0.662	1.000	3	2.49	0.548	0.665	0.579	0.022	3	2.89	0.586	0.636	0.572	0.000	3	2.89	0.516	0.529	0.466	0.022	5	4.29	0.563	0.852	0.832	0.044
HCM01	9	7.00	0.214	0.892	0.865	0.000	9	8.89	0.194	0.917	0.894	0.000	8	7.00	0.207	0.909	0.885	0.000	2	1.98	0.355	0.506	0.374	0.000	9	7.75	0.244	0.942	0.934	0.000
HCM02	5	4.00	0.643	0.788	0.737	1.000	4	3.68	0.581	0.747	0.685	0.004	9	8.02	0.517	0.886	0.857	0.000	4	3.00	0.387	0.690	0.628	1.000	5	4.38	0.529	0.880	0.864	0.891
HCM08	7	5.96	0.214	0.933	0.910	0.000	9	8.78	0.387	0.914	0.892	0.000	7	6.57	0.345	0.889	0.862	0.000	8	7.67	0.290	0.940	0.920	0.000	7	6.69	0.311	0.971	0.965	0.000
HCM11	6	5.89	0.464	0.756	0.711	0.000	7	6.57	0.290	0.852	0.818	0.000	7	6.38	0.414	0.865	0.832	0.000	6	6.00	0.355	0.821	0.779	1.000	6	4.89	0.378	0.916	0.906	0.000
HCM13	5	4.89	0.536	0.746	0.690	0.015	3	2.79	0.484	0.721	0.658	0.002	11	10.92	0.414	0.905	0.880	0.000	7	6.89	0.484	0.876	0.846	0.001	5	4.25	0.479	0.920	0.910	0.000
HCM14	4	3.67	0.429	0.694	0.624	0.011	5	4.89	0.452	0.787	0.744	0.000	10	8.96	0.276	0.917	0.893	0.000	3	2.18	0.613	0.743	0.682	0.006	4	3.46	0.445	0.899	0.887	0.000
HCM29	11	10.81	0.286	0.920	0.896	0.000	7	6.99	0.355	0.764	0.716	0.000	9	7.99	0.276	0.910	0.885	0.000	7	6.29	0.355	0.861	0.828	0.000	11	9.85	0.319	0.947	0.941	0.000
MP19	10	8.90	0.321	0.896	0.868	0.000	6	5.89	0.452	0.774	0.726	0.002	8	7.93	0.310	0.822	0.781	0.000	11	10.10	0.419	0.898	0.874	1.000	10	8.72	0.378	0.912	0.901	0.021
APS28	4	3.90	0.321	0.847	0.811	0.000	8	7.99	0.323	0.851	0.817	0.000	10	9.99	0.345	0.905	0.879	0.000	8	7.71	0.355	0.833	0.796	0.000	4	3.70	0.336	0.956	0.950	0.000
APS45	18	16.62	0.714	0.948	0.927	0.007	16	14.90	0.581	0.941	0.921	0.000	6	5.79	0.724	0.943	0.922	0.000	21	19.85	0.581	0.943	0.924	0.000	18	16.75	0.647	0.981	0.976	0.000
Mean	7.600	6.758	0.455	0.835	0.795		7.067	6.777	0.417	0.803	0.756		8.267	7.743	0.412	0.868	0.836		7.400	6.861	0.415	0.791	0.744		7.600	6.750	0.424	0.918	0.907	

PY, Poyang Lake; DT, Dongting Lake; HZ, Hung-tse Lake; AQ, Anqing Lake.

Table 2 Pairwise F_{ST} (below the diagonal) and the number of migrants per generation, *N*m (above the diagonal) among four *Lamprotula leai* stocks estimated from 15 microsatellite loci

	PY	DT	HZ	AQ
PY		1.46	3.18	1.47
DT	0.146*		1.75	1.87
HZ	0.073*	0.125*		1.52
AQ	0.146*	0.118*	0.142*	

PY, Poyang Lake; DT, Dongting Lake; HZ, Hung-tse Lake; AQ, Anqing Lake. *: $P<0.05$.

Table 3 AMOVA of 15 microsatellites in the four *Lamprotula leai* stocks

Source of variation	*df*	Sum of squares	Variance components	Percentage of variation
Among stocks	3	187.47	0.90	12.56*
Among individuals within stocks	115	1065.96	3.04	42.76*
Within individuals	119	378.50	3.18	44.68*
Total	237	1631.93	7.12	100

*: $P<0.05$.

Table 4 Nei's unbiased genetic identity (above diagonal) and genetic distance (below diagonal)

	PY	DT	HZ	AQ
PY		0.287	0.563	0.361
DT	0.890		0.398	0.574
HZ	0.438	0.578		0.298
AQ	0.672	0.192	0.768	

PY, Poyang Lake; DT, Dongting Lake; HZ, Hung-tse Lake; AQ, Anqing Lake.

Hardy-Weinberg equilibrium

A total of 12 loci significantly deviated from HWE after Bonferroni correction. Departure from HWE can be attributed to random genetic drift, inbreeding, and null alleles which contribute to heterozygote deficiency (Nei, 1987; Zheng et al, 2009). Using Micro-checker, we found five loci including GQ302635, *HCM08*, *HCM29*, *MP19* and *APS45* with null alleles. This phenomenon is not unusual when analyzing conservation genetics using cross-amplification methods (Harper et al, 2003). However, each locus which departured from HWE can amplify at least one allele in all samples which means that the frequency of null alleles were not enough to affect the analysis (Goodman et al, 2001). In this study, F_{is} was positive and both H_O and H_E had large differences, suggesting an ongoing inbreeding among the tested stocks of *L. leai*. If accurate, then inbreeding is likely a critical factor accounting for departure from HWE, highlighting the need for better management and planned breeding.

Feasibility of cross-species amplification in shellfish

To date, 18 microsatellite loci for *L. leai* have been screened, but developing further microsatellite loci is essential for further more targeted research and for more cross-species applications. The primers derived from the relatively conservative flanking sequences can be used for amplification across species. Some studies in shellfish have shown the feasibility of cross-species amplification method. For instance, Xu et al (2011) isolated and characterized 18 loci in *L. leai*, 10 of which were successfully amplified in three *H. cumingii* populations. Wang et al (2006) confirmed that 13 loci from 32 polymorphic microsatellite primers of *Crassostrea gigas* can amplify specific products in *H. cumingii*. Hai et al (2009) indicated that 17 primers of *Perca schrenkii* were amplified in *P. fluviatilis* and *P. flavescens*, among which 10 pairs showed versatility in the same genus. The microsatellite loci isolated in this study may then provide useful information for further inquiries into shellfish genetic resource information collecting using cross-amplification.

CONCLUSION

In conclusion, the four tested stocks of *L. leai* examined in this study showed both high genetic diversity and medium genetic differentiation, but we also encountered evidence suggesting ongoing inbreeding among the stocks. These results may be related to the life habits and reproductive characteristics of *L. leai,* or to the currently employed methods of farming and aquaculture. Given this result, genetic management should be carried out in order to maintain the genetic integrity before the situation deteriorates (Jia et al, 2012). Based on our results, we suggest that specimens from Hung-tse Lake may be viable parents for systematic breeding and hybrid efforts that may result in offspring that could offset the apparent inbreeding and maintain the genetic diversity we observed. On the whole, however, our results and methodology may be useful in identifying growth traits associated markers, constructing of genetic linkage maps, and marker-assisted breeding of *L. leai*.

ACKNOWLEDGEMENTS

We would like to thank the Weiwang Pearl Cultivation Base for providing

samples. We are also grateful to Professor Yongjiu Chen (Zhejiang Ocean University) for assistance with the manuscript.

REFERENCES

Afanas'ev KI, Rubtsova GA, Malinina TV, Salmenkova EA, Omel'chenko VT, Zhivotovsky LA. 2006. Microsatellite variability and differentiation of hatchery stocks of chum salmon *Oncorhynchus keta* Walbaum in Sakhalin. *Russian Journal of Genetics,* **42**(12): 1694-1702.

An H, Kim MJ, Park K, Cho K, Bae BS, Kim J, Myeong JI. 2012. Genetic diversity and population structure in the heavily exploited Korean rockfish, *Sebastes schlegeli*, in Korea. *Journal of the World Aquaculture Society,* **43**(1): 73-83.

Bai ZY, Yin YX, Hu SN, Wang GL, Zhang XW, Li JL. 2009. Identification of genes involved in immune response, microsatellite, and SNP markers from expressed sequence tags generated from hemocytes of freshwater pearl mussel (*Hyriopsis cumingii*). *Marine Biotechnology,* **11**(4): 520-530. (in Chinese)

Botstein D, White RL, Skolnick M, Davis RW. 1980. Construction of a genetic linkage map in man using restriction fragment length polymorphisms. *American Journal of Human Genetics,* **32**(3): 314-331.

Excoffier L, Laval G, Schneider S. 2005. Arlequin ver. 3.0: An integrated software package for population genetics data analysis. *Evolutionary Bioinformatics,* **1**: 47-50.

Geist J, Rottmann O, Schroder W, Kuhn R. 2003. Development of microsatellite markers for the endangered freshwater pearl mussel *Margaritifera margaritifera* L. (Bivalvia:Unionoidea). *Molecular Ecology Notes,* **3**(1): 444-446.

Goodman SJ, Tamate HB, Wilson R, Nagata J, Tatsuzawa S, Swanson GS, Pemberton JM, McCullough DR. 2001. Bottlenecks, drift and differentiation: the population structure and demographic history of sika deer (*Cervus nippon*) in the Japanese archipelago. *Molecular Ecology,* **10**(6): 1357-1370.

Hai S, Li JL, Liu F, Feng JB. 2009. Isolation of microsatellite loci from *Perca schrenkii* and its universal in related species. *Chinese Journal of Zoology,* **44**: 17-23. (in Chinese)

Hale ML, Burg TM, Steeves TE. 2012. Sampling for microsatellite-based population genetic studies: 25 to 30 individuals per population is enough to accurately estimate allele frequencies. *Plos One,* **7**(9): 1-10.

Harper GL, Maclean N, Goulson D. 2003. Microsatellite markers to assess the influence of population size, isolation and demographic change on the genetic structure of the UK butterfly *Polyommatus bellargus*. *Molecular Ecology,* **12**(12): 3349-3357.

Huvet A, Boudry P, Ohresser M, Delsert C, Bonhomme F. 2000. Variable microsatellites in the Pacific oyster *Crassostrea gigas* and other cupped oyster species. *Animal Genetics,* **31**(1): 71-72.

Hered GJ. 1995. FSTAT (Version 1.2): A computer program to calculate F-statistics. *Journal of Heredity,* **86**(6): 485-486.

Hu ZQ. 2005. Geographical distribution of endemic species of Chinese freshwater bivalves. *Chinese Journal of Zoology,* **40**(6): 80-83. (in Chinese)

Ji W. 2007. Genetic Diversity of Five Freshwater Mussels and Isolation of Microsatellite DNA for *Hyriopsis cumingii* in Qinglan Lake, Jiangxi Province. Master's thesis. Huazhong Agricultural University, Wuhan. (in Chinese)

Ji W, Wei KJ, Zhang GR, Shi ZC. 2007. Microsatellite DNA analysis of genetic diversity in five freshwater mussels in Qinglan Lake Jiangxi Province. *Journal of Agricultural Biotechnology,* **15**(3): 429-433. (in Chinese)

Jia ZY, Zhang YY, Chen SQ, Shi LY. 2012. Genetic diversity and differentiation of masu salmon (*Oncorhynchus masou masou*) between and within cultured populations inferred from microsatellite DNA analysis. *Zoological Research,* **33**(E3-4): E33-E39.

Jones JW, Culver M, David V, Struthers SJ, Ajohnson N, Neves RJ, Brien SJO, Hallerman EM. 2004. Development and characterization of microsatellite loci in the endangered oyster mussel *Epioblasma capsaeformis* (Bivalvia: Unionidae). *Molecular Ecology Notes,* **4**(1): 649-652.

Launey S, Hedgecock D. 2001. High genetic load in the pacific oyster *Crassostrea gigas*. *Genetics,* **159**(1): 255-265.

Laikre L, Palm S, Ryman N. 2005. Genetic population structure of fishes: implications for coastal zone management. *Ambio,* **34**(2): 111-119.

Li JL, Wang GL, Bai ZY. 2009. Genetic variability in four wild and two farmed stocks of the Chinese freshwater pearl mussel (*Hyriopsis cumingii*) estimated by microsatellite DNA markers. *Aquaculture,* **287**(3-4): 286-291.

Li JL, Wang GL, Bai ZY, Yue GH. 2007. Ten polymorphic microsatellites from freshwater pearl mussel, *Hyriopsis cumingii*. *Molecular Ecology Notes,* **7**(6): 1357-1359.

Ling G. 2005. Primary Studies on Conservation Biology of *Lamprotula leai* (Gray). Master's Thesis. Nanchang University, Nanchang. (in Chinese)

Ling G, Wu XP, Ouyang S, Gao JH, Wu HS. 2005. The age and growth of *Lamprotula leal* Gray 1835. *Journal of Nanchang University* (*Natural Science Edition*), **29**(5): 497-499, 507. (in Chinese)

Liu XH, Yao YG. 2013. Characterization of 12 polymorphic microsatellite markers in the Chinese tree shrew (*Tupaia belangeri chinensis*). *Zoological Research,* **34**(E2): E62-E68.

Liu YY, Zhang WZ, Wang YX, Wang EY. 1979. China's Economic Fauna: Freshwater Mollusks. Beijing: Science Press. (in Chinese)

Liu ZJ, Cordes JF. 2004. DNA marker technologies and their applications in aquaculture genetics. *Aquaculture,* **238**: 1-37.

Luo YM. 2006. Genetic Diversity of Four *Hyriopsis cumingii* (Bivalvia: Unionidae) Populations by SSR Analysis. Master's Thesis. Huazhong Agricultural University, Wuhan. (in Chinese)

Ma HT, Chang YM, Yu DM, Sun XW. 2007. Microsatellite variations among four populations of *Eriocheir sinensis*. *Zoological Research,* **28**(2): 126-133. (in Chinese)

Magoulas A, Gjetvag B, Terzoglou V, Zouros E. 1998. Three polymorphic microsatellites in the Japanese oyster, *Crassostrea gigas* (Thunberg). *Animal Genetics,* **29**(1): 69-70.

Maudet C, Miller C, Bassano B, Breitenmoser-Wursten C, Gauthier D, Obexer-Ruff G, Michallet J, Taberlet P, Luikart G. 2002. Microsatellite DNA and recent statistical methods in wild conservation management: applications in Alpine ibex *Capra ibex* (*ibex*). *Molecular Ecology,* **11**(3): 421-436.

Nei M. 1978. Estimation of average heterozygosity and genetic distance from a small number of individuals. *Genetics,* **89**(3): 583-590.

Nei M. 1987. Molecular Evolutionary Genetics. New York: Columbia University Press,

Rousset F. 2008. Genepop'007: a complete re-implementation of the Genepop software for Windows and Linux. *Molecular Ecology Resources,* **8**(1): 103-106.

Sambrook J, Russell DW. 2001. Molecular Cloning: A Laboratory Manual, 3rd ed. New York: Cold Spring Harbor Laboratory Press.

Sekino M, Hamaguchi M, Aranishi F. 2003. Development of novel microsatellite DNA markers from the Pacific oyster *Crassostrea gigas*. *Marine*

Biotechnology (NY), **5**(3): 227- 233.

Shen YB, Bai ZY, Guo SZ, Li JL. 2013. Polymorphic microsatellite loci for population genetics of the hard shelled mussel, *Mytilus coruscus*. *Conservation Genetics Resources,* **5**(1): 121-123.

Slatkin M. 1985. Gene flow in natural populations. *Annual Review of Ecology and Systematics,* **16**(1): 393-430.

Sun M. 1996. Effects of population size, mating system, and evolutionary origin on genetic diversity in *Spiranthes sinensis* and *S. hongkongensis*. *Conservation Biology,* **10**(3): 785-795.

Sun XW, Zhang XF, Zhao YY, Zhang Y, Jia ZY, Chang YM, Lu CY, Liang LQ. 2008. Development and application of microsatellite markers in aquatic species. *Journal of Fishery Sciences of China,* **15**(4): 689-703. (in Chinese)

Van Oosterhout C, Hutchinson WF, Wills DPM, Shipley P. 2004. Microchecker: software for identifying and correcting genotyping errors in microsatellite data. *Molecular Ecology Notes,* **4**(3): 535-538.

Wang GL, Su X, Li JL, Bai ZY. 2011a. Characterization of $(GT)_n$ microsatellite in *Anodonta woodiana* genome. *Chinese Journal of Ecology,* **30**(1): 1-6. (in Chinese)

Wang GL, Wang JJ, Li JL. 2006. Preliminary study on applicability of microsatellite primers developed from *Crassostrea gigas* to genomic analysis of *Hyriopsis cumingii*. *Journal of Fisheries of China,* **30**(1): 15-20. (in Chinese)

Wang GL, Yuan YM, Li JL. 2007. SSR analysis of genetic diversity and phylogenetic relationships among different populations of *Hyriopsis cumingii* from the five lakes of China. *Journal of Fisheries of China,* **31**(2): 152-158. (in Chinese)

Wang L, Meng ZN, Liu XC, Zhang Y, Lin HR. 2011b. Genetic diversity and differentiation of the orange-spotted grouper (*Epinephelus coioides*) between and within cultured stocks and wild populations inferred from microsatellite DNA analysis. *International Journal of Molecular Sciences,* **12**(7): 4378-4394.

Wright S. 1965. The interpretation of population structure by F-statistics with special regard to systems of mating. *Evolution,* **19**(3): 395-420.

Wu SZ, Guan YY, Huang XD, He MX. 2013. Development of 25 novel microsatellite loci and genetic variation analysis in breeding populations of the pearl oyster, *Pinctada fucata*. *Journal of the World Aquaculture Society,* **44**(4): 600-609.

Xu B, Li JL, Wang GL. 2011. Development and characterization of microsatellite loci in *Lamprotula leai*, with cross-amplification in *Hyriopsis cumingii*. *Conservation Genetics Resources,* **3**(3): 545-547.

Xu B, Wang GL, Li JL. 2012. Development of microsatellite markers from *Lamprotula leai*: A comparison of magnetic beads hybridization and 5'-anchored PCR methods. *Chinese Journal of Ecology,* **31**(4): 923-930. (in Chinese)

Xu N, Yang Z, Que YF, Shi F, Zhu B, Xiong MH. 2013. Genetic diversity and differentiation in broodstocks of the endangered Chinese sucker, *Myxocyprinus asiaticus*, using microsatellite markers. *Journal of the World Aquaculture Society,* **44**(4): 520-527.

Xu QQ, Xie J, Zhang SH, Zhao CY, Yuan HW. 2010. Isolation, characterization and polymorphism of microsatell markers in triangle mussel *Hyriopsis cumingii*. *Journal of Fishery Sciences of China,* **17**(6): 1200-1207. (in Chinese)

Yan LN, Zhang DX. 2004. Effects of sample size on various genetic diversity measures in population genetic study with microsatellite DNA markers. *Acta Zoologica Sinica,* **50**(2): 279-290. (in Chinese)

Yan XC, Tong GX, Kuang YY, Liang LQ, Sun XW. 2009. Analysis of genetic diversity between in two cultured populations of *Pinctada Martensii* Dunker cultured populations using microsatellite markers. *Chinese Journal Fisheries,* **22**(1): 5-9. (in Chinese)

Yeh FC, Yang RC, Boyle T. 1999. Popgene version 1.32. Microsoft window-base software for population genetic analysis: a quick user's guide. A joint Project development by the authors, University of Alberta, Center for International Forestry Research, Alberta, Canada.

Zhang GF, Xu SJ, Fang AP. 2009. Preliminary study on the embryonic development of *Lamprotula leai*. *Chinese Journal of Zoology,* **44**(4): 96-101. (in Chinese)

Zhang GF, Xu SJ, Fang AP. 2010a. Parasitic metamorphosis development and effective accumulated temperature of glochidia of *Lamprotula leai*. *Freshwater Fisheries,* **40**(3): 18-22. (in Chinese)

Zhang GF, Xu SJ, Fang AP. 2010b. Development and growth of juvenile *Lamprotula leai*. *Chinese Journal of Zoology,* **45**(5): 105-110. (in Chinese)

Zhang Y, Yu DN, Du WG, Zheng RQ, Yang G. 2010c. Microsatellite DNA analysis of genetic diversity among captive breeding stocks of Chinese pond turtle (*Chinemys reevesii*). *Journal of Fisheries of China,* **34**(11): 1636-1644. (in Chinese)

Zheng RQ, Ye RH, Yu YY, Yang G. 2009. Fifteen polymorphic microsatellite markers for the giant spiny frog, *Paa spinosa*. *Molecular Ecology Resources,* **9**(1): 336-338.

Zhu XY, Zhou YF, Shu MA. 2010. Isolation and genetic diversity analysis of microsatellite in *Hyriopsis cumingii*. *Jiangsu Journal of Agricultural Sciences,* **26**(5): 1026-1031. (in Chinese)

Hydrophilic/hydrophobic characters of antimicrobial peptides derived from animals and their effects on multidrug resistant clinical isolates

Cun-Bao LIU[1], Bin SHAN[2], Hong-Mei BAI[1], Jing TANG[3], Long-Zong YAN[4], Yan-Bing MA[1,*]

[1] *Yunnan Key Laboratory of Vaccine Research and Development on Severe Infectious Diseases, Institute of Medical Biology, Chinese Academy of Medical Sciences and Peking Union Medical College, Kunming Yunnan* 650118*, China*

[2] *Department of Clinical Lab, the First Affiliated Hospital of Kunming Medical University, Kunming Yunnan* 650032*, China*

[3] *Department of Biochemistry and Molecular Biology, Kunming Medical University, Kunming Yunnan* 650500*, China*

[4] *Department of Burn*, *the Second Affiliated Hospital of Kunming Medical University*, *Kunming Yunnan* 650101, *China*

ABSTRACT

Multidrug resistant (MDR) pathogen infections are serious threats to hospitalized patients because of the limited therapeutic options. A novel group of antibiotic candidates, antimicrobial peptides (AMPs), have recently shown powerful activities against both Gram-negative and Gram-positive bacteria. Unfortunately, the viability of using these AMPs in clinical settings remains to be seen, since most still need to be evaluated prior to clinical trials and not all of AMPs are potent against MDR clinical isolates. To find a connection between the characteristics of several of these AMPs and their effects against MDR pathogens, we selected 14 AMPs of animal origin with typical structures and evaluated their *in vitro* activities against clinical strains of extensive drug-resistant *Acinetobacter baumannii*, methicillin-resistant *Staphylococcus aureus*, extended spectrum β-lactamase-producing *Pseudomonas aeruginosa* and extended spectrum β-lactamase-producing *Escherichia coli.* Our results showed that these peptides' hydrophilic/hydrophobic characteristics, rather than their secondary structures, may explain their antibacterial effects on these clinical isolates. Peptides that are amphipathic along the longitudinal direction seemed to be effective against Gram-negative pathogens, while peptides with hydrophilic terminals separated by a hydrophobic intermediate section appeared to be effective against both Gram-negative and Gram-positive pathogens. Among these, cathelicidin-BF was found to inhibit all of the Gram-negative pathogens tested at dosages of no more than 16 mg/L, killing a pandrug-resistant *A. baumannii* strain within 2 h at 4×MICs and 4 h at 2×MICs. Tachyplesin III was also found capable of inhibiting all Gram-negative and Gram-positive pathogens tested at no more than 16 mg/L, and similarly killed the same *A. baumannii* strain within 4 h at 4×MICs and 2×MICs. These results suggest that both cathelicidin-BF and tachyplesin III are likely viable targets for the development of AMPs for clinical uses.

Keywords: Hydrophilic/hydrophobic character; Multidrug resistant clinical isolate; Cathelicidin-BF; Tachyplesin III

INTRODUCTION

Multidrug resistant (MDR) pathogens continue to pose serious threats to hospitalized patients because there are limited effective therapies capable of combatting the infection. Among these pathogens, *Acinetobacter baumannii* is particularly intractable because several of its clinical isolates have gained resistance to nearly all currently available antibiotics, leading it to be described as "extensive drug resistant" (XDR) (Falagas & Karageorgopoulos, 2008). Though work on developing novel cocktails of antibiotics that can be used in tandem may help in the short-run, a long-term solution is urgently needed.

One promising candidate source of novel antibiotic treatments, antimicrobial peptides (AMPs), have gained increased attention. These AMPs, which are innate immune

Received: 28 July 2014; Accepted: 06 November 2014

Foundation items: This study was supported by the Peking Union Medical College (PUMC) Youth Fund and the Fundamental Research Funds for the Central Universities, China (333203084)

*Corresponding author, E-mail: yanbingma@126.com

DOI:10.13918/j.issn.2095-8137.2015.1.41

molecules that are widely distributed among animals, have previously exhibited powerful killing effects to both Gram-negative and Gram-positive bacteria. Unfortunately, clinical applications of these AMPs have made relatively little progress over the last decade and have been rarely reported (Hancock & Sahl, 2006; Lipsky et al, 2008; Vaara, 2009). The reasons for this lack of progress are multifaceted; aside from the instability of these peptides *in vivo*, three further reasons warrant some explanation. First, not all of the currently AMPs reported are potent AMPs. Traditionally, AMPs are purified directly from tissues following their activities, which may assure their antimicrobial activities. Currently, a growing number AMPs are simply predicted via bioinformatics, and then sometimes synthesized as peptides to test for antimicrobial activities. Typically, these synthetic AMPs are found to exhibit comparatively weak antimicrobial effects. Second, the structures of AMPs are highly diversified. It is nearly impossible to test the antimicrobial activities of these AMPs one by one, largely due to the intensive time and financial requirements. To get around this obstacle, it is usually necessary to select typical AMPs and then estimate the antibacterial activities of their corresponding groups, of which four predominate: helix, beta-sheet formed with 2-3 disulfide bridges, linear peptides rich in special amino acids and loop peptides formed by one disulfide bridge (Vaara, 2009). Third, the primary laboratory screening procedure of AMPs usually involves testing their antibacterial activities on several type culture strains (e.g., American Type Culture Collection, or ATCC strains) or several randomly selected clinical isolates. Though occasionally insightful, these findings are rarely translatable to combatting clinical MDR strains.

To date, more than 2 300 AMPs have been discovered, and more are constantly being reported (http://aps. unmc.edu/AP/main.php). This growing pool of usable materials is quite timely (Wang et al, 2009). In the present study, we have attempted and elucidate some relationship between the characters of several discovered AMPs and their activities against MDR clinical pathogens, so as to provide clues to the screening procedure of clinically valuable candidates. Here, we selected 14 AMPs of animal origin with typical structures to test their *in vitro* effects on XDR *A. baumannii*, methicillin-resistant *Staphylococcus aureus* (MRSA), extended spectrum β-lactamase (ESBL)-producing *Pseudomonas aeruginosa,* and ESBL-producing *Escherichia coli*.

MATERIALS AND METHODS

Ethics

The protocols of this study were approved by the ethics committee of Kunming Medical University and ethics committee of Institute of Medical Biology, Chinese Academy of Medical Sciences and Peking Union Medical College. Isolation of multidrug resistant clinical strains were undertaken with the informed and written consent of each patient. The study methodologies conformed to the standards set by the Declaration of Helsinki and all other relevant national and international regulations.

Bacterial strains

XDR *A. baumannii* strains Ab5753 and Ab5755 were isolated from sputum samples of two different ICU patients in the First Affiliated Hospital of Kunming Medical University. All other strains were isolated from patients at the Second Affiliated Hospital of Kunming Medical University. These strains tested in this study include the following: (I) XDR *A. baumannii* strain Ab1408 isolated from the sputum sample of one oncology department patient; (II) MRSA strain Sa1390 isolated from the sputum sample of one surgery intensive care unit (SICU) patient; (III) ESBL *P. aeruginosa* strains Pa1409 and Pa4216 isolated from the sputum samples of two different oncology department patients; and (IV) ESBL *E. coli* strain Ec513 isolated from the blood sample of one general surgery department patient. Bacterial identification was performed using a Vitek 32 system (bioMérieux, France).

Antimicrobial peptides and antibiotics

All tested AMPs were supplied by GL Biochem Ltd (Shanghai, China), and had a purity ≥95%. The tested AMPs were dissolved in water at 2 mg/mL and stored at −20 °C before use. Determining whether the AMPs are amidated on the C-terminus or not was made through the previously published literature (Table 1). Antibiotics used as references were supplied by Sigma-Aldrich, and dissolved in water at 2 mg/mL prior use, and included colistin sulfate salt (colistin), vancomycin hydrochloride hydrate (vancomycin), and tigecycline hydrate (tigecycline).

Susceptibility testing

The minimal inhibitory concentrations (MICs) of all AMPs and antibiotic references to clinical isolates were determined by broth dilution method in MHII following Clinical and Laboratory Standards Institute (CLSI) recommendations (Clinical and Laboratory Standards Institute, 2013).

Time-killing curves

Time-kill studies of tachyplesinIII, cathelicidin-BF, colistin, and tigecycline on XDR *A. baumannii* strain Ab1408 with initial inocula between 1×10^6 and 1×10^7 CFU/mL were performed using 4×MICs, 2×MICs, 1×MIC, and 0.5×MIC concentrations. Samples were taken at 0, 0.5, 2, 4, 8, and 24 h after incubation. The effects of drug carryover were addressed via three dilution steps. Only plates with between 30 and 300 colonies were counted. An antibiotic was considered bactericidal when a reduction of 3 $\log_{10}$ CFU/mL was achieved, as compared with the initial inocula (Isenberg, 2004). These tests were each performed in duplicate.

Antimicrobial peptide structure prediction

Human LL-37 and beta-defensin-2—both of which are longer than 30 amino acids—were sourced directly from NCBI PDB database PDB 2K6O and PDB 1FD3. The other 12 AMPs were predicted by the structure prediction software PEP-FOLD at http://bioserv.rpbs. univ-paris-diderot.fr/PEP-FOLD/ (Thévenet et al, 2012), and model 1 of each peptide with the best conformation was selected for further analysis.

Table 1 Peptides tested for antimicrobial effects against drug resistant bacteria

Name	Sequence	Structure	Source and references
CA(1-7)M(2-9)	KWKLFKKIGAVLKVL-NH_2	Helix	*Hyalophora cecropia* (silk moth)+*Apis mellifera* (bee venom) (Giacometti et al, 2003)
[E4K]Alyteserin-1c	GLKKIFKAGLGSLVKGIAAHVAS-NH_2	Helix	*Alytes obstetricans* (midwife toad) (Conlon et al, 2009)
[D4K]B2RP	GIWKTIKSMGKVFAGKILQNL-NH_2	Helix	*Lithobates septentrionalis* (mink frog) (Conlon et al, 2010)
Cathelicidin-BF	KFFRKLKKSVKKRAKEFFKKPRVIGVSIPF	Helix	*Bungarus fasciatus* (banded krait) (Wang et al, 2008)
LL-37	LLGDFFRKSKEKIGKEFKRIVQRIKDFLRN LVPRTES	Helix	*Homo sapiens* (Thomas-Virnig et al, 2009)
Cramp	GLLRKGGEKIGEKLKKIGQKIKNFFQKLVP QPEQ	Helix	*Mus musculus* (house mouse) (Chromek et al, 2006)
Oncocin	VDKPPYLPRPRPPRRIYNR-NH_2	Linear, Proline/Arginine rich	*Oncopeltus fasciatus* (milkweed bug) (Knappe et al, 2010)
Indolicidin	ILPWKWPWWPWRR-NH_2	Linear, Tryptophane rich	*Bos taurus* (cattle) (Selsted et al, 1992)
Histatin	AKRHHGYKRKFH-NH_2	Linear, Histatine rich	*Homo sapiens* (Giacometti et al, 2005)
Thanatin	GSKKPVPIIY*C*NRRTGK*C*QRM[a]	Loop, one disulfide bridge	*Podisus maculiventris* (spined soldier bug) (Pagès et al, 2003)
Ranalexin-1Ca	FLGGLMKAFPALI*C*AVTKK*C*[a]	Loop, one disulfide bridge	*Rana clamitans* (green frog) (Halverson et al, 2000)
Tachyplesin III	KW*C*FRVCYRGICYRK*C*R-NH_2[a]	Beta-sheet, two disulfide bridges	*Tachypleus gigas* (Southeast Asian horseshoe crab) (Cirioni et al, 2007)
Beta-Defensin-2	GIGDPVT**C**LKSGAI*C*HPVFCPRRYKQIG-TC*G*LPGTK**C**CKKP[a]	Beta-sheet, three disulfide bridges	*Homo sapiens* (Routsias et al, 2010)
Alpha-defensin-2	LRDLV**C**YCRTRGCKRRERMNGTC*R*KGH LMYTLC**C**R[a]	Beta-sheet, three disulfide bridges	*Mus musculus* (house mouse) (Ouellette et al, 1992)

[a]: For antimicrobial peptides with disulfide bridges, cysteine (C) with the same type font or underlined formed one disulfide.

RESULTS

Minimal inhibitory concentrations (MICs)

All MICs are listed in Table 2. We found that all three *A. baumannii* strains were resistant to colistin according to CLSI standards (i.e., ≥4 mg/L). According to the susceptibility/ resistance breakpoints of tigecycline, as interpreted by the European Committee on Antimicrobial Susceptibility Testing (EUCAST) (susceptible, ≤1 mg/L; resistant, ≥4 mg/L) (The European Committee on Antimicrobial Susceptibility Testing (EUCAST) Steering Committee, 2006), Ab5753 has intermediate resistance to tigecycline (XDR) whereas Ab5755 and Ab1408 are resistant to tigecycline (Pandrug resistance, PDR). Four AMPs, including CA(1-7)M(2-9), [D4K] B2RP, cathelicidin-BF, and Tachyplesin III, showed MICs between 4 and 16 mg/L to all of the three *A. baumannii* strains. Given that the molecular weights of these peptides (from 1 770 to 3 638) are about three times to six times that of tigecycline (586), these peptides are considered as effective as tigecycline in inhibiting XDR *A. baumannii*.

ESBL *E. coli* and *P. aeruginosa* are still sensitive to colistin, but the two *P. aeruginosa* strains were resistant to tigecycline. Four AMPs, namely, CA(1-7)M(2-9), [D4K]B2RP, cathelicidin-BF, and tachyplesinIII, showed MICs of between 4 and 8 mg/L to Ec513. By contrast, only two AMPs, namely, cathelicidin-BF and tachyplesin III, showed MICs between 4 and 8 mg/L to Pa4216 and Pa1409. This phenomenon is consistent with the results on tigecycline; that is, ESBL *P. aeruginosa* is more resistant than ESBL *E. coli* is.

MRSA strain Sal1390 is sensitive to vancomycin, but intermediately resistant to tigecycline. Three AMPs, namely, CA(1-7)M(2-9), [D4K]B2RP, and tachyplesin III, showed MICs of 16 mg/L to this MRSA strain. Notably, [E4K]Alyteserin-1c and cathelicidin-BF, which showed a generally effective inhibitory activity on all MDR Gram-negative bacteria, had no effect on Gram-positive MRSA.

Time-killing kinetics

Figure 1 shows the time-killing kinetics. Cathelicidin-BF kills XDR *A. baumannii* strain Ab1408 within 4 h at 2×MICs and 2 h at 4×MICs respectively. This is similar to the action of colistin, i.e., Cathelicidin-BF was also able to rapidly kill bacteria. By comparison, tachyplesin III kills XDR *A. baumannii* after 4 h of incubation at 2×MICs and 4×MICs. Compared with colistin, tigecycline showed a markedly slower killing effect (after 8 h of incubation at 2×MICs and 4×MICs), but this effect lasted longer (24 h at 4×MICs). The optimum killing effects of cathelicidin-BF and tachyplesin III appeared to be 4 h of incubation, and afterward gradually declined.

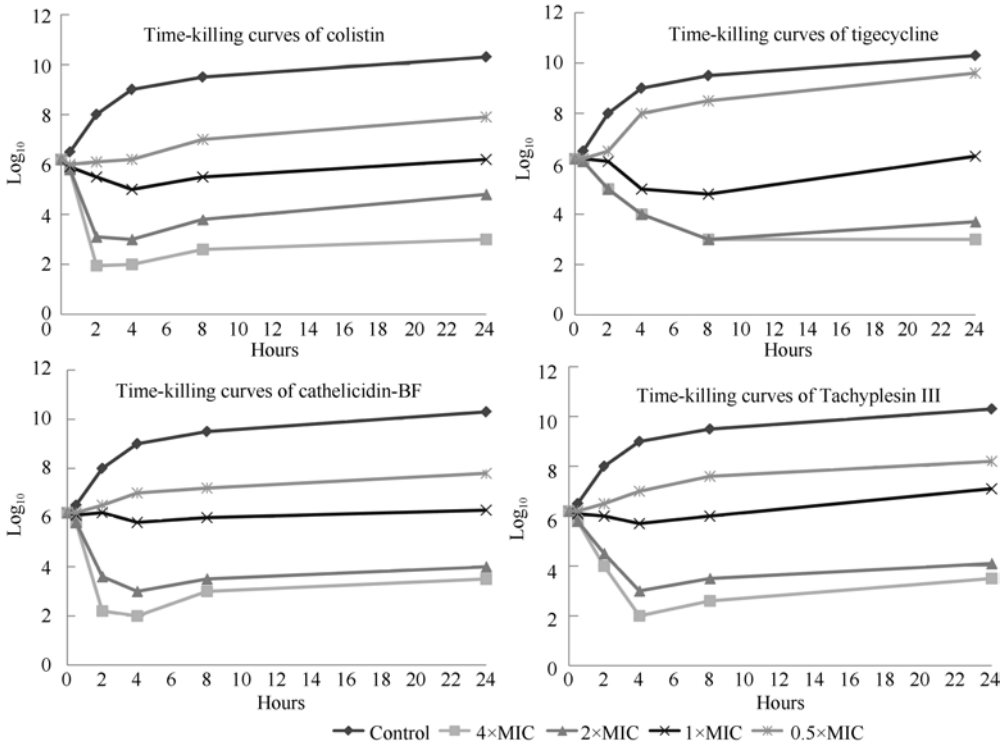

Figure 1 **Time-killing curves of colistin, tigecycline, cathelicidin-BF, and tachyplesin III on one XDR *Acinetobacter baumannii* strain (Ab1408)**

Initial inocula between 1×10^6 and 1×10^7 CFU/mL were performed using 4×MICs, 2×MICs, 1×MIC, and 0.5×MIC concentrations. Samples were obtained at 0, 0.5, 2, 4, 8, and 24 h after incubation.

Amphipathic structure distributions of AMPs

Although CA(1-7)M(2-9), [D4K]B2RP, [E4K]Alyteserin-1c, cathelicidin-BF, LL-37, and cramp are all classified as helical peptides by their secondary structures, these AMPs showed different antibacterial effects. Since the amphipathic structure distributions are generally considered crucial for AMPs to kill bacteria (Brogden, 2005), we studied the three-dimensional structures of the eight AMPs that were found to be effective on our tested MDR clinical isolates (Figure 2). [E4K]Alyteserin-1c and cathelicidin-BF, which were effective on all three Gram-negative bacteria, both have classical long linear amphipathic structures, withhydrophobic regions on one side and hydrophilic regions on the other side along the linear peptides. Similar structures exist in LL-37 and cramp, but these AMPs only showed slight activity on a portion of these Gram-negative strains. The helical peptides of CA(1-7)M(2-9) and [D4K]B2RP, which could inhibit not only Gram-negative but also Gram-positive bacteria, tend to manifest a more contractive style, with hydrophilic terminals separated by a hydrophobic intermediate section. A similar amphipathic structure distribution can be seen in tachyplesin III, which is also effective on both Gram-negative and Gram-positive clinical isolates, but is classified as a beta-sheet formed by two disulfide bridges according to its secondary structure. Interestingly, a similar structure also exists in Ranalexin-1Ca, which only showed slight activity to Gram-positive strains, but was ineffective on Gram-negative strains.

AMPs (mainly beta-sheet AMPs like beta-defensin-2 and alpha-defensin-2 that are formed with 3 disulfide bridges, and linear AMPs like oncocin, indolicidin, histatin and thanatin, which are rich in special amino acids) with neither classical long linear amphipathic structures nor hydrophilic terminals separated by hydrophobic intermediate sections, showed no effects on the tested MDR clinical isolates (Table 2, Figure 3).

DISCUSSION

In total, more than 2 300 antimicrobial peptides have been reported to date, but as we mentioned earlier, clinical applications of these AMPs are held up by a number of roadblocks. In this study, we collected a set of AMPs with different structures to evaluate their *in vitro* effects on typical MDR clinical isolates, which included XDR *A. baumannii*, MRSA, ESBL-producing *P. aeruginosa* and *E. coli.* Our results showed that helical AMPs appear to be more effective at killing MDR bacteria than other types of AMPs. By contrast, linear AMPs rich in special amino acids and AMPs with

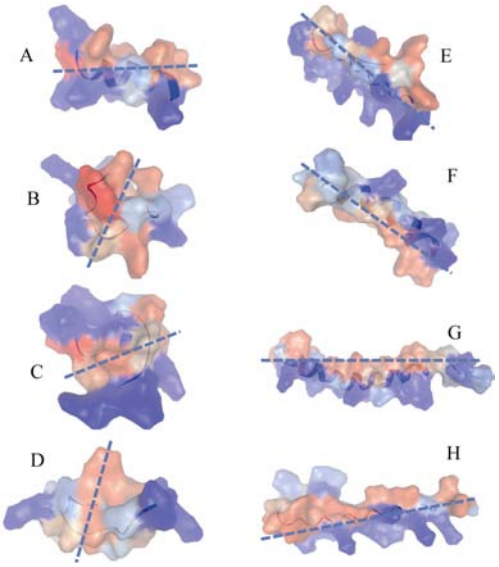

Figure 2 Structures and three-dimensional hydrophilic /hydrophobic arrangements of effective antimicrobial peptides

The backbones of these AMPs are shown in flat ribbons, and the three-dimensional surfaces of these AMPs are shown in solid. Blue: hydrophilic regions; Red: hydrophobic regions. A: CA(1-7)M(2-9); B: [D4K]B2RP; C: Tachyplesin III; D: Ranalexin-1Ca; E: cathelicidin-BF; F: [E4K]Alyteserin-1c; G: LL-37; H: cramp. Dotted lines indicate different hydrophilic/ hydrophobic region arrangement styles between A-D (both Gram-negative and Gram-positive effective, except for D, i.e., Ranalexin-1Ca, which is only Gram-positive effective) and E-H (Gram-negative effective).

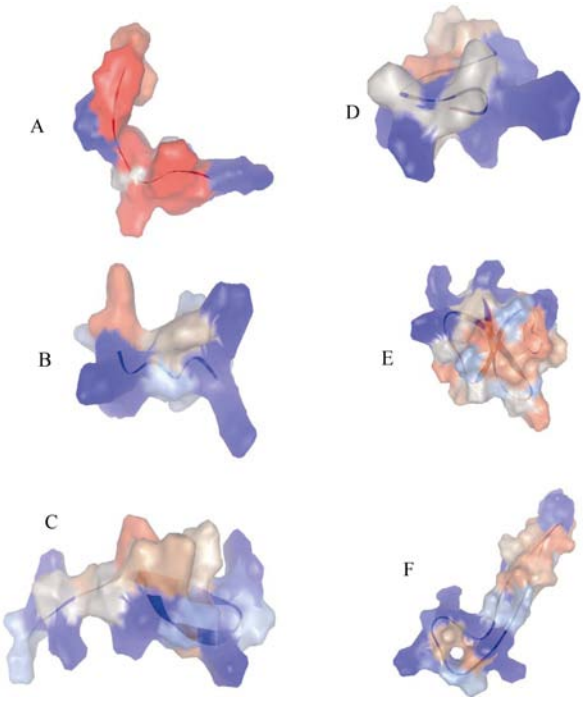

Figure 3 Structures and three-dimensional hydrophilic/ hydrophobic arrangements of ineffective antimicrobial peptides

The backbones of these AMPs are shown in flat ribbons, and the three-dimensional surfaces of these AMPs are shown in solid. Blue: hydrophilic regions; Red: hydrophobic regions. A: Indolicidin; B: Histatin; C: Thanatin; D: Oncocin; E: beta-Defensin-2; F: alpha-defensin-2.

Table 2 MICs (mg/L) of AMPs and antibiotics against drug resistant bacteria

AMPs & antibiotics	XDR *A.baumannii*			ESBLs *E.coli* & *P. aeruginosa*			MRSA
	Ab5753	Ab5755	Ab1408	Ec513	Pa1409	Pa4216	Sa1390
CA(1-7)M(2-9)	8	4	8	8	64	32	16
[D4K]B2RP	8	4	16	8	32	32	16
[E4K]Alyteserin-1c	64	8	64	32	>128	64	>128
Cathelicidin-BF	16	4	16	8	8	4	>128
LL-37	>128	32	>128	128	>128	>128	>128
Cramp	>128	128	>128	128	>128	>128	>128
Oncocin	>128	>128	>128	>128	>128	>128	>128
Indolicidin	>128	>128	>128	>128	>128	>128	>128
Histatin	>128	>128	>128	>128	>128	>128	>128
Thanatin	>128	>128	>128	>128	>128	>128	>128
Ranalexin-1Ca	>128	>128	>128	>128	>128	>128	64
Tachyplesin III	8	8	16	4	8	8	16
Beta-Defensin-2	>128	>128	>128	>128	>128	>128	>128
Alpha-defensin-2	>128	>128	>128	>128	>128	>128	>128
Colistin	>128	16	8	<1	<1	<1	>128
Vancomycin	>128	>128	>128	>128	>128	>128	2
Tigecycline	2	4	4	2	16	16	2

Abbreviations: AMP: antimicrobial peptides; MIC: minimum inhibitory concentration; XDR: extensive drug resistance; ESBLs: extended spectrum beta-lactamase producing; MRSA: methicillin-resistant *S. aureus*.

disulfide bridges (with the exception of tachyplesin III) are generally less effective in combatting MDR bacteria as compared with helical AMPs. Three-dimensional analysis showed that the hydrophilic/hydrophobic arrangements of these peptides, and not their secondary structures, seem to contribute more to their efficacy and position on the antimicrobial spectra. Peptides with long linear amphipathic structures were found to be effective only on Gram-negative pathogens, whereas peptides with more contractive styles with hydrophilic terminals separated by a hydrophobic intermediate section appeared to be effective on both Gram-negative and Gram-positive pathogens. Even though all AMPs are reported as antimicrobial peptides, only 2 of the 14 tested AMPs (tachyplesin III and cathelicidin-BF) were effective against all the tested MDR pathogens within their antimicrobial spectrum and with low MICs (≤16 mg/L). Since the net charge these AMPs carried does not correlate with their antibacterial activities (data not shown), the underlying mechanisms that lead to different MICs to kill bacteria remains to be further determined in more targeted follow-up studies.

Our results also showed that Cathelicidin-BF kills bacteria as quickly as colistin (within 4 h at 2×MICs and 2 h at 4×MICs), while Tachyplesin III is slower (after 4 h of incubation at 2×MICs and 4×MICs) than colistin, but faster than tigecycline. Considering the difference of the amphipathic structure distributions between these two peptides, the different rate of killing bacteria may imply a difference in the mechanism underlying their activities. Notably, the killing effects of these two potent peptides all declined after 4 h of incubation, which may, in part, be due to the nature of the peptides. Again, further targeted studies are needed to shed more light into the differences of these AMPs.

In conclusion, in the present study not all of the reported AMPs were effective against several tested MDR clinical isolates. Of the 14 potential AMPs, only two, Tachyplesin III and cathelicidin-BF, which differ in both their secondary structures and three-dimensional hydrophilic/ hydrophobic arrangements, showed potent activities (≤16 mg/L) against nearly all of the MDR clinical isolates within corresponding antimicrobial spectrum *in vitro*. What differentiates these two AMPs in terms of their efficacy to kill bacteria compared with other AMPs with similar hydrophilic/ hydrophobic arrangements remains to be determined.

REFERENCES

Brogden KA. 2005. Antimicrobial peptides: pore formers or metabolic inhibitors in bacteria? *Nature Reviews Microbiology,* **3**(3): 238-250.

Chromek M, Slamová Z, Bergman P, Kovács L, Podracká L, Ehrén I, Hökfelt T, Gudmundsson GH, Gallo RL, Agerberth B, Brauner A. 2006. The antimicrobial peptide cathelicidin protects the urinary tract against invasive bacterial infection. *Nature Medicine,* **12**(6): 636-641.

Cirioni O, Ghiselli R, Silvestri C, Kamysz W, Orlando F, Mocchegiani F, Di Matteo F, Riva A, Łukasiak J, Scalise G, Saba V, Giacometti A. 2007. Efficacy of tachyplesin III, colistin, and imipenem against a multiresistant *Pseudomonas aeruginosa* strain. *Antimicrobial Agents and Chemotherapy,* **51**(6): 2005-2010.

Clinical and Laboratory Standards Institute. 2013. Performance standards for antimicrobial susceptibility testing; 23rd informational supplement. M100-S23. Wayne, PA.

Conlon JM, Ahmed E, Condamine E. 2009. Antimicrobial properties of brevinin-2-related peptide and its analogs: Efficacy against multidrug-resistant *Acinetobacter baumannii*. *Chemical Biology & Drug Design,* **74**(5): 488-493.

Conlon JM, Ahmed E, Pal T, Sonnevend A. 2010. Potent and rapid bactericidal action of alyteserin-1c and its [E4K] analog against multidrug-resistant strains of *Acinetobacter baumannii*. *Peptides,* **31**(10): 1806-1810.

Falagas ME, Karageorgopoulos DE. 2008. Pandrug resistance (PDR), extensive drug resistance (XDR), and multidrug resistance (MDR) among Gram-negative bacilli: need for international harmonization in terminology. *Clinical Infectious Diseases,* **46**(7): 1121-1122.

Giacometti A, Cirioni O, Kamysz W, D'Amato G, Silvestri C, Del Prete MS, Łukasiak J, Scalise G. 2003. Comparative activities of cecropin A, melittin, and cecropin A-melittin peptide CA(1-7)M(2-9)NH_2 against multidrug-resistant nosocomial isolates of *Acinetobacter baumannii*. *Peptides,* **24**(9): 1315-1318.

Giacometti A, Cirioni O, Kamysz W, D'Amato G, Silvestri C, Del Prete MS, Licci A, Riva A, Łukasiak J, Scalise G. 2005. In vitro activity of the histatin derivative P-113 against multidrug-resistant pathogens responsible for pneumonia in immunocompromised patients. *Antimicrobial Agents and Chemotherapy,* **49**(3): 1249-1252.

Halverson T, Basir YJ, Knoop FC, Conlon JM. 2000. Purification and characterization of antimicrobial peptides from the skin of the North American green frog *Rana clamitans*. *Peptides,* **21**(4): 469-476.

Hancock RE, Sahl HG. 2006. Antimicrobial and host-defense peptides as new anti-infective therapeutic strategies. *Nature Biotechnology,* **24**(12): 1551-1557.

Isenberg HD. 2004. Clinical Microbiology Procedures Handbook. Washington DC: ASM Press.

Knappe D, Piantavigna S, Hansen A, Mechler A, Binas A, Nolte O, Martin LL, Hoffmann R. 2010. Oncocin (VDKPPYLPRPRPPRRI YNR-NH_2): a novel antibacterial peptide optimized against gram-negative human pathogens. *Journal of Medicinal Chemistry,* **53**(14): 5240-5247.

Lipsky BA, Holroyd KJ, Zasloff M. 2008. Topical versus systemic antimicrobial therapy for treating mildly infected diabetic foot ulcers: a randomized, controlled, double-blinded, multicenter trial of pexiganan cream. *Clinical Infectious Diseases,* **47**(12): 1537-1545.

Ouellette AJ, Miller SI, Henschen AH, Selsted ME. 1992. Purification and primary structure of murine cryptdin-1, a Paneth cell defensin. *FEBS Letters,* **304**(2-3): 146-148.

Pagès JM, Dimarcq JL, Quenin S, Hetru C. 2003. Thanatin activity on multidrug resistant clinical isolates of *Enterobacter aerogenes* and *Klebsiella pneumoniae*. *International Journal of Antimicrobial Agents,* **22**(3): 265-269.

Routsias JG, Karagounis P, Parvulesku G, Legakis NJ, Tsakris A. 2010. *In vitro* bactericidal activity of human β-defensin 2 against nosocomial strains. *Peptides,* **31**(9): 1654-1660.

Selsted ME, Novotny MJ, Morris WL, Tang YQ, Smith W, Cullor JS. 1992. Indolicidin, a novel bactericidal tridecapeptide amide from neutrophils. *The Journal of Biological Chemistry,* **267**(7): 4292-4295.

The European Committee on Antimicrobial Susceptibility Testing (EUCAST) Steering Committee. 2006. EUCAST technical note on tigecycline. *Clinical Microbiology and Infection,* **12**(11): 1147-1149.

Thévenet P, Shen YM, Maupetit J, Guyon F, Derreumaux P, Tufféry P. 2012. PEP-FOLD: an updated *de novo* structure prediction server for both linear and disulfide bonded cyclic peptides. *Nucleic Acids Research,* **40**(W1): W288-293.

Thomas-Virnig CL, Centanni JM, Johnston CE, He LK, Schlosser SJ, Van Winkle KF, Chen RB, Gibson AL, Szilagyi A, Li LJ, Shankar R, Allen-Hoffmann BL. 2009. Inhibition of multidrug-resistant *Acinetobacter baumannii* by nonviral expression of hCAP-18 in a bioengineered human skin tissue. *Molecular Therapy,* **17**(3): 562-569.

Vaara M. 2009. New approaches in peptide antibiotics. *Current Opinion in Pharmacology,* **9**(5): 571-576.

Wang G, Li X, Wang Z. 2009. APD2: the updated antimicrobial peptide database and its application in peptide design. *Nucleic Acids Research,* **37**(Database issue): D933- D937.

Wang YP, Hong J, Liu XH, Yang HL, Liu R, Wu J, Wang AL, Lin DH, Lai R. 2008. Snake cathelicidin from *Bungarus fasciatus* is a potent peptide antibiotics. *PLos One,* **3**(9): e3127.

Effects of senescence on the expression of BDNF and TrkB receptor in the lateral geniculate nucleus of cats

Chuan-Wang TONG[1,2], Zi-Lu WANG[1], Peng LI[1], Hui ZHU[1], Cui-Yun CHEN[1], Tian-Miao HUA[1,*]

[1] *College of Life Science, Anhui Normal University, Wuhu* 241000*, China*

[2] *College of Biological Engineering, Wuhu Institute of Technology, Wuhu* 241000*, China*

ABSTRACT

To explore the neural mechanisms mediating aging-related visual function declines, we compared the expressions of brain-derived neurotrophic factor (BDNF) and its high affinity receptor-tyrosine kinase B (TrkB) between young and old adult cats. Nissl staining was used to display neurons in each layer of the lateral geniculate nucleus (LGN). The BDNF- and TrkB receptor-immunoreactive neurons were labeled immunohistochemically, observed under optical microscope and photographed. Their neuronal density and immunoreactive intensity were measured. Results showed that the mean density of the Nissl stained neurons in each LGN layer were comparable between old and young adult cats, and their BDNF and TrkB proteins were widely expressed in all LGN layers. However, compared with young adult cats, both the density and optical absorbance intensity of BDNF- and TrkB-immunoreactive cells in each LGN layer in old cats were significantly decreased. These findings indicate that the decreased expressions of BDNF and TrkB proteins in the LGN may be an important factor inducing the compromised inhibition in the central visual nucleus and the functional visual decline in senescent individuals.

Keywords: Cat; Lateral geniculate nucleus; BDNF; TrkB; Age-related change

INTRODUCTION

Progressive recession in visual capacity, which includes decreased visual acuity, insensitiveness to visual contrast, inability to determine orientation or direction of objects and slowdown in processing visual information, can be found during the normal course of aging (Hua et al, 2006; Schmolesky et al, 2000). However, the neuronal mechanisms underlying age-related functional visual decline are still unclear (Hua et al, 2011; Zhou et al, 2011). How changes in neuronal plasticity affect age-related functional visual decline and the correlated molecular or cellular mechanisms are quite controversial (Hua et al, 2006; Liang et al, 2012b; Schmolesky et al, 2000; Zhou et al, 2013). For example, previous electrophysiological studies reported that the reactive characters of neurons in the lateral geniculate nucleus (LGN) were not significantly correlated with age and that aging might affect neuronal functions of the visual cortex, especial the advanced visual cortex (Hua et al, 2006; Liang et al, 2012a, 2012b; Zhou et al, 2011). However, these results could not rule out the possibility that both the morphology and neurotransmitter systems had changed during aging (Vidal et al, 2004), and these changes could influence the reactive characters of the visual cortical neurons to visual stimuli through synaptic connections. Other studies reported that aging was also accompanied with decreased expression of inhibitory neurotransmitters (such as GABA) in the visual cortex (Hua et al, 2008), which might induce the insensitiveness and decline in selectivity of the visual cortical neurons to visual stimuli (Hua et al, 2006; Leventhal et al, 2003; Zhou et al, 2011). Studies on neurotrophic factors found that brain-derived neurotrophic factors (BDNF) are vital in the development, survival, and lesion repair of neurons and neuronal plasticity via receptor mediated signal transductions (Ichim et al, 2012; Kwon et al, 2011; Numakawa et al, 2010). Some reports have shown that the BDNF signal system can modulate activity-dependent intracortical inhibitory (Rutherford et al, 1997) and promote the synthesis and transportation of GABA (Sánchez-Huertas & Rico, 2011; Vaz et al, 2011; Waterhouse et al, 2012). However, although a few studies

Received: 21 August 2014; Accepted: 21 October 2014

Foundation items: This study was supported by the National Natural Science Foundation of China (31171082); the Key Project of Natural Science Research of the Education Bureau of Anhui Province (KJ2014A284); the Foundation of Key Laboratories of Anhui Province and Key Laboratories of Universities of Anhui Province

*Corresponding author, E-mail: tmhua@mail.ahnu.edu.cn

DOI:10.13918/j.issn.2095-8137.2015.1.48

reported that age-related changes were found in the cerebral expressions of BDNF and receptors (Erickson et al, 2010; Hayakawa et al, 2008; Luellen et al, 2007; Silhol et al, 2005), it is too early to conclude that the decreased expression of BDNF and its receptors during senescence is the reason for a decline of inhibitory neurotransmitter GABA.

Our previous immunohistochemistry results showed that the expression of GABA in the dorsal LGN (dLGN) decreased significantly during aging (Tong et al, 2006); however, whether this phenomena is correlated with the expression down-regulation of BDNF and its receptors remains unclear. To understand the cellular and molecular mechanisms of age-related functional visual decline, we explored the expression differences of BDNF and its high affinitive receptor, tyrosine kinase receptor B (TrkB), in the dLGN of young and old adult cats.

MATERIALS AND METHODS

Animal subjects and experimental reagents

Four young (1-3 years old, 2-3.5 kg) and four old (10-13 years old, 2-3.5 kg) adult cats were examined ophthalmoscopically prior to experimentation to confirm that no optical or retinal problems impaired their visual function. All experiment procedures were performed strictly in accordance with the guidelines published in the NIH Guide for the Care and Use of Laboratory Animals. After a deep anesthesia by ketamine HCl (40 mg/kg, im) injection, cardiac perfusion was immediately performed on the animals (0.9% saline water). When pale livers were observed, a pre-fixture with 0.1 mol/L PBS (10% formalin, 2.5% glutaraldehyde, pH 7.2-7.4, 200 mL/kg) was performed. The isolated brainstem was fixed for 2 h and the LGN was then separated from it and transferred into a fixing solution (10% formalin, 2.5% glutaraldehyde, 30% sucrose) till the tissue sank to the bottom. Every four continuous coronal frozen slices (30 μm) were selected as a group for Nissl staining, BDNF and TrkB immunohistochemistry labels and negative controls. The slice groups were separated from each other by an interval of five slices. Every cat included 10 groups of slices.

Neuronal Nissl staining

Slices were stained in 0.1% cresyl violet solution for 5 min at room temperature, rinsed with distilled water, dehydrated by gradient alcohol, transparentized by xylene and then sealed with gum. Stained slices were used to determine the layering structures of the LGN and the neuronal density of each layer.

Immunohistochemical labeling

The frozen slices were incubated in 3% H_2O_2 for 15 min at room temperature to eliminate endogenous peroxidase activity and were then rinsed with distilled water, incubated in 0.3% TritonX-100 PBS for 20 min at room temperature, incubated in solution with 5% fetal bovine serum protein for 20 min at room temperature to seal the specific reactive areas, incubated in rabbit-anti-mouse BDNF and rabbit-anti-human TrkB multiclonal antibodies (1:100, primary antibodies) for 36 hours at 4°C and then rinsed three times with PBS for 5 min, incubated in biotinylated secondary antibody (goat-ant-rabbit) for 20 min at room temperature and then rinsed three times with PBS for 5 min, incubated in streptavidin-biotin complex (SABC) working solution for 20 min at room temperature and then rinsed three times with PBS for 5 min, developed by DAB to produce colorimetric end products, dehydrated by gradient (80%, 95% and 100%) alcohol, transparentized by xylene and then sealed with neutral gum. The only difference in the treatment of the negative control slices was replacing primary antibodies with PBS. All immunohistochemistry kits and the DAB substrate were products of Boster, Wuhan, China.

Statistical analysis

Nissl stained slices and BDNF and TrkB immuno-reactive slices were observed under a microscope (Olympus BX-51). Images were collected by Image-Pro Express 6.0 software. All related morphological parameters went through quantitative analysis, including the Nissl stained neuronal densities in each LGN layer, densities of BDNF and TrkB immuno-reactive positive neurons and intensities of immuno-reactions (evaluated by average optical absorbance, where higher absorbance values indicated stronger immuno-reactions). Data analyses were performed unbiased.

Images of slices were initially acquired under 40× ocular magnification and the layering structures (layer A, layer A_1 and layer C) of the LGN were then discriminated under 100× ocular magnification. Ten view fields (50 μm×50 μm) of each layer were randomly selected under 400× ocular magnification to calculate the densities of Nissl stained neurons and BDNF and TrkB immuno-positive neurons (cells/mm^2), respectively. A typical Nissl stained neuron was characterized with royal purple Nissl bodies and a clear nucleus in soma, and a typical BDNF/TrkB immuno-positive neuron was characterized with obvious immuno-positive matter and a clear nucleus in soma. The optical absorbance values of 20 immuno-positive neurons from each slice were randomly selected by Image-Pro Express 6.0 software, and the mean value was taken as the index indicating the intensity of immuno-reactions. All data were analyzed via SPSS 13.0 software and expressed as means±*SD*, with $P<0.05$ being considered statistically significant.

RESULTS

Densities of Nissl stained neurons

A three-layer-structure of the LGN (layer A, layer A_1 and layer C) (Figure 1) was shown in the Nissl stained slices. Blue or dark blue somas in various shapes, such as oval, tapered or polygon, were visualized in each layer. The results showed that age-independently, the neuronal density of layer A was significantly higher than that of layer A_1 ($F_{(1,158)}=31.04$, $P<0.001$), and neuronal densities of layer A and A_1 were both higher than that of layer C ($F_{(1,158)}=212.04$, $P<0.001$; $F_{(1,158)}=85.72$, $P<0.001$). No differences were found in the neuronal densities of each layer between young and old adult cats ($F_{(1,238)}=1.88$, $P=0.17$, Table 1).

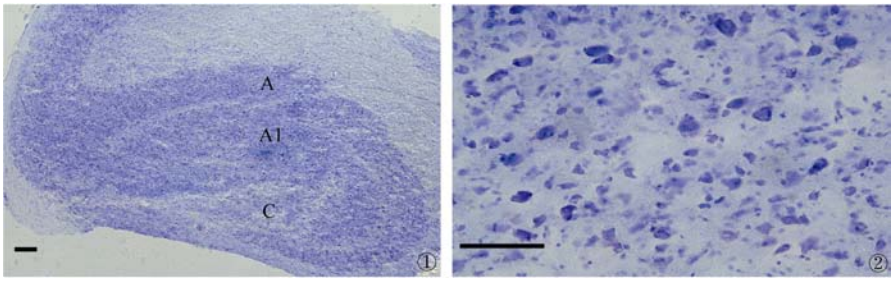

Figure 1 Nissl stained laminar organization (left, layer A, A_1 and C) and neurons (right) in the LGN of cats (Scale bar=50 μm)

Densities of BDNF and TrkB immuno-positive neurons

Immunohistochemical staining results showed that BDNF and TrkB immuno-positive neurons with brown or dark brown somas and their fiber distributions were found in every layer of the LGN in young and old adult cats (Figure 2). Age-independently, the densities of BDNF immuno-positive neurons in layer A and A_1 were both significantly higher than that of layer C ($F_{(1,158)}$=27.12, P<0.001; $F_{(1,158)}$=40.06, P<0.001, Table 1), whereas, those between layer A and A_1 were comparable ($F_{(1,158)}$=1.33, P=0.25). However, although no differences were found in the densities of BDNF immuno-positive neurons in each layer among cats at similar ages ($F_{(3,236)}$=1.11, P=0.35), those in old adult cats were significantly lower than those in young adult cats ($F_{(1,238)}$= 125.39, P<0.001, Table 1).

Age-independently, the densities of TrkB immuno-positive neurons in layer A and A_1 were both significantly higher than that of layer C ($F_{(1,158)}$=28.16, P<0.001; $F_{(1,158)}$=29.92, P<0.001, Table 1), whereas, those between layer A and A_1 were comparable ($F_{(1,158)}$=0.02, P=0.89). However, although no differences were found in the densities of BDNF immuno-positive neurons in each layer among cats at similar ages ($F_{(3,236)}$=0.22, P=0.88), those in old adult cats were significantly lower than those in young adult cats ($F_{(1,238)}$= 208.54, P<0.001, Table 1).

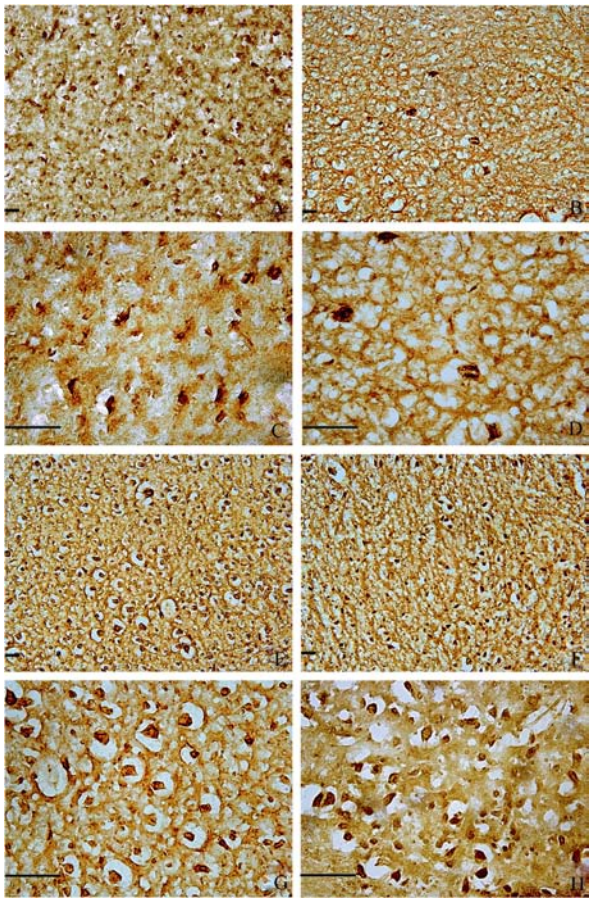

Figure 2 BDNF immuno-positive neurons (A, B, C, D) and TrkB immuno-positive neurons (E, F, G, H) in layer A of the LGN in young (A, C, E, G) and old (B, D, F, H) adult cats (Scale bar=50 μm)

Immuno-intensities of BDNF and TrkB immuno-positive neurons

The mean optical absorbance values of the BDNF immuno-positive neurons in the LGN of old cats were significantly lower than those in young cats ($F_{(1,78)}$=18.74, P<0.001), specifically, the mean absorbance values of layer A, A_1 and C were decreased by 26.4%, 20.3% and 36.3%, respectively. The mean absorbance values of the TrkB immuno-positive neurons in the LGN of old cats were also significantly lower than those in young cats ($F_{(1,78)}$=28.46. P<0.001), specifically, the mean optical absorbance values of layer A, A_1 and C were decreased by 25.6%, 26.5% and 35.3%, respectively (Figure 3).

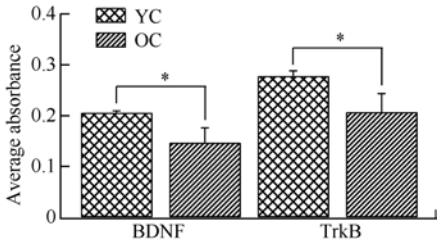

Figure 3 Mean optical absorbance values of BDNF and TrkB immuno-positive neurons in the LGN of young and old adult cats (*: P<0.01)

DISCUSSION

Vision is the most important way for higher animals, including

Table 1 Densities of BDNF, TrkB immuno-positive neurons in the dLGN of young and old cats

Animal subjects	Lamina organization of LGN		
	A	A_1	C
Densities of Nissl stained neurons (cells/mm^2)			
YC1	3 510.0±587.8	2 650.0±462.5	2 030.0±336.8
YC2	2 510.0±481.8	2 430.0±432.2	1 590.0±159.5
YC3	2 550.0±259.3	2 440.0±320.4	1 880.0±312.0
YC4	2 850.0±406.2	2 510.0±587.7	1 920.0±234.8
Mean	2 855.0±592.7$^{\#}$	2 507.5±451.4$^{\#}$	1 855.0±307.1$^{\#}$
OC1	2 700.0±434.6	2 380.0±482.6	1 980.0±278.1
OC2	2 810.0±481.8	2 430.0±503.4	1 680.0±193.2
OC3	2 930.0±490.0	2 390.0±296.1	1 750.0±222.4
OC4	2 690.0±486.4	2 020.0±297.4	1 830.0±231.2
Mean	2 782.5±465.7$^{\#}$	2 305.0±425.4$^{\#}$	1 810.0±250.9$^{\#}$
Densities of BDNF immuno-positive neurons (cells/mm^2)			
YC1	2 320.0±315.6	2 640.0±430.0	2 040.0±350.2
YC2	2 400.0±461.9	2 280.0±423.7	2 000.0±326.6
YC3	2 320.0±253.0	2 120.0±379.5	2 160.0±337.3
YC4	2 360.0±397.8	2 440.0±461.9	1 840.0±337.3
Mean	2 350.0±353.0**	2 370.0±451.1**	2 010.0±344.8**
OC1	1 640.0±295.1	2 000.0±377.1	1 280.0±253.0
OC2	1 760.0±337.3	1 840.0±386.4	1 520.0±367.6
OC3	1 960.0±350.2	1 800.0±282.8	1 080.0±270.0
OC4	1 560.0±295.2	1 920.0±367.6	1 240.0±227.1
Mean	1 730.0±343.6**	1 890.000±350.7**	1 280.0±316.4**
Density of TrkB immuno-positive neurons (cells/mm^2)			
YC1	2 280.0±369.5	2 520.0±329.3	2 000.0±326.6
YC2	2 360.0±397.8	2 280.0±388.7	2 040.0±266.7
YC3	2 320.0±168.7	2 160.0±386.4	2 120.0±423.7
YC4	2 400.0±533.3	2 480.0±454.1	1 880.0±379.5
Mean	2 340.0±379.5**	2 360.0±410.6**	2 010.0±350.8**
OC1	1 600.0±266.7	1 760.0±279.7	1 200.0±188.6
OC2	1 800.0±339.9	1 560.0±227.1	1 600.0±233.0
OC3	1 920.0±367.6	1 670.0±259.7	1 120.0±315.5
OC4	1 640.0±350.2	1 960.0±380.2	1 280.0±253.0
Mean	1 740.0±345.5**	1 737.5±311.2**	1 300.0±289.3**

YC1-4 and OC1-4 represent four different young and four different old adult cats, respectively. $^{\#}$:P>0.05; **: P<0.001.

humans, to acquire environmental information. Age-related functional visual decline can therefore directly lower life quality. Understanding neuronal networks and the molecular and cellular mechanisms underlying age-related functional visual decline is helpful in delaying the effects of senescence on vision and stimulating visual ability in seniors (Zhang et al, 2008a).

In higher animals and humans, the processing of visual information includes three different levels, that is, the retina, LGN and visual cortex from low to high. Previous electrophysiological studies indicate that aging may change the reactive characters of visional neurons to visional stimuli, e.g., the ability to determine the locations of visional stimuli and confirm moving directions, sensitivity to contrasts and selectivity in dimensional and temporal frequencies (Fu et al, 2013; Hua et al, 2006; Leventhal et al, 2003; Liang et al, 2010;

Schmolesky et al, 2000; Wang et al, 2005; Yang et al, 2009; Zhang et al, 2008b; Zhou et al, 2011). However, although these studies did not show significant influences of senescence on the characteristics of neurons on the LGN (Spear et al, 1994; Zhou et al, 2013), it is still possible that age-related changes are happening at the molecular or cellular level in the LGN. Our earlier work found that GABA expressions in the LGN of old cats were significantly lower than those in young adult cats (Tong et al, 2006). We assume that the functional effects of decreasing GABA may be compensated by downstream pathways or other factors, and therefore senescence may influence the function of LGN at the cellular level.

Tong et al (2006) reported that during the course of aging, the neuronal densities of the LGN maintained relatively stable, while the expression of GABA was significantly decreased; however, the underlying mechanisms for this remain unclear. Studies on neurotrophic factors showed that BDNF and its receptor (including high affinitive Trk receptor and low high affinitive p75 receptor) introduced signal transductions play vital roles in the development, survival and synaptic plasticity of neurons (Ichim et al, 2012; Kwon et al, 2011; Numakawa et al, 2010; Wong et al, 2013), including GABAnergic neurons (Cheng & Yeh, 2005; Jiao et al, 2011; Rutherford et al, 1997; Sakata et al, 2009; Waterhouse et al, 2012), and may be directly involved in the synthesis and transportations of GABA (Sánchez-Huertas & Rico, 2011; Vaz et al, 2011). However, whether the age-related GABA decrease is also correlated with the abnormal BDNF signal transduction still needs further evidence.

In the present study, no differences were found in the neuronal densities of each LGN layer, indicating relative stable neuronal quantities during the aging course, which is consistent with previous research (Tong et al, 2006). However, both the densities and intensities of the immuno-activity of BDNF and TrkB immuno-positive neurons in each LGN layer of old adult cats were significantly lower than those in young adult cats, which is consistent with results observed in old rats and the hippocampus of patients with Alzheimer's disease (Chapman et al, 2012; Erickson et al, 2010; Luellen et al, 2007; Tapia-Arancibia et al, 2008), indicating that the expressions of BDNF and TrkB decrease and the BDNF-TrkB signal transductions decline during the course of aging.

In summary, the present study indicated that senescence could induce the decreased expression of BDNF and TrkB receptors in each LGN layer, and the BDNF-TrkB signal transduction decline could decrease the expression of GABA. The weakening inhibitory effects of nerve endings on synaptic connections could influence the sensitivity and selectivity of visual neurons to visual stimuli and then induce age-related functional visual decline.

REFERENCES

Chapman TR, Barrientos RM, Ahrendsen JT, Hoover JM, Maier SF, Patterson SL. 2012. Aging and infection reduce expression of specific brain-derived neurotrophic factor mRNAs in hippocampus. *Neurobiology of Aging,* **33**(4): 832.e1-832.e14.

Cheng Q, Yeh HH. 2005. PLCγ signaling underlies BDNF potentiation of Purkinje cell responses to GABA. *Journal of Neuroscience Research,* **79**(5): 616-627.

Erickson KI, Prakash RS, Voss MW, Chaddock L, Heo S, Mclaren M, Pence BD, Martin SA, Vieira VJ, Woods JA, Mcauley E, Kramer AF. 2010. Brain-derived neurotrophic factor is associated with age-related decline in hippocampal volume. *The Journal of Neuroscience,* **30**(15): 5368-5375.

Fu Y, Yu S, Ma YY, Wang YC, Zhou YF. 2013. Functional degradation of the primary visual cortex during early senescence in rhesus monkeys. *Cerebral Cortex,* **23**(12):2923-2931.

Hayakawa N, Abe M, Eto R, Kato H, Araki T. 2008. Age-related changes of NGF, BDNF, parvalbumin and neuronal nitric oxide synthase immunoreactivity in the mouse hippocampal CA1 sector. *Metabolic Brain Disease,* **23**(2): 199-211.

Hua GP, Shi XM, Zhou J, Peng QS, Hua TM. 2011. Decline of selectivity of V1 neurons to visual stimulus spatial frequencies in old cats. *Neuroscience Bulletin,* **27**(1): 9-14.

Hua TM, Kao CC, Sun QY, Li XR, Zhou YF. 2008. Decreased proportion of GABA neurons accompanies age-related degradation of neuronal function in cat striate cortex. *Brain Research Bulletin,* **75**(1): 119-125.

Hua TM, Li XR, He LH, Zhou YF, Wang YC, Leventhal AG. 2006. Functional degradation of visual cortical cells in old cats. *Neurobiology of Aging,* **27**(1): 155-162.

Ichim G, Tauszig-Delamasure S, Mehlen P. 2012. Neurotrophins and cell death. *Experimental Cell Research,* **318**(11): 1221-1228.

Jiao YY, Zhang Z, Zhang CZ, Wang XJ, Sakata K, Lu B, Sun QQ. 2011. A key mechanism underlying sensory experience-dependent maturation of neocortical GABAergic circuits in vivo. *Proceedings of the National Academy of Sciences of the United States of America,* **108**(29): 12131-12136.

Kwon M, Fernández JR, Zegarek GF, Lo SB, Firestein BL. 2011. BDNF-promoted increases in proximal dendrites occur via CREB-dependent transcriptional regulation of cypin. *The Journal of Neuroscience,* **31**(26): 9735-9745.

Leventhal AG, Wang YC, Pu ML, Zhou YF, Ma YY. 2003. GABA and its agonists improved visual cortical function in senescent monkeys. *Science,* **300**(5620): 812-815.

Liang Z, Yang Y, Li GX, Zhang J, Wang YC, Zhou YF, Leventhal AG. 2010. Aging affects the direction selectivity of MT cells in rhesus monkeys. *Neurobiology of Aging,* **31**(5): 863-873.

Liang Z, Chen YM, Meng X, Wang Y, Zhou BZ, Xie YY, He WS. 2012a. Aging affects early stage direction selectivity of MT cells in rhesus monkeys. *Zoological Research,* **33**(5): 498-502.

Liang Z, Li HX, Yang Y, Li GX, Tang Y, Bao PL, Zhou YF. 2012b. Selective effects of aging on simple and complex cells in primary visual cortex of rhesus monkeys. *Brain Research,* **1470**: 17-23.

Luellen BA, Bianco LE, Schneider LM, Andrews AM. 2007. Reduced brain-derived neurotrophic factor is associated with a loss of serotonergic innervation in the hippocampus of aging mice. *Genes, Brain and Behavior,* **6**(5): 482-490.

Numakawa T, Suzuki S, Kumamaru E, Adachi N, Richards M, Kunugi H. 2010. BDNF function and intracellular signaling in neurons. *Histology and Histopathology,* **25**(2): 237-258.

Rutherford LC, Dewan A, Lauer HM, Turrigiano GG. 1997. Brain-derived neurotrophic factor mediates the activity-dependent regulation of inhibi-

tion in neocortical cultures. *The Journal of Neuroscience,* **17**(12): 4527-4535.

Sakata K, Woo NH, Martinowich K, Greene JS, Schloesser RJ, Shen L, Lu B. 2009. Critical role of promoter IV-driven BDNF transcription in GABAergic transmission and synaptic plasticity in the prefrontal cortex. *Proceedings of the National Academy of Sciences of the United States of America,* **106**(14): 5942-5947.

Sánchez-Huertas C, Rico B. 2011. CREB-dependent regulation of *GAD65* transcription by BDNF/TrkB in cortical interneurons. *Cerebral Cortex,* **21**(4): 777-788.

Schmolesky MT, Wang YC, Pu ML, Leventhal AG. 2000. Degradation of stimulus selectivity of visual cortical cells in senescent rhesus monkeys. *Nature Neuroscience,* **3**(4): 384-390.

Silhol M, Bonnichon V, Rage F, Tapia-Arancibia L. 2005. Age-related changes in brain-derived neurotrophic factor and tyrosine kinase receptor isoforms in the hippocampus and hypothalamus in male rats. *Neuroscience,* **132**(3): 613-624.

Spear PD, Moore RJ, Kim CB, Xue JT, Tumosa N. 1994. Effects of aging on the primate visual system: spatial and temporal processing by lateral geniculate neurons in young adult and old rhesus monkeys. *Journal of Neurophysiology,* **72**(1): 402-420.

Tapia-Arancibia L, Aliaga E, Silhol M, Arancibia S. 2008. New insights into brain BDNF function in normal aging and Alzheimer disease. *Brain Research Reviews,* **59**(1): 201-220.

Tong CW, Wang SY, Wan A, Zhang DY, Hua TM. 2006. Age-related morphological changes in the lateral geniculate nucleus of the cat. *Chinese Journal of Histochemistry and Cytochemistry*, **15**(5): 532-536. (in Chinese)

Vaz SH, Jørgensen TN, Cristóvão-Ferreira S, Duflot S, Ribeiro JA, Gether U, Sebastião AM. 2011. Brain-derived neurotrophic factor (BDNF) enhances GABA transport by modulating the trafficking of GABA transporter-1 (GAT-1) from the plasma membrane of rat cortical astrocytes. *Journal of Biological Chemistry,* **286**(47): 40464-40476.

Vidal L, Ruíz C, Villena A, Díaz F, Pérez De Vargas I. 2004. Quantitative age-related changes in dorsal lateral geniculate nucleus relay neurons of the rat. *Neuroscience Research,* **48**(4): 387-396.

Wang YC, Zhou YF, Ma YY, Leventhal AG. 2005. Degradation of signal timing in cortical areas V_1 and V_2 of senescent monkeys. *Cerebral Cortex,* **15**(4): 403-408.

Waterhouse EG, An JJ, Orefice LL, Baydyuk M, Liao GY, Zheng K, Lu B, Xu BJ. 2012. BDNF promotes differentiation and maturation of adult-born neurons through GABAergic transmission. *The Journal of Neuroscience,* **32**(41): 14318-14330.

Wong AW, Xiao JH, Kemper D, Kilpatrick TJ, Murray SS. 2013. Oligodendroglial expression of TrkB independently regulates myelination and progenitor cell proliferation. *The Journal of Neuroscience,* **33**(11): 4947-4957.

Yang Y, Liang Z, Li GX, Wang YC, Zhou YF. 2009. Aging affects response variability of V1 and MT neurons in rhesus monkeys. *Brain Research,* **1274**: 21-27.

Zhang CZ, Hua TM, Li GZ, Tang CH, Sun QY, Zhou PL. 2008a. Visual function declines during normal aging. *Current Science,* **95**(11): 1544-1550.

Zhang J, Wang XS, Wang YC, Fu Y, Liang Z, Ma YY, Leventhal AG. 2008b. Spatial and temporal sensitivity degradation of primary visual cortical cells in senescent rhesus monkeys. *European Journal of Neuroscience,* **28**(1): 201-207.

Zhou BZ, Yao ZM, Liang Z, Wang ZC, Yuan N, Liu ZG, Zhou YF. 2013. Aging affects on the response irregularity of cells in different visual areas of cats. *Journal of Biomedical Engineering,* **30**(2): 229-233.

Zhou J, Shi XM, Peng QS, Hua GP, Hua TM. 2011. Decreased contrast sensitivity of visual cortical cells to visual stimuli accompanies a reduction of intracortical inhibition in old cats. *Zoological Research,* **32**(5): 533-539. (in Chinese)

Effects of alcohol on H3K9 acetylation in mouse pre-implantation embryos

Fang DING[1,2], Li CHEN[1,2], Yong LIU[2,3], Feng-Rui WU[2,3], Biao DING[2,3], Wen-Yong LI[3], Rong WANG[2,*]

[1] *School of Life Science, Anhui University, Hefei* 230601, *China*

[2] *School of biological and food engineering, Fuyang Teachers College, Fuyang* 236037, *China*

[3] *Key Laboratory of Embryo Development and Reproductive Regulation in Anhui*, *Fuyang* 236037, *China*

ABSTRACT

It is well known that excessive long-term alcohol consumption is harmful, especially in pregnant women. In the present study, the Kunming white mouse was used as an animal model and indirect immunofluorescence was performed to analyze the toxic effects of alcohol on early pre-implantation embryos. H3K9 acetylation immunofluorescence could not be detected in MII oocytes. H3K9 acetylation levels in the treatment group were higher than in the control group during the morula stage, and contrary to results during the blastocyst stage. Other stages showed no obvious differences for in vivo embryos. For in vitro embryos, almost no difference was found between the two experimental groups across all stages, and both groups showed increasing H3K9 acetylation levels (except at the 2-cell stage). This study shows that H3K9 acetylation levels in early pre-implantation embryos are notably impacted by excessive alcohol ingestion by females. These data are the first step in understanding the epigenetic mechanism of alcohol toxicity in early pre-implantation mouse embryos.

Keywords: Alcohol intake; Pre-implantation embryos; H3K9 acetylation; Mice; Embryo development

INTRODUCTION

Long-term excessive drinking is severely harmful, especially in pregnant women. Fetal alcohol spectrum disorder (FASD), with syndromes including pre- and postnatal developmental retardation, craniofacial paramorphia, central nervous abnormalities, congenital heart diseases and mental and behavior disorders, can be induced by excessive drinking during progestation or gestational periods (Mattson et al, 2011). Studies into the toxicology of alcohol have mainly focused on the effects of excessive drinking on tissues, such as alcohol induced fatty liver (Li, 2003), cerebral injury (Zhao & Feng, 2012) and retinopathy (Jiang et al, 2007), or neonatal risks and syndromes following maternal alcohol exposure (Mattson et al, 2011). Few studies have been done on the toxicology of alcohol on early pre-implantation embryos in mice. Huang et al (2013a,b) found that alcoholism reduces germocyte activity and induces abnormal DNA methylation in early pre-implantation embryos. The aim of the present study is to understand the effects of alcoholism on H3K9 acetylation levels of pre-implantation embryos in mice from an epigenetic perspective.

The influence of epigenetic modification on biological phenotype has become a research hotspot. Most congenital diseases are the result of genetic and environmental factors and genetic mutation itself may not fully explain their nosogenesis. Epigenetic modifications include DNA methylation, genomic imprinting, histone modification and non-encoding RNA, etc. Histones are highly alkaline proteins found within chromosomes that package and order DNA into structural units. Histone H3 and H4 feature a N-terminal tail protruding from the globular nucleosome core, which can undergo several different types of post-translational modification that influence cellular processes, including reversible covalent modifications, such as histone acetylation, etc. Histone acetylation plays a vital role in the development of mammals and its abnormality results in chromatin reorganizing, and genetic transcriptional disorders in the cell cycle, cell differentiation and apoptosis (Vigushin & Coombes, 2002). Histone acetyltransferase (HATs) and histone deacetylases (HDACs) are a pair of enzymes that regulate genetic acetylation and deacetylation. By adjusting the

Received: 14 July 2014; Accepted: 25 October 2014

Foundation items: This study was supported by the National Natural Science Foundation of China (31372273, 31201789); Academic Renovation Research Project of Anhui University (yqh100125); Natural Science Foundation of the Education Bureau of Anhui Province (KJ2013A202); Major project of discipline construction in Anhui province ([2014]No.28); and Natural Science Foundation of Anhui Province (1408085MC44, 1408085QC65)

*Corresponding author, E-mail:wangrbnu@aliyun.com

DOI:10.13918/j.issn.2095-8137.2015.1.54

electrostatic attraction and sterical hinderence between DNA and histone, thereafter influencing the tightness of chromosomes, HATs and HDACs can repress or initiate gene transcription (Haycock, 2009). Histone H3K9 acetylation is one of the signs of gene transcription initiation (Morinobu et al, 2004) and its abnormal acetylation can induce abnormal chromatin structure and abnormal gene expression. Fetal malformations or abnormal developments are usually the result of protein misexpression. For example, imbalanced histone acetylation can cause the misexpression of cardiogenesis-related genes and bring on obstacles during the differentiation of mesenchymal stem cells (MSCs) to myocardial cells (Lin, 1981). Fisher et al (1986) reported that alcohol elevates acetylation levels of histone H3K9 in myocardial progenitor cells and then induces misexpression of cardiogenesis-related genes.

Earlier studies from our group suggest that epigenetic modifications of pre-implantation embryos in mice are extremely sensitive to environmental change. Alcohol-induced genomic DNA methylation in germocytes and zygotes, H3K9 methylation and H3K27 acetylation could interfere with the orderly establishment of epigenetic patterns in pre-implantation embryos in mice (Huang et al, 2013a, 2013b). To better understand epigenetic patterns under the influence of alcohol we force-fed Kunming (KM) mice with alcohol to stimulate external inducing conditions of FASD, and then monitored the acetylation level of H3K9.

MATERIALS AND METHODS

Experimental animals

Female KM mice (4–5 weeks old, 30±2 g) were provided by the Experimental Animal Center of Anhui Medical University and were housed at 24±2 ℃ with lights on from 0800h–2200 h. Food and water were available *ad libitum*. Animals were allowed to adapt to the housing condition for one week. All animal procedures were carried out in accordance with Fuyang Teachers College Animal Care and Use Committee.

Experimental reagents and equipments

Pregnant mare serum hormone (PMSG) and human chorionic gonadotrophin (hCG) were products of the Second Hormone Factory of Ningbo, China. Saline water was from Shanghai Huayuan Anhui Jinhui Pharmaceutical, China. The antibody of H3K9 acetylation was from Epigentek Group Inc. (New York, USA). Secondary goat-anti-rabbit antibody, IgG-FITC, was from Bioss Biotechnology (Beijing, China). Petri dishes were from Corning and all other reagents were products of Sigma. Equipment included a stereomicroscope (SMZ1500, Nikon, Japan), CO_2 incubator (2323-2, Thermo, USA), electronic balance (AR224CN, Ohaus, USA) and laser scanning cofocal microscope (TCS-SP5, Leica, Germany).

Animal model establishment and animal grouping

Animal models were established according to previous publications (Dole & Gentry, 1984; Dole et al, 1985; Griffin et al, 2009; Hwa et al, 2011) indicating that the behavioral and physiological features in mice force-fed with 20% (4–5 g/kg) alcohol bear a resemblance to those in human alcoholics. Mice were randomly separated into *in vivo* and *in vitro* groups. In the *in vivo* group, animals were further divided into an alcohol group and control group. The alcohol treatment animals (*n*=20) were force-fed 20% (4-5 g/kg) alcohol for 30 days and then force-fed saline water (4-5 g/kg) for another 4 days, *ad libitum*; control animals (*n*=20) were force-fed saline water 34 days. In the *in vitro* group, animals were divided into an alcohol group and control group. The alcohol treatment animals (*n*=10) were force-fed 20% (4-5 g/kg) alcohol for 30 days *ad libitum*; the control animals (*n*=10) were force-fed saline water 30 days. Zygotes and embryos at different stages were cultured in Petri dishes for 4 days.

Collection of MII stage ovum and pre-implantation embryos from *in vivo* and *in vitro* groups

Animals were given 10 U PMSG (i.p.) at 1730h on the last day of force-feeding and given 10 U hCG (i.p.) 48 hours later.Five females were randomly selected to not mate with males and 14 hours after hCG injection, their ampulla were punctured to collect MII stage ovum. The other females were mated with adult males (1:1). At 0800h on the day after mating, vaginal suppositories were checked and if the vaginal suppository was identified then female fertilization was confirmed. *In vivo* flushing method (using syringe, HCZB fluid and observation under a stereomicroscope) was applied in the *in vivo* group to collect zygotes (at 14 hours after fertilization and zygotes can be obtained by puncturing ampulla directly), 2-cell-, 4-cell-, 8-cell-embryo, morula and blastula (at 30, 48, 60, 72 and 88 hours after fertilization) at different stages of embryonic development. For the *in vitro* group, zygotes collected 14 hours after fertilization were rinsed with CZB sugar-free culture fluid and then cultured with CZB fluid (sugar-free) in the incubator at 37 ℃, 5% CO_2. Forty-eight hours later, 4-cell-embryos were transferred into CZB fluid (with sugar) and cultured in the incubator at 37 ℃, 5% CO_2. Zygotes, 2-cell-, 4-cell-, 8-cell-embryo, morula and blastula collected *in vitro* were rinsed with PBS (0.1% PVA), fixed with 4% paraform and saved.

Indirect immunofluorescence detection of H3K9 acetylation in pre-implantation embryos at different developmental stages

Fixed zygotes and embryos at different stages were rinsed with PBS (0.1% PVA) and then incubated in PBS with 0.2% TritonX-100 at 37.5 ℃ for 1 hour; rinsed with PBS (0.1% BSA); sealed with PBS (0.1% BSA) for 1-2 hours at 37.5 ℃; incubated in H3K9 acetylation antibody (1:100, diluted with PBS (1% BSA)) over night at 37.5 ℃; rinsed for 5 min, 3 times with PBS (0.1% Tween 20 and 0.01% TritonX-100); incubated in secondary goat-anti-rabbit antibody, IgG-FITC (1:100, diluted with PBS (1% BSA), inspired with 488 nm waves), in the dark for 3 hours at 37.5 ℃; rinsed with PBS (0.1% PVA) 3 times and then stained in propidium iodide (PI, 10 μg/mL, inspired with 568 nm waves) in the dark for 10 min; and finally rinsed with PBS (0.1% PVA) and fixed on slides for observing and photographing under a laser scanning cofocal microscope.

Statistical analysis

Fluorescence densities were analyzed using LAS AF Lite and Image Pro-Plus. Every sample group was repeated three times and at least 20 zygotes or embryos at different stages were examined. Corresponding fluorescence data were obtained by running Image Pro-Plus. Data from alcohol treatment groups and control groups were compared with *t*-tests (Kim et al, 2002). GraphPad Prism 5 was used to produce histograms and fluorograms.

RESULTS

H3K9 acetylation of MII stage ovum

Indirect immunofluorescence detection of H3K9 acetylation in MII stage ovum showed that no immunofluorescence could be found in the alcohol treatment groups or controls. However, immunofluorescences were found by DNA PI staining (data not shown).

Immunofluorescence of H3K9 acetylation in pre-implantation embryos at different developmental stages in the *in vivo* groups

Indirect immunofluorescence detection of H3K9 acetylation in pre-implantation embryos at different developmental stages in the *in vivo* groups is shown in Figure 1.

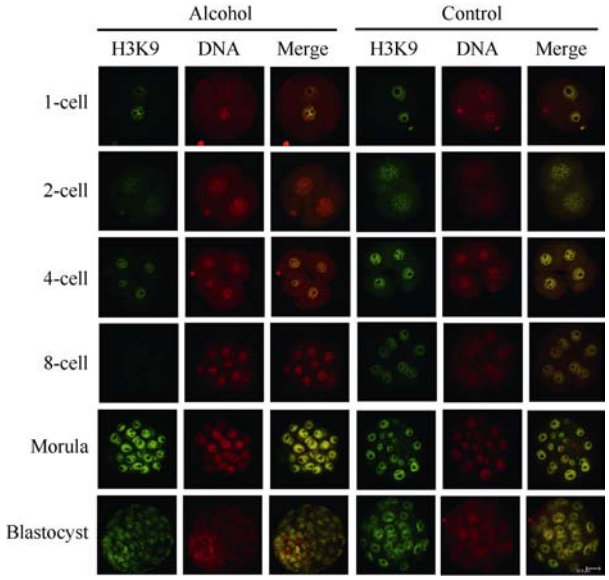

Figure 1 Different stages of mouse pre-implantation embryos and H3K9 acetylation immunofluorescence *in vivo*

1-cell, 2-cell, 4-cell, 8-cell, morula and blastocyst *in vivo* treatment and control groups collected separately. Embryos were immunostained with specific antibodies against resistance to H3K9 acetylation antibody (H3K9 in histone); in red (middle), DNA; Merged (right) . Scale bar=20 μm.

Semi-quantitative analysis of H3K9 acetylation in pre-implantation embryos at different developmental stages in the *in vivo* groups

The analysis of fluorescence data showed that at the morula stage, H3K9 acetylation levels in the *in vivo* alcohol treatment group were higher than in the control group, whereas at the blastocyst stage H3K9 acetylation levels in the control group were higher than in the alcohol treatment group. No differences were found for other stages. An abrupt reduction in H3K9 acetylation only occurred in the alcohol treatment group at the blastocyst stage. For other stages in both groups, H3K9 acetylation levels all initially decreased, then increased. High expression was found in the prokaryotic phase. Expression levels were rather low in the 2-cell stage and later increased.

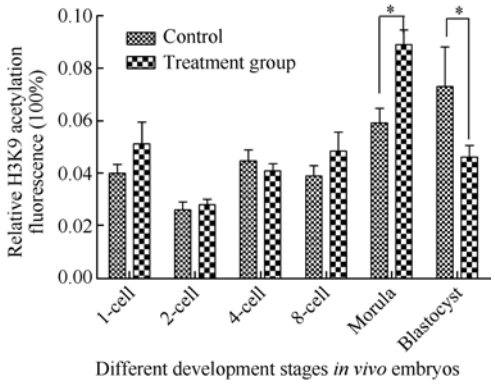

Figure 2 Semi-quantification of H3K9 acetylation levels of mouse pre-implantation embryos *in vivo*

H3K9 acetylation intensities of mouse pre-implantation embryos *in vivo* from control group and treatment group quantified with Image Pro-Plus 6.0. Different columns and bars represent mean±*SE*, *: $P<0.05$, control group *in vivo* compared with treatment group *in vivo*.

Immunofluorescence of H3K9 acetylation in pre-implantation embryos at different developmental stages in the *in vitro* groups

Indirect immunofluorescence detection of H3K9 acetylation in pre-implantation embryos at different developmental stages in the *in vitro* groups is shown in Figure 3.

Semi-quantitative analysis of H3K9 acetylation in pre-implantation embryos at different developmental stages in the *in vitro* groups

The analysis of fluorescence data showed that H3K9 acetylation levels of the *in vitro* alcoholic treatment and control groups were comparable (except at the 2-cell stage) and that H3K9 acetylation levels increased (Figure 4).

Patterns of H3K9 acetylation in the *in vivo* and *in vitro* alcohol treatment groups were different (Figure 2, 4). At the 2-cell stage *in vivo* a reduction in H3K9 acetylation was found, and then increased. *In vitro*, the H3K9 acetylation level increased, after which it decreased and increased again. For control groups, H3K9 acetylation levels *in vivo* at the 2-cell and blastocyst stages were lower than *in vitro*, while at the 4-cell-stage *in vivo* were higher than *in vitro*; no differences

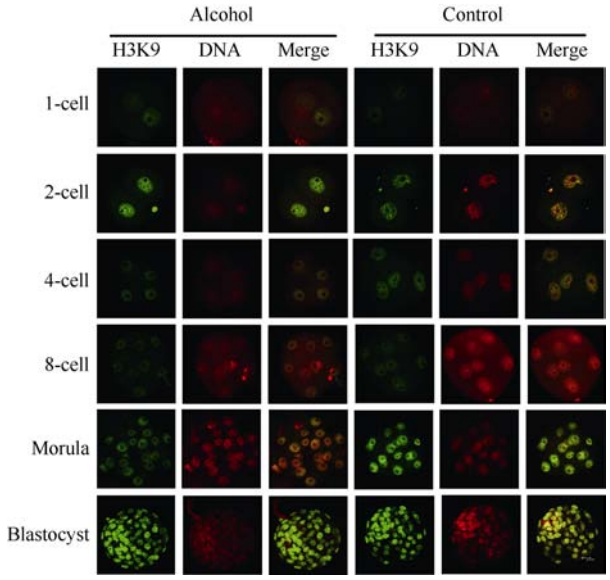

Figure 3 Different stages of mouse pre-implantation embryos and H3K9 acetylation immunofluorescence figure *in vitro*

1-cell, 2-cell, 4-cell, 8-cell, morula and blastocyst in the *in vitro* treatment and control groups were collected separately. Embryos were immunostained with specific antibodies against resistance to H3K9 acetylation antibody (H3K9 in histone); in red (middle), DNA ; Merged (right). Scale bar=20μm .

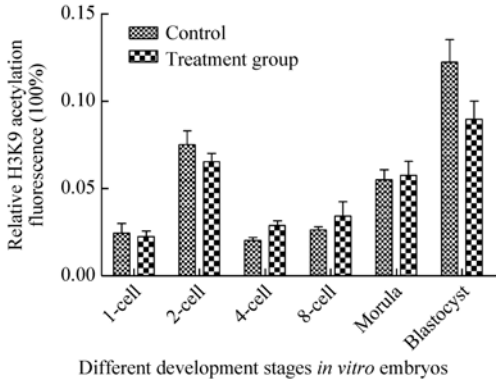

Figure 4 Semi-quantification of H3K9 acetylation levels of mouse pre-implantation embryos *in vitro*

Different columns and bars represent mean±*SE*, control group compared with treatment group *in vitro.*

were found for other stages. For alcohol treatment groups, H3K9 acetylation levels *in vivo* at the 1-cell and morula stages were higher than *in vitro*, while at the 2-cell and blastocyst stages *in vivo* were lower than *in vitro*. No differences were found for other stages.

We found that the blastocyst rates of *in vitro* alcohol treatment group and their controls were comparable. However, for the morula and blastocyst rates of *in vivo* groups, the alcohol treatment group was lower than the control group.

DISCUSSION

Histone acetylation influences chromatin remodeling and gene expression. As one of the signs of gene transcription initiation, H3K9 acetylation functions as an important form of histone acetylation and changes in its level can directly affect gene expression, induce protein misexpression and lead to phenotypic defects or maldevelopment. Here, no H3K9 acetylation indirect immunofluorescences in MII stage ovum were observed in either alcohol treatment groups or their controls and we assume this is because MII stage ovum were already in maturation and H3K9 deacetylated.

In vivo results showed that H3K9 acetylation levels in the 2-cell stage were low, and then increased. The mechanisms responsible is likely that during the 2-cell stage zygotic genes are activated, accumulated activation effects suppress gene transcription, and then under the regulation of zygotic genes many development-related genes start to transcript (Wang et al, 2013). Pan et al (2013) claim that increased H3K9 acetylation in mice embryos lays the ground for transcription initiation of development-related genes, which is in accordance with our data. From zygotes to the 8-cell stage in *vivo*, although H3K9 acetylation in the alcohol group was only slightly higher than the control group, a difference induced by alcohol occurred at the morula stage when many development-related genes would be activated. Under these circumstances, alcohol treated morula turned mature in advance and then cells began to deacetylate, and thereafter H3K9 acetylation levels were lower compared to the control group. Alcohol can harm female mice and affect H3K9 acetylation of pre-implantation embryos in multiple ways. Studies on hepatic cells show that alcohol related high histone acetylation may be correlated with the MAPK signal pathway (Yeh et al, 2008).

In vitro abnormal 4-cell stage H3K9 acetylation could be the result of activation delay of zygotic genes (Ma et al, 2001; Qiu et al, 2003). Zygotic gene activation (ZGA) is the initiation of embryo development from maternal regulation to embryonic regulation when the embryo will start to synthesize its own mRNAs and proteins and no long depends on maternally-sourced mRNAs and proteins (Kidder, 1993). The 2-cell stage is a vital period in mice embryonic development and is also the initiation phase of ZGA. *In vitro* culture may delay ZGA and prolong the procedure from maternal regulation to embryonic regulation.

Fluctuations in H3K9 acetylation levels observed in the *vivo* and *in vitro* control and alcohol groups from zygotes to blastocytes indicate that environmental differences can induce H3K9 acetylation imbalance in pre-implantation embryos. This imbalance may be correlated with the activation delay of zygotic genes and the postponing of 2-cell stage development; however, the mechanism for *in vitro* 2-cell stage development postponement remain unclear. Some studies have shown that at the 2-cell stage *in vitro*, the active oxygen content in embryos was much higher than that of other stages and the lesion caused by excessive active oxygen may be one of the reasons for 2-cell stage development postponement in mice

(Tang, 2006). Zhao et al (2005) reported that *in vitro* culture could suppress or decrease GCN5 and HDAC1 protein expressions in mice pre-implantation embryos and influence *in vitro* histone acetylation. Both *in vivo* and *in vitro* data suggest that long-term excessive alcohol consumption, even without alcohol intake during pregnancy, could still influence H3K9 acetylation in pre-implantation embryos because of remnant alcohol inside the body or metabolism products. Changes in H3K9 acetylation may also interfere with the correct establishment of epigenetic patterns in pre-implantation embryos. Alcohol may influence H3K9 acetylation in pre-implantation embryos and then induce gene misexpression by adjusting the activities of HATs; however, the underlying mechanisms at play here require further exploration.

ACKNOWLEDGEMENTS

I would like to express my appreciation to Prof. Rong WANG, Dr. Ji-Chang HUANG and staff and students at our lab for generous help with this study.

REFERENCES

Dole VP, Gentry RT. 1984. Toward an analogue of alcoholism in mice: scale factors in the model. *Proceedings of the National Academy of Sciences of the United States of America,* **81**(11): 3543-3546.

Dole VP, Ho A, Gentry RT. 1985. Toward an analogue of alcoholism in mice: criteria for recognition of pharmacologically motivated drinking. *Proceedings of the National Academy of Sciences of the United States of America,* **82**(10): 3469-3471.

Fisher SE, Duffy L, Atkinson M. 1986. Selective fetal malnutrition: effect of acute and chronic ethanol exposure upon rat placental Na, K-ATPase activity. *Alcoholism: Clinical and Experimental Research,* **10**(2): 150-153.

Griffin WC III, Lopez MF, Becker HC. 2009. Intensity and duration of chronic ethanol exposure is critical for subsequent escalation of voluntary ethanol drinking in mice. *Alcoholism, Clinical and Experimental Research,* **33**(11): 1893-1900.

Haycock PC. 2009. Fetal alcohol spectrum disorders: the epigenetic perspective. *Biology of Reproduction,* **81**(4): 607-617.

Huang JC, Wang CH, Liu Y, Wu FR, Li WY, Wang R. 2013a. Chronic alcohol ingestion influences sperm semen quality and global DNA methylation in pre-implantation embryos. *Chinese Journal of Cell Biology,* **35**(8): 1103-1109. (in Chinese)

Huang JC, Wang CH, Liu Y, Wu FR, Ding B, Li WY, Wang R. 2013b. Female rats ingested alcohol before and after pregnancy impact DNA methylation patterns in pre-implantation embryo. *Chinese Journal of Cell Biology,* **35**(12): 1765-1771. (in Chinese)

Hwa LS, Chu A, Levinson SA, Kayyali TM, Debold JF, Miczek KA. 2011. Persistent escalation of alcohol drinking in C57BL/6J mice with intermittent access to 20% ethanol. *Alcoholism, Clinical and Experimental Research,* **35**(11): 1938-1947.

Jiang QY, Hu YQ, Cheng XS, Deng JB. 2007. Neuroapoptosis in visual cortex of offspring mouse after prenatal ethanol exposure. *Acta Anatomica Sinica,* **38**(4): 400-404. (in Chinese)

Kidder GM. 1993. Genes involved in cleavage, compaction, and blastocyst formation. *In*: Gwatkin RBL. Genes in Mammalian Reproduction. New York: Wiley-Liss, 45-47.

Kim JM, Ogura A, Nagata M, Aoki F. 2002. Analysis of the mechanism for chromatin remodeling in embryos reconstructed by somatic nuclear transfer. *Biology of Reproduction,* **67**(3): 760-766.

Li YM. 2003. New insight on the pathogenesis of alcoholic liver diseases. *Chinese Journal of Hepatalogy,* **11**(11): 690-691. (in Chinese)

Lin GW. 1981. The effect of ethanol consumption during gestation on maternal-fetal amino acid metabolism in the rat. *Currents in Alcoholism,* **8**: 479-483.

Mattson SN, Crocker N, Nguyen TT. 2011. Fetal alcohol spectrum disorders: neuropsychological and behavioral features. *Neuropsychology Review,* **21**(2): 81-101.

Ma J, Svoboda P, Schultz RM, Stein P. 2001. Regulation of zygotic gene activation in the preimplantation mouse embryo: global activation and repression of gene expression. *Biology of Reproduction,* **64**(6): 1713-1721.

Morinobu A, Kanno Y, O'shea JJ. 2004. Discrete roles for histone acetylation in human T helper 1 cell-specific gene expression. *The Journal of Biological Chemistry,* **279**(39): 40640-40646.

Pan B, Sun HC, Lv TW, Wu XY, Zhu J, Tian J. 2013. Hyperacetylation imbalance and epimutation of H3K9 induced by alcoholconsumed during gestation in mice. *Journal of Clinical Cardiology,* **29**(5): 395-398. (in Chinese)

Qiu JJ, Zhang WW, Wu ZL, Wang YH, Qian M, Li YP. 2003. Delay of ZGA initiation occurred in 2-cell blocked mouse embryos. *Cell Research,* **13**(3): 179-185.

Tang GE. 2006. Detection of Reactive Oxygen Species (ROS) in Different Developmental Stage Mouse Embryos in Vivo and in vitro. Master Thesis, Agriculture College of Yanbian University, Jilin. (in Chinese)

Vigushin DM, Coombes RC. 2002. Histone deacetylase inhibitors in cancer treatment. *Anti-cancer Drugs,* **13**(1): 1-13.

Wang CH, Liu Y, Huang JC, Wu FR, Ding B, Zhang Y, Wang R, Li WY. 2013. The difference of the patterns of H3K27 acetylation between parthenogenetic embryos and in vivo mouse embryos and the effect on development. *Sichuan Journal of Zoology,* **32**(5): 684-688. (in Chinese)

Yeh CH, Chang JK, Wang YH, Ho ML, Wang GJ. 2008. Ethanol may suppress Wnt/β-catenin signaling on human bone marrow stroma cells: a preliminary study. *Clinical Orthopaedics and Related Research,* **466**(5): 1047-1053.

Zhao DM, Xu CM, Huang HF, Qian YL, Jing F. 2005. Expression patterns of GCN5 and HDAC1 in preimplantational mouse embryos and effects of in-vitro cultures on their expressions. *Acta Biologiae Experimentalis Sinica,* **38**(6): 513-519. (in Chinese)

Zhao MQ, Feng LD. 2012. Biomarkers of alcohol binge-drinking Induced brain damage in mice. *Journal of Medical Research,* **41**(8): 169-171. (in Chinese)

Update on the distribution range of the white-browed crake (*Porzana cinerea*): a new record from mainland China

Li-Jiang YU[1,*], Ai-Wu JIANG[2], Fang ZHOU[1]

[1] *College of Animal Science and Technology, Guangxi University, Nanning Guangxi* 530005*, China*

[2] *College of Forestry, Guangxi University, Nanning Guangxi* 530005*, China*

ABSTRACT

Since 1980, the white-browed crake (*Porzana cinerea*) has been experiencing an expansion from south of the Isthmus of Kra, northward to China. Recently, this species was observed in several locations throughout Southwest China, including Ningming and Baise, Guangxi (2012, 2013), and Xichang, Sichuan (2013). These sightings are the first distribution record of this species in mainland China, suggesting that the white-browed crake is following a natural species dispersal northward into mainland China from Southeast Asia.

Keywords: *Porzana cinerea*; New record; Mainland China

INTRODUCTION

The white-browed crake (*Porzana cinerea*) is a small, slim-body crake with striking diagnostic face pattern that typically resides in vegetated coastal and freshwater wetlands, ranging from Malaysia and Greater Sundas through Philippines, Sulawesi, Moluccas and Lesser Sundas to New Guinea and north Australia, and east through Micronesia and Melanesia to Polynesia (Fiji and Samoa) (Taylor, 1996). The species was not included in the early avian checklist of China (Cheng, 1987), though the first recorded observation was in Southern Taiwan between 1984 and 1985 (Lin, 1997). Later, one vagrant was observed in 1991 at Mai Po, Hong Kong (Kennerley, 1992). To date, this species has never been recorded in mainland China (Wang et al, 2006; Zheng, 2011). During a recent survey of birds in Guangxi and Sichuan, several recent sightings in the area suggest that a new distribution record of this species in mainland China is warranted.

OBSERVATIONS

On 28 August 2012, one adult white-browed crake was observed at Honggu reservoir, Ningming Town, Southwestern of Guangxi, China. This sighting was treated as vagrant record, and no photographic evidence was obtained or published. Several months later on 2 February 2013, a sole crake was found and photographed in a suburban pond locating in Baise City, in Northwestern Guangxi Zhuang Autonomous Region. According to this species' typical face pattern and behaviour, it was identified as an adult white-browed crake. Later, one juvenile was found at farmland on 15 November (Figure 1) and another at Longjing reservoir on 24 December 2013 in Baise City, Guangxi. In addition, one juvenile white-browed crake was found by Min Xue, a birdwatcher, in Xichang Wetland Park, Sichuan Province, on 25 October 2013 (Table 1, Figure 2).

Figure 1 A white-browed crake (right) in Baise, Guangxi, South-western China (Photo by Dong-Sheng GUO)

Received: 28 August 2014; Accepted: 24 December 2014

Foundation item: This work was supported by the National Natural Science Foundation of China (31172123)

*Corresponding author, E-mail: yulj1709@126.com

DOI:10.13918/j.issn.2095-8137.2015.1.59

Table 1 Records of white-browed crake in Mainland China

Date	Age class	Number (*n*)	Site recorded	Longitude	Latitude	Altitude (m)	Habitat
28 Aug. 2012	Adult	1	Ningming, Guangxi	E107° 09'	N22° 03'	164	Reservoir
02 Feb. 2013	Adult	1	Baise, Guangxi	E106° 36'	N23° 52'	142	Pond
25 Oct. 2013	Juvenile	1	Xichang, Sichuan	E102° 18'	N27° 48'	1 511	Wetland park
15 Nov. 2013	Juvenile	1	Baise, Guangxi	E106° 36'	N23° 52'	147	Farmland
24 Dec. 2013	Juvenile	1	Baise, Guangxi	E106° 36'	N23° 52'	142	Reservoir

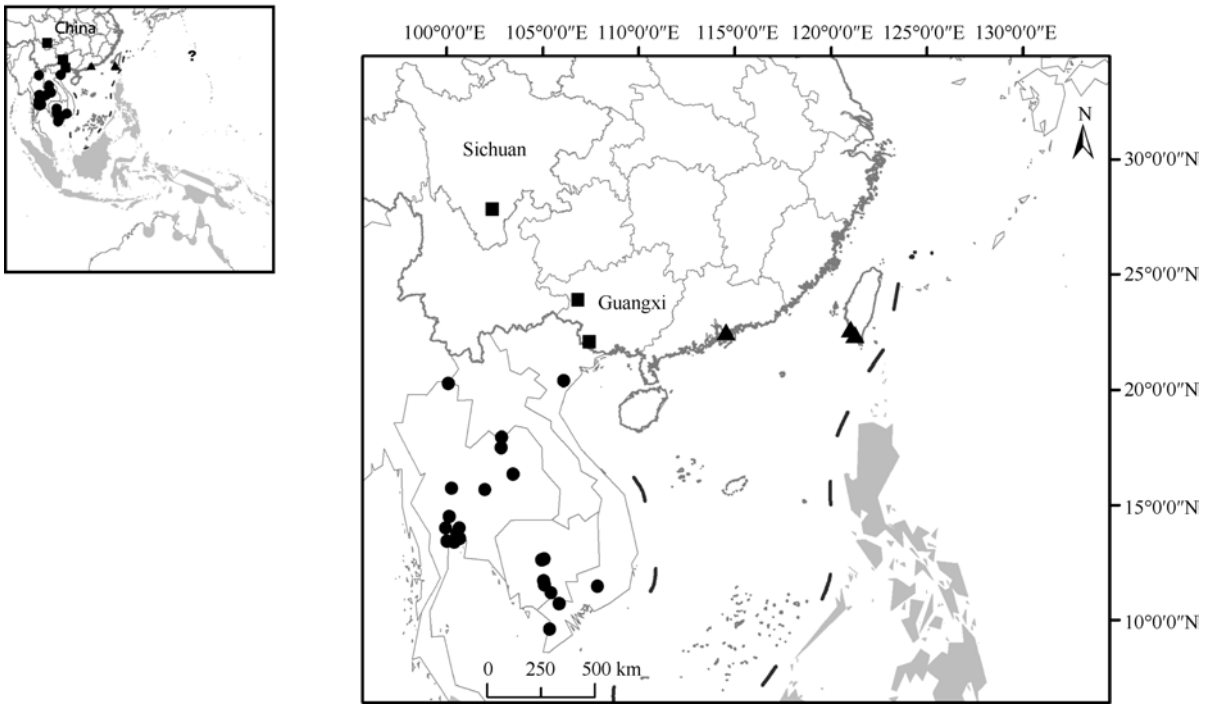

Figure 2 The distribution range and records of white-browed crake

■: New records for mainland China from this study; ▲: Previous records in Hong Kong and Taiwan; ●: Records from non-Sundaic mainland Asia since 1980 (Duckworth & Evans, 2007); grey shadow: The distribution range (Handbook of the Birds of the World, 1996); ?: Extinct site.

DISCUSSION

The white-browed crake was previously thought to distribute mainly in south of the Isthmus of Kra, which includes Malaysia, Singapore, Philippines, Indonesia, New Guinea and North Australia (Taylor, 1996). Accordingly, in Southeast Asia, early records were from Malay Peninsula (Robinson & Chasen, 1936). In the 1990s, new distribution sites were found across Southeast Asia, including Thailand, Cambodia, Vietnam and Laos (Buckton & Safford, 2004; Mundkur et al, 1995; Robson, 2000, 2004, 2011). Duckworth & Hedges (2007) analyzed this species distribution records since 1980 and proposed that white-browed crake has been expanding northward from a purely Sundaic distribution and moving almost to China. This hypothesis was well supported by the studied records: one distribution site in Laos was ~800 km north of any historical sighting, while the site in northern Vietnam at Van Long Nature Reserve—quite close to the southwestern Chinese border—was considered as an “amazing range extension” (Duckworth & Hedges, 2007). Taking our distribution data of the crake in mainland China alongside several recent records for other birds in this region (Jiang & Ning, 2010; Jiang et al, 2013), it seems likely that the white-browed crake’s distribution range is quickly expanding in Asia. Indeed, the distance between Baise and Van Long Nature Reserve is ~400 km, and Xichang to Van Long is ~900 km.

ACKNOWLEDGEMENTS

We are grateful to the birdwatchers, Dongsheng Guo, Yongmao Lin from Baise and Min Xue from Xichang, for providing the sighting information.

REFERENCES

Buckton ST, Safford RJ. 2004. The avifauna of the Vietnamese Mekong

Delta. *Bird Conservation International,* **14**(4): 279-322.

Cheng TH. 1987. A Synopsis of the Avifauna of China. Beijing: Science Press. (in Chinese)

Duckworth JW, Evans TD. 2007. First records of white-browed crake (*Porzana cinerea*) for Laos and its current range in Southeast Asia. *The Wilson Journal of Ornithology,* **119**(2): 253-258.

Jiang AW, Ning YX. 2010. A new distribution site of the Asian open-billed stork (*Anastomus oscitans*) in southwestern China. *Chinese Birds,* **1**(4): 259-260.

Jiang AW, Pan HQ, Lu Z, Liu NF. 2013. A new record of the bird subspecies black-crested bulbul (*Pycnonotus flaviventris johnsoni*) in China. *Zoological Research,* **34**(1): 53-54. (in Chinese)

Kennerley PR. 1992. White-browed crake at Mai Po: the first record for Hong Kong and China. *In*: Hong Kong Bird Report 1991. Hong Kong: Hong Kong Bird Watching Society.

Lin W-H. 1997. The History of Taiwan Birds Discovery. Taipei: Yushan Publishing Co. Ltd.. (in Chinese)

Mundkur T, Carr P, Sun H, Chhim S. 1995. Surveys for large waterbirds in Cambodia, March-April 1994. IUCN. United Kingdom: Gland, Switzerland, and Cambridge.

Robinson HC, Chasen FN. 1936. Coots, rails and crakes. *In*: Robinson HC, Chasen FN. The Birds of the Malay Peninsula. Volume 3. Sporting Birds; Birds of the Shore and Estuaries. London: H. F. & G. Witherby Ltd., 67-84.

Robson C. 2000. From the field: Laos. *Oriental Bird Club Bulletin,* **32**: 70.

Robson C. 2004. From the field: Vietnam. *Birding Asia,* **2**: 105.

Robson C. 2011. Field Guide to the Birds of South-East Asia. London: New Holland Publishes Ltd.

Taylor PB. 1996. Family Rallidae (rails, gallinules and coots). *In*: del Hoyo J, Elliott A, Sargatal J. Handbook of the Birds of the World. Volume 3. Hoatzin to Auks. Barcelona: Lynx Edicions, 108-209.

Wang QS, Ma M, Gao RY. 2006. Family Rallidae. *In*: Fauna Sinica, Aves. Volume 5. Gruiformes, Charadriiformes and Lariformes. Beijing: Science Press, 57-128. (in Chinese)

Zheng GM. 2011. A Checklist on the Classification and Distribution of the Birds of China. 2nd ed. Beijing: Science Press, 1-456. (in Chinese)

Evaluating the effect of habitat diversity on the species-area relationship using land-bridge islands in Thousand Island Lake, China

Zhi-Feng DING[1,2], Hui-Jian HU[2], Ping DING[1,*]

[1] *The Key Laboratory of Conservation Biology for Endangered Wildlife of the Ministry of Education, College of Life Sciences, Zhejiang University, Hangzhou* 310058*, China*

[2] *Guangdong Entomological Institute & South China Institute of Endangered Animals*, *Guangzhou* 510260 *China*

DEAR EDITOR:

The species-area relationship (SAR) describes the phenomenon whereby the number of plant and animal species found in an area of wild habitat is strongly correlated with the size of that area. As one of the few ecological laws, the SAR plays a vital role in the design and assessment of biodiversity protection regions (Lomolino et al, 2010; Ladle & Whittaker, 2011).

Increasing area and habitat promote species richness (Triantis et al, 2003) and both these mechanisms have theoretical support. Basically, the notion of area *per se* claims that the effects of area are embodied in the chance of species extinction (Preston, 1960, 1962; MacArthur & Wilson, 1963, 1967). In contrast, the habitat diversity hypothesis states that the highly diversified habitats often found in large patches positively impact species addition (Williams, 1964). Although it remains controversial which mechanism is more important in influencing species richness, some ecologists believe that the area *per se* and habitat diversity are mutually complementary and not mutually exclusive (Triantis et al, 2003).

Land-bridge islands are characterized by well-delineated boundaries, an inhospitable surrounding matrix and relatively homogeneous habitats (Hu et al, 2011). Land-bridge islands are considered excellent models for studying the relationship between area *per se* and habitat diversity. Located in Chun'an County in Zhejiang, eastern China (N29º22′-29º50′, E118º34′-119º15′), Thousand Island Lake is a large man-made lake following dam construction on the Xin'an River in 1959. With a water surface area of approximately 580 km^2, the lake contains 1 078 land-bridge islands larger than 0.25 ha (108 m in water level elevation).

To understand correlations between area *per se* and habitat diversity we used bird data for 41 land-bridge islands in Thousand Island Lake from 2006 to 2009. This data was used to compare the goodness-of-fit of the classical Arrhenius SAR model, and the choros (*K*) model integrating both area and habitats (Triantis et al, 2003). The canonical power function model (log$S$=log$c$× z×log$A$, in which S represents the number of species and A is the size of the area; c and z are constants) was used to investigate the effect of area on bird species richness. Choros (*K*) (K=H×A, in which H represents habitat diversity and A is the area of the study island) was adopted to assess correlations between area and habitat diversity (Zhang et al, 2008; Wang et al, 2010). The classical SAR model can be expressed as:

$$\text{Log}(S)=\log(c)+z\log(A) \quad (1)$$

and the K model can be expressed as:

$$\text{Log}(S)=\log(c)+z\log(K) \quad (2)$$

Akaike Information Criterion (AIC) was used to determine the optimum model and the model with the lowest AICc (modification of AIC for small n) was considered better (Burnham & Anderson, 2002). Statistical differences in z values among regression equations were compared by referencing the methods of Zar (1996) $t=(b1-b2)/S_{b1,b2}$ in which $b1$ and $b2$ are both regression coefficients and $S_{b1,b2}$ are standard errors of regression coefficients).

Our results show that the lowest AICc was found in the *SAR* model (Table 1), however, no differences in z values were found between the two models ($P>0.05$). These findings indicate that the Arrhenius SAR model gives a better fit than the K model and there is no effect of habitat diversity on the SAR. This finding is in contrast with that of Triantis et al (2003)

Table1 Comparison of the SAR and choros (*K*) models

Models	z	Adjusted r2	AICc
(logS-logA)	0.12	0.64	–219.71
(logS-logK)	0.11	0.62	–217.94

Received: 27 September 2014; Accepted: 23 October 2014

Foundation items: This study was supported by the National Natural Science Foundation of China (31170397)

*Corresponding author, E-mail: dingping@zju.edu.cn

DOI:10.13918/j.issn.2095-8137.2015.1.62

in which the *K* model better explained the effect of area and habitat diversity on species richness.

One possible explanation for this discrepancy is that due to the relatively homogeneous habitats on the islands of Thousand Island Lake, insignificant differences in habitat diversity may be all that exists between the largest and smallest islands. Therefore, compared with changes in area, habitat homogeneity is more prominent in Thousand Island Lake and bird richness is strongly correlated with area (Hu et al, 2011; Ding et al, 2013). The weak effect of habitat diversity found in this study may also be the result of different statistical methods. There are various ways to define habitat diversity (Looijen, 1995, 1998); for example, Ricklefs (1979) defines habitat as vegetation coverage in a given area but Whittaker et al (1973) defines habitat as the multidimensional space occupied by plant and animal species. Although the latter definition (with minor improvements) has been widely accepted by ecologists (Krebs, 1988, 1994; Looijen, 1995, 1998), the definition itself is too broad and has been difficult to apply consistently across different studies (Newmark, 1986).

Here, only island area was important when explaining the relationship between area, habitat and species richness. Consequently, eliminating habitat diversity alters the results only subtly and in protection practice, area has the highest authority in maintaining bird richness. Effective evaluation of species biodiversity can be obtained by choosing area as a parameter, and priority protection areas can be determined accordingly. This finding suggests that more attention should be given to large islands with high species richness in Thousand Island Lake (Wang et al, 2010).

REFERENCES

Burnham KP, Anderson DR. 2002. Model Selection and Multimodel Inference: a Practical Information-theoretic Approach. 3rd ed. New York: Springer.

Ding ZF, Feeley KJ, Wang YP, Pakeman RJ, Ding P. 2013. Patterns of bird functional diversity on land-bridge island fragments. *Journal of Animal Ecology,* **82**(4): 781-790.

Hu G, Feeley KJ, Wu JG, Xu GF, Yu MJ. 2011. Determinants of plant species richness and patterns of nestedness in fragmented landscapes: evidence from land-bridge islands. *Landscape Ecology,* **26**(10): 1405-1417.

Krebs CJ. 1988. The Message of Ecology. New York: Harper & Row.

Krebs CJ. 1994. Ecology: the Experimental Analysis of Distribution and Abundance. New York: Harper & Row.

Ladle RJ, Whittaker RJ. 2011. Conservation Biogeography. Oxford: Wiley-Blackwell.

Lomolino MV, Riddle BR, Whittaker RJ, Brown JH. 2010. Biogeography. 4th ed. Sunderland, Massachusetts: Sinauer Associates, Inc.

Looijen RC. 1995. On the distinction between habitat and niche, and some implications for species' differentiation. *Poznań Studies in the Philosophy of the Sciences and the Humanities,* **45**: 87-108.

Looijen RC. 1998. Holism and Reductionism in Biology and Ecology. The Mutual Dependence of Higher and Lower Level Research Programmes. Ph.D. thesis, University of Groningen, Groningen.

MacArthur RH, Wilson EO. 1963. An equilibrium theory of insular zoogeography. *Evolution,* **17**(4): 373-387.

MacArthur RH, Wilson EO. 1967. The Theory of Island Biogeography. New Jersey: Princeton University Press.

Newmark WD. 1986. Species-area relationship and its determinants for mammals in western North American national parks. *Biological Journal of the Linnean Society,* **28**(1-2): 83-98.

Preston FW. 1960. Time and space and the variation of species. *Ecology,* **41**(4): 611-627.

Preston FW. 1962. The canonical distribution of commonness and rarity: Part I. *Ecology*, **43**(2): 185-215, 410-432.

Preston FW. 1962. The canonical distribution of commonness and rarity: Part II. Ecology, 43(3): 410-432 .

Ricklefs RE. 1979. Ecology. 2nd ed. New York: Chiron Press.

Triantis KA, Mylonas M, Lika K, Vardinoyannis K. 2003. A model for the species-area-habitat relationship. *Journal of Biogeography,* **30**(1): 19-27.

Wang YP, Bao YX, Yu MJ, Xu GF, Ding P. 2010. Nestedness for different reasons: the distributions of birds, lizards and small mammals on islands of an inundated Lake. *Diversity and Distributions,* **16**(5): 862-873.

Whittaker RH, Levin SA, Root RB. 1973. Niche, habitat, and ecotope. *The American Naturalist,* **107**(955): 321-338.

Williams CB. 1964. Patterns in the Balance of Nature. London: Academic Press.

Zar JH. 1996. Biostatistical Analysis. New Jersey: Prentice-Hall.

Zhang JC, Wang YP, Jiang PP, Li P, Yu MJ, Ding P. 2008. Nested analysis of passeriform bird assemblages in the Thousand Island Lake region. *Biodiversity Science,* **16**(4): 321-331. (in Chinese)

Author Guidelines for Submitting Manuscripts to *Zoological Research*

Published bimonthly, *Zoological Research* is an interdisciplinary, peer-reviewed, open-access journal publishing original articles, review articles, research reports, letter to the editor, editorial and notes focusing on Genome Evolution and Genetic Diversity, Animal Ecology and Ethology, Primates and Animal Models of Human Diseases. The journal also publishes high quality papers related to taxonomy and DNA barcoding, developmental biology, physiology, biochemistry, immunology, and neuroscience. To assist you in formatting your articles correctly for submission to *ZR*, please use this attached guide.

SUBMISSIONS

All paper submitted to *Zoological Research* must follow the submission instructions. Failure to do so may result in rejection of the manuscript or delays in publication. Please be aware that we only publish articles in English, and not Chinese. If you have a Chinese-language manuscript you are interested in publishing, please contact one of our editors and they can assist you in getting the article translated into English, which will then be polished by our English speaking editors.

Manuscripts and editorial correspondence should either be e-mailed to zoores@mail.kiz.ac.cn, or submitted through our website at http://www.zoores.ac.cn/.

FORMATTING

All papers should follow the standard format for *Zoological Research* and be double spaced, in 12 point Times New Roman font, with 1" inch margins. The paper should include the following elements:

1) A full title, no more than 250 characters;

2) An abbreviated running title of around 50 characters which succinctly explains the purpose of the paper;

3) A cover letter or email, briefly explaining (a) the relevance of their research; (b) stating that the paper being submitted for publication must not have been published, accepted for publication, or be under consideration for publication, either in whole or in part, elsewhere in any other language; and (c) that all authors and co-authors agree to the paper's submission to *Zoological Research*.

4) Any accompanying tables, figures or data the authors wish to have appended to the published paper.

NOTE on Copyright: If tables, figures or other data have from another source, authors should submit a letter from the copyright holder granting authorization for use of the material. Authors may use their article elsewhere after publication provided that prior permission is obtained from the publisher.

PUBLICATION PROCESS

All articles undergo initial review by our editors and then are either sent out for peer-review or language editing if they are deemed acceptable. Following peer-review, the corresponding author is invited to return the revision within three months after receiving the reviewers' and editors comments. If we or the reviewers recommend that your article could benefit from English-language editing, jointly the editorial staff and the submitting author will arrange the schedule with our English speaking editors, who will revise the language of the manuscript and then return it to the author for final review. Pending acceptance of this version, a final revision will be approved by our editorial staff and review board, and proofs will be sent to the corresponding author directly preceding publication. Acceptance of the final proof should be sent back to the editorial office as soon as possible, ideally within three days.

ETHICS

All submitted manuscripts should abide by ethnics rules and Uniform Requirements for Manuscripts Submitted to Biomedical Journals produced by International Committee of Medical Journal Editors (ICMJE). For papers that deal with either human or animal experimentation, please submit a disclaimer that all procedures were approved by your local ethics review board and that your procedures obey all relevant national and international regulations.

STYLE & LENGTH

Manuscripts should be no longer than 15,000 words, including references and all figures and/or tables. Whenever possible, authors should try to avoid abbreviations or complex technical terminology. When needed, all abbreviations should be standard, abiding by common zoological and genetic nomenclature and using standard unit measurements.

All manuscripts should contain the following information and be organizing in this order:

I. Title Page

The title page should include (i) full title of the paper, not to exceed 250 characters, (ii) full names of all authors with listings of their respective institutional affiliations, (iii) full postal, email, and telephone contact information for the corresponding author; (iv) a brief, running title of no more than 50 characters that will appear at the top of each page.

II. Abstract

Each paper should be preceded by an **abstract** of no more than 250 that presents the purpose, importance, basic methods and key findings of the research. Avoid using abbreviations, citations or references to other parts of the text whenever possible.

III. Keywords

Each papers should include around 5 **keywords** (for indexing), provided immediately below the abstract.

IV. Text

The main text of a manuscript should be organized into four parts:

Introduction should summarize the rationale and give a concise background. Use references to provide the most salient background rather than an exhaustive review.

Materials and methods provide technical information to allow the fieldwork or experiments to be repeated. Describe new methods or modifications and identify unusual instruments and procedures in detail.

Results emphasize or summarize only important observations. Simple data may be set forth in the text without the need of tables and figures. This section can be combined with the discussion if needed.

Discussion should deal with the interpretation of results that emphasizes any new and important aspect of the research as it relates to the broader field and scholarship. The discussion should also end with a brief conclusion, recapping the major findings and contributions of the paper.

V. Acknowledgment(s)

Acknowledgements may indicate (a) contributors that do not warrant authorship; (b) technical help or assistance; and (c) material support. Foundation items should be put in the footnote of the first page.

VI. Tables and figures

All tables and figures must be numbered consecutively by Arabic numerals based on the order they appear in the manuscript. The captions to illustrations can be bonded with the tables, and the figure legends should be separated from the illustration. Only high-quality drawings and original photographs (preferably as JPEG or TIFF files) suitable for reproduction can be accepted. Actual enlarging multiples or the length unit (bar, in μm or nm) should be marked in photos produced by microscopy. Three-line tables (no vertical line) are requested.

VII. References

Citations should appear in the text using the (Author, Date) system with corresponding references appearing at the end of the paper. Listed references should be complete in all details if possible. The full list should be collected and typed at the end of the paper and arranged alphabetically by authors and chronologically for each author as shown below. If originally published in Chinese or another non-European language, please translate the article title into English and provide a note at the end, denoting the original language, *e.g.,* [in Chinese], [in Vietnamese], [in Marathi], etc.. The EndNote reference style file of *Zoological Research* and its instructions can be downloaded from our website: http://www.zoores.ac.cn/EN/column/column86.shtml.
For a sample guide for references and in-text citations, please see the accompanying document on using EndNote to format your citations.

SUBMISSION CHECKLIST

Please ensure all of the following elements are included in your final submission to our journal:

- Cover letter / email specifying appropriate details
- Title page with author information, corresponding author contact data, full & running titles
- Abstract less than 250 words
- Properly organized manuscript
- Standardized abbreviations, measurements and nomenclature
- All figures, tables and supplementary materials
- Cross-checked references

Zoological Research Editorial Board

ZOOLOGICAL RESEARCH

动物学研究 DONGWUXUE YANJIU

Bimonthly, Since 1980

中国精品科技期刊 中国科技核心期刊 动物学类核心期刊

Editor-in-Chief: Yong-Gang YAO

Executive Editor-in-Chief: Yun ZHANG

Editors: Su-Qing LIU Long NIE Andrew Willden

Edited by Editorial Office of Zoological Research

(Kunming Institute of Zoology, Chinese Academy of Sciences, 32 Jiaochang Donglu, Kunming, Yunnan, Post Code: 650223 Tel: +86 871 65199026 E-mail: zoores@mail.kiz.ac.cn

Sponsored by Kunming Institute of Zoology, Chinese Academy of Sciences; China Zoological Society©

Supervised by Chinese Academy of Sciences

Published by Science Press (16 Donghuangchenggen Beijie, Beijing 100717, China)

Printed by Kunming Xiaosong Plate Making & Printing Co, Ltd

Domestic distribution by Yunnan Post and all local post offices in China

International distribution by China International Book Trading Corporation (Guoji Shudian) P.O.BOX 399, Beijing 100044, China

Advertising Business License 广告经营许可证：滇工商广字66号

Domestic Postal Issue No.: 64-20

Price: 10.00 USD/60.00 CNY Post No.: BM358

ISSN 2095-8137